N-terminal acetyltransferases and Translation

Gholson J. Lyon, M.D. Ph.D.

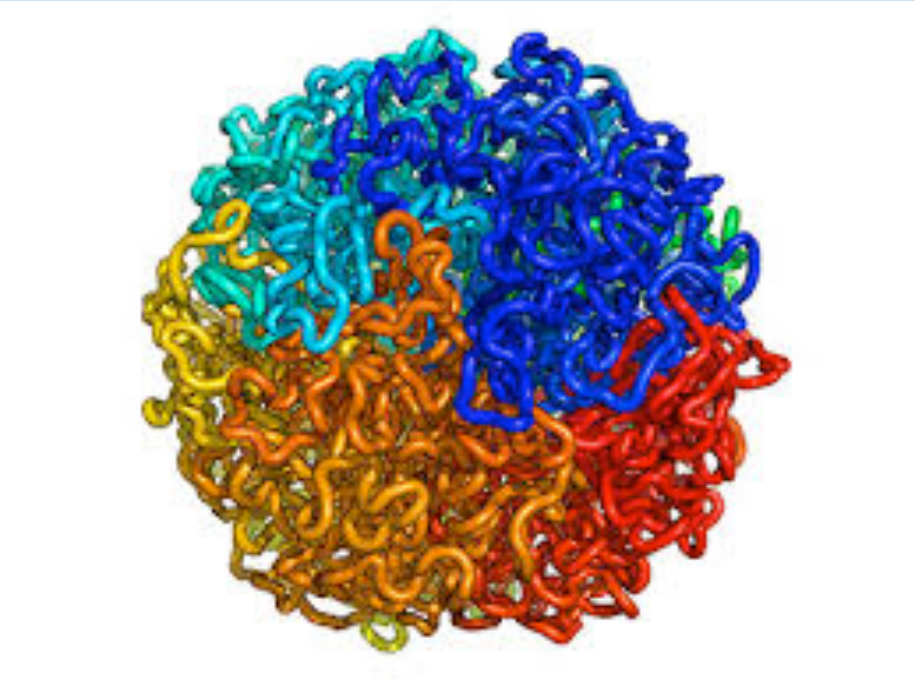

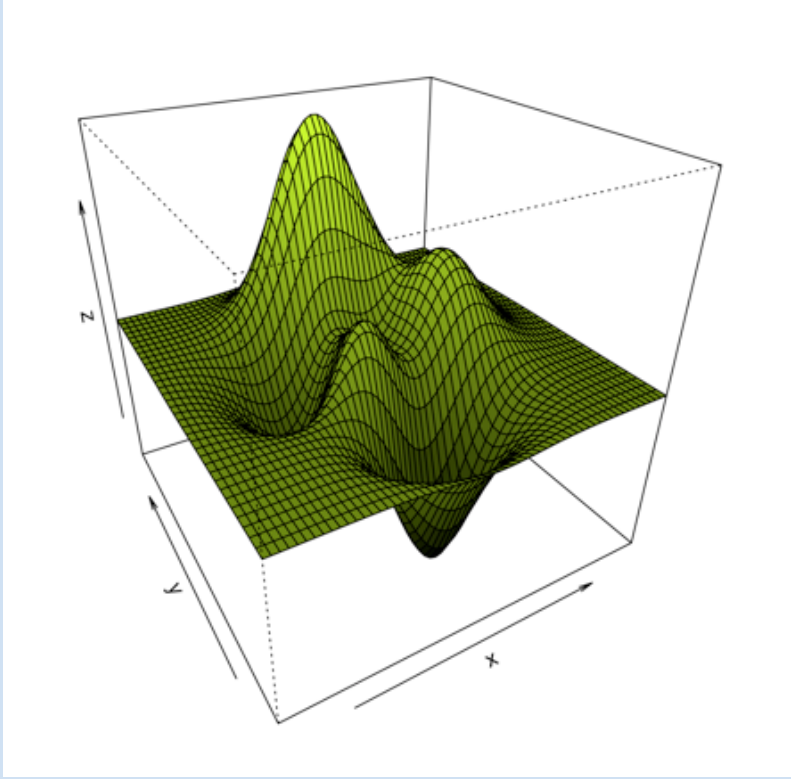

“There are ~12 billion nucleotides in every cell of the human body, and there are ~25-100 trillion cells in each human body. Given somatic mosaicism, epigenetic changes and environmental differences, no two human beings are the same, particularly as there are only ~7 billion people on the planet”.

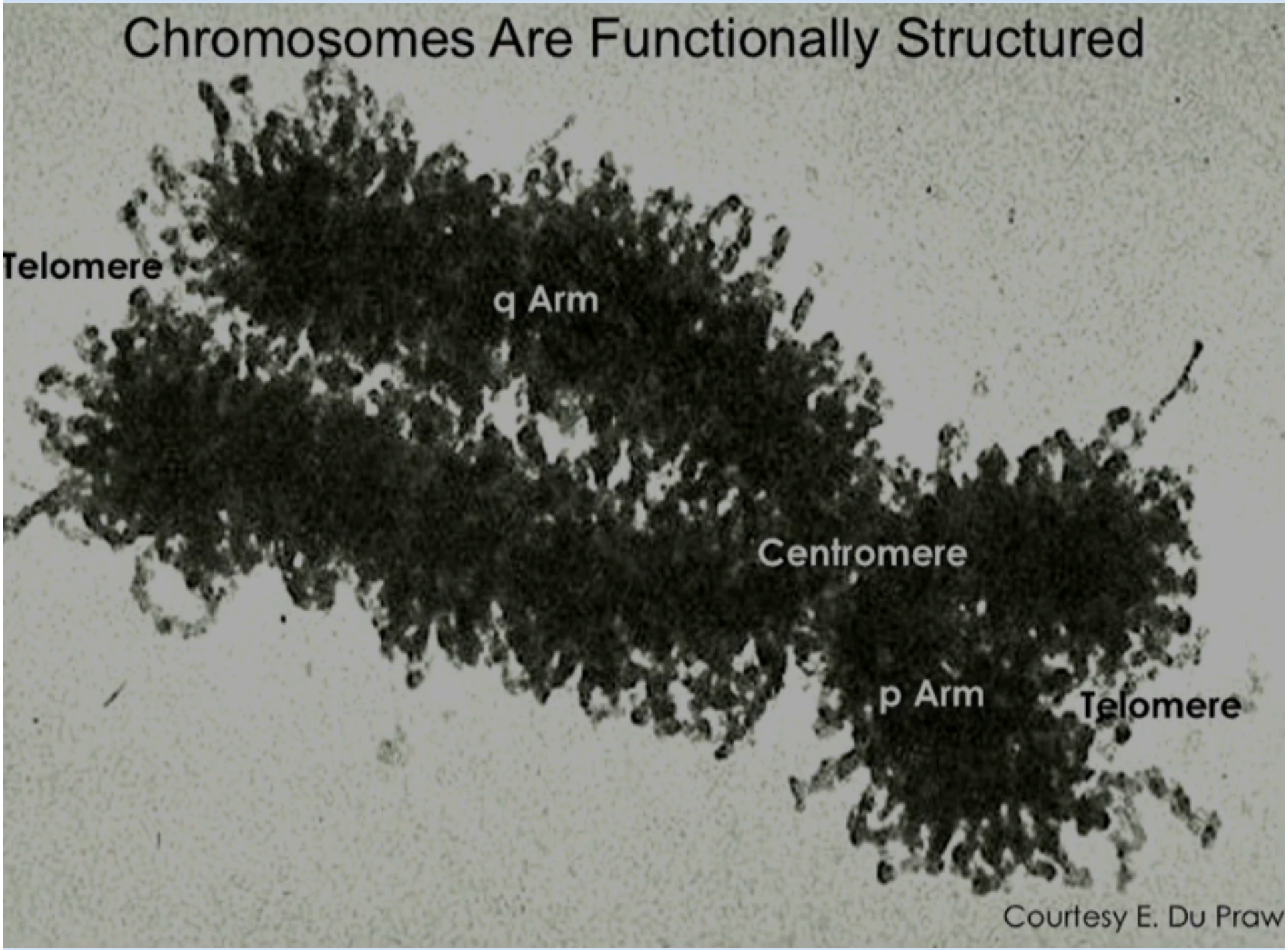
Chromosomes Are Functionally Structured
Telomere
q Arm
Centromere
p Arm
Telomere
Courtesy E. Du Praw

Hi-C schematic

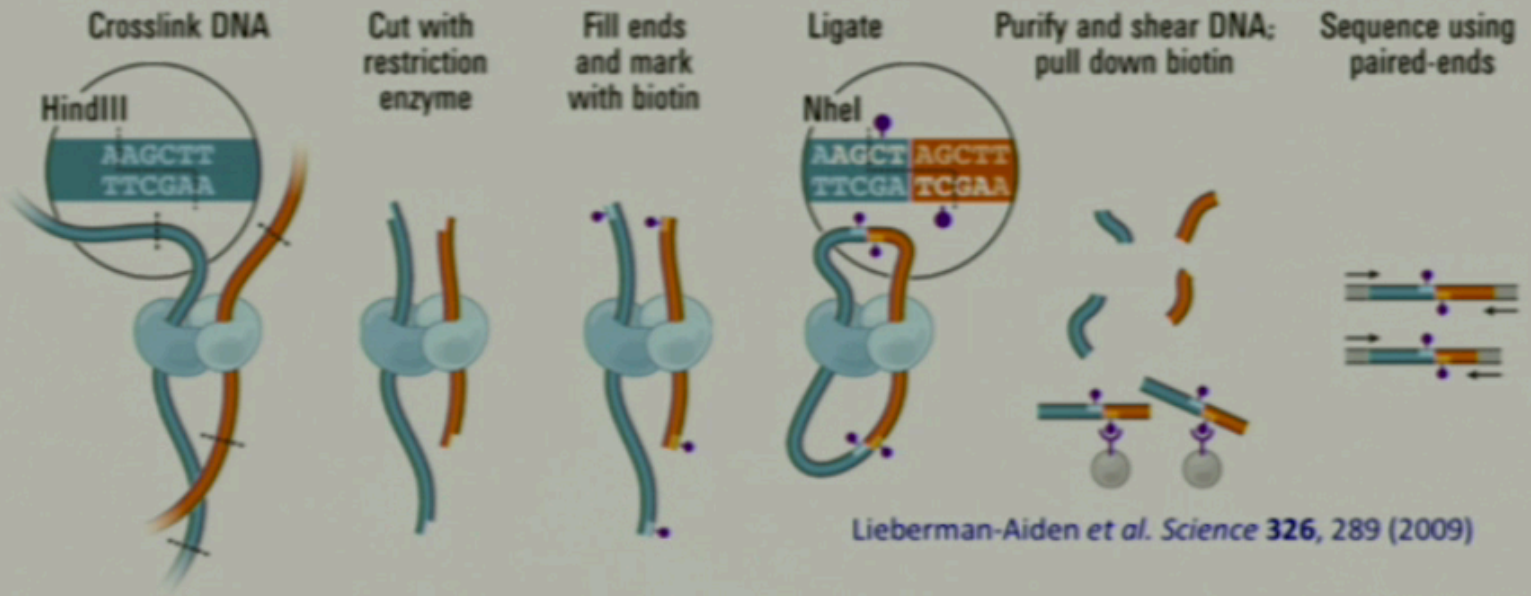

Lieberman-Aiden *et al. Science* **326**, 289 (2009)

3D model of yeast genome

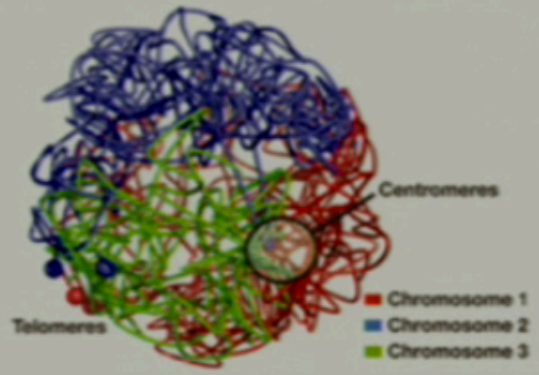

Ken-ichi Noma

The Fractal Globule model

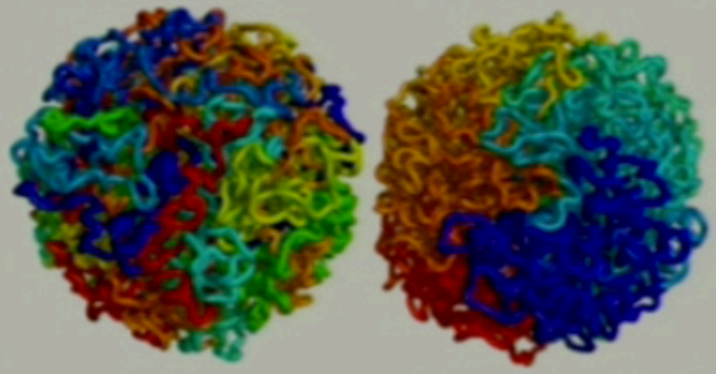

Job Dekker

Hi-C evidence of Mb scale compacted structural domains

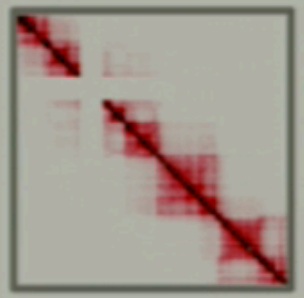

Nora *et al. Nature* (2012)

There is a dedicated mRNA export machinery

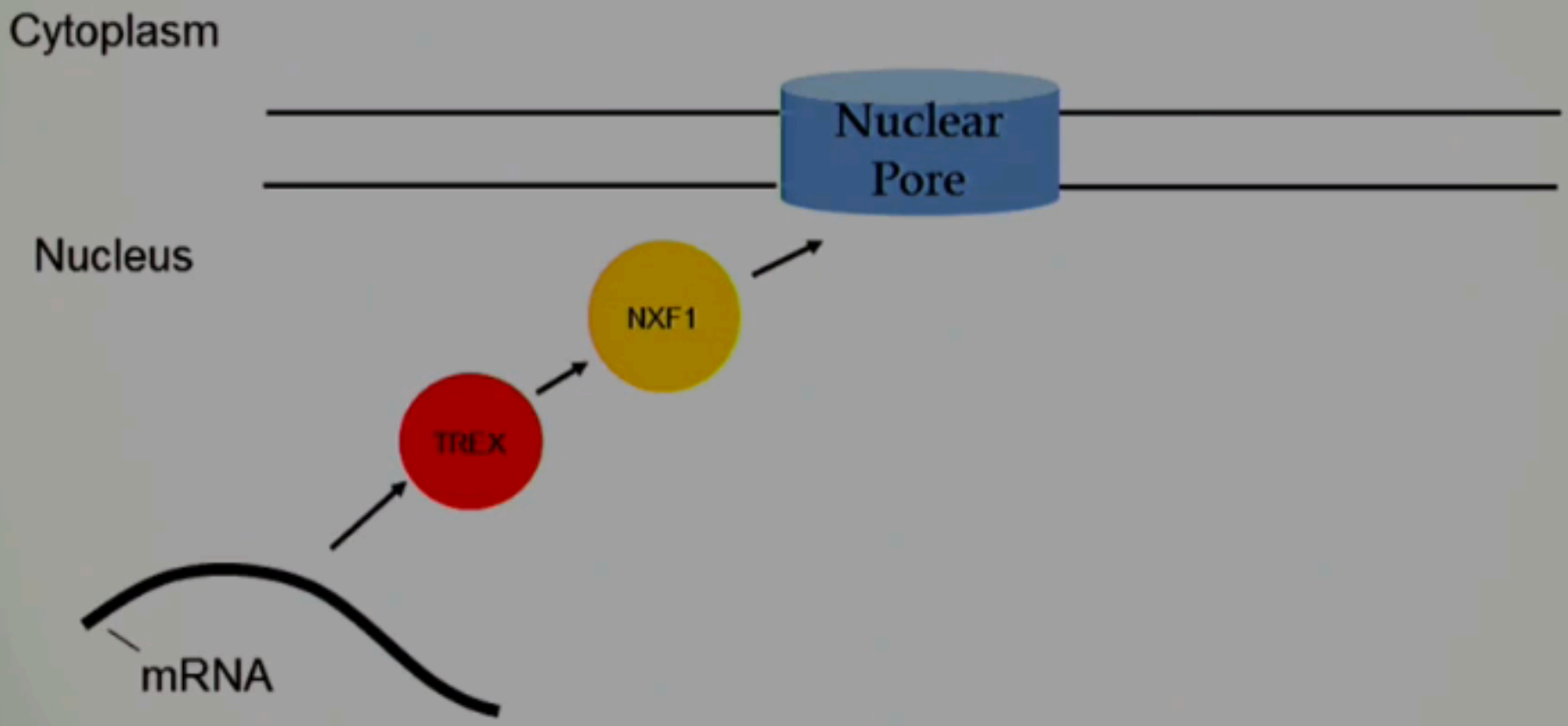

Canonical mRNA Export Pathway

The Nucleus is Functionally Compartmentalized

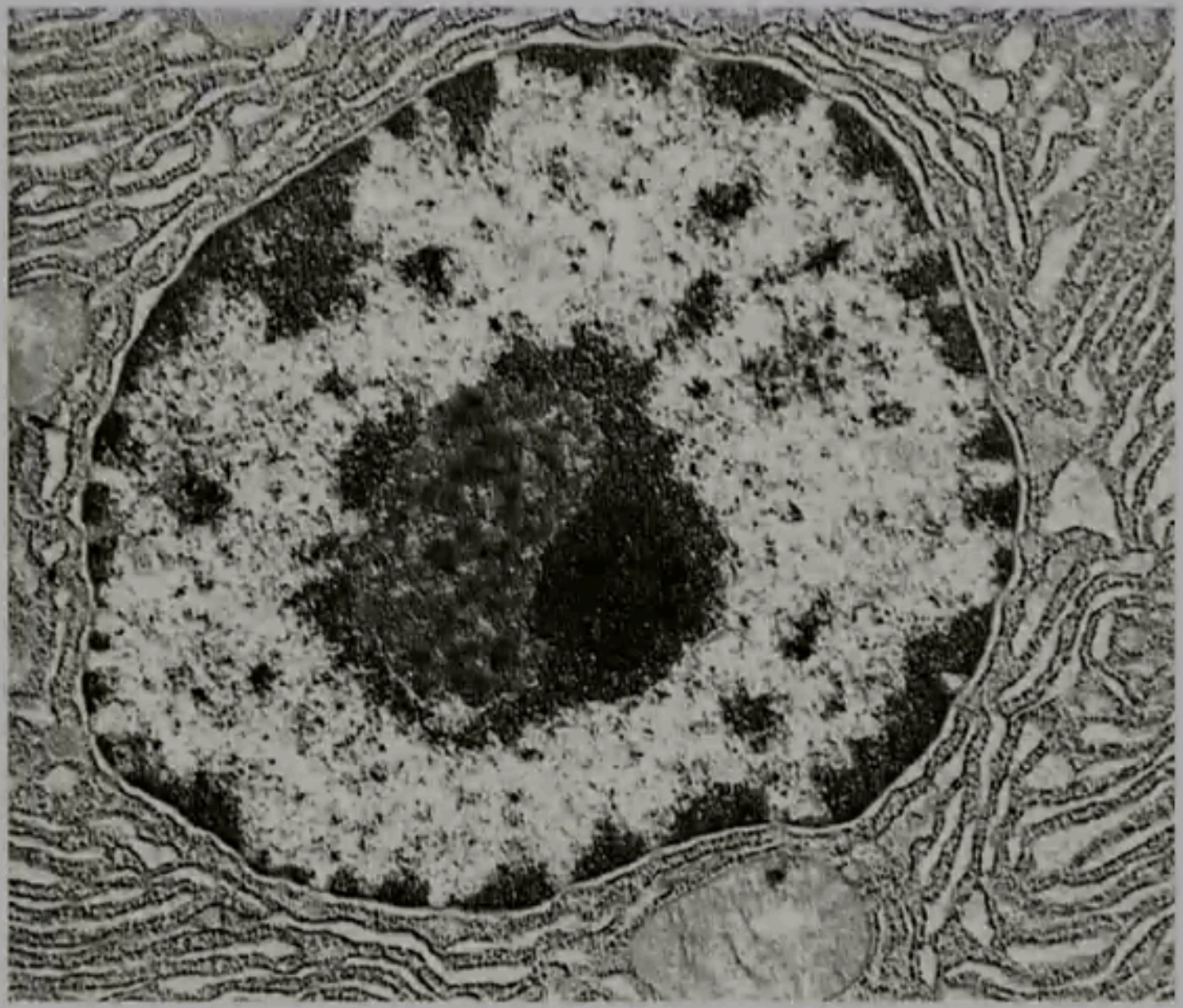

Courtesy Kenneth M. Bart

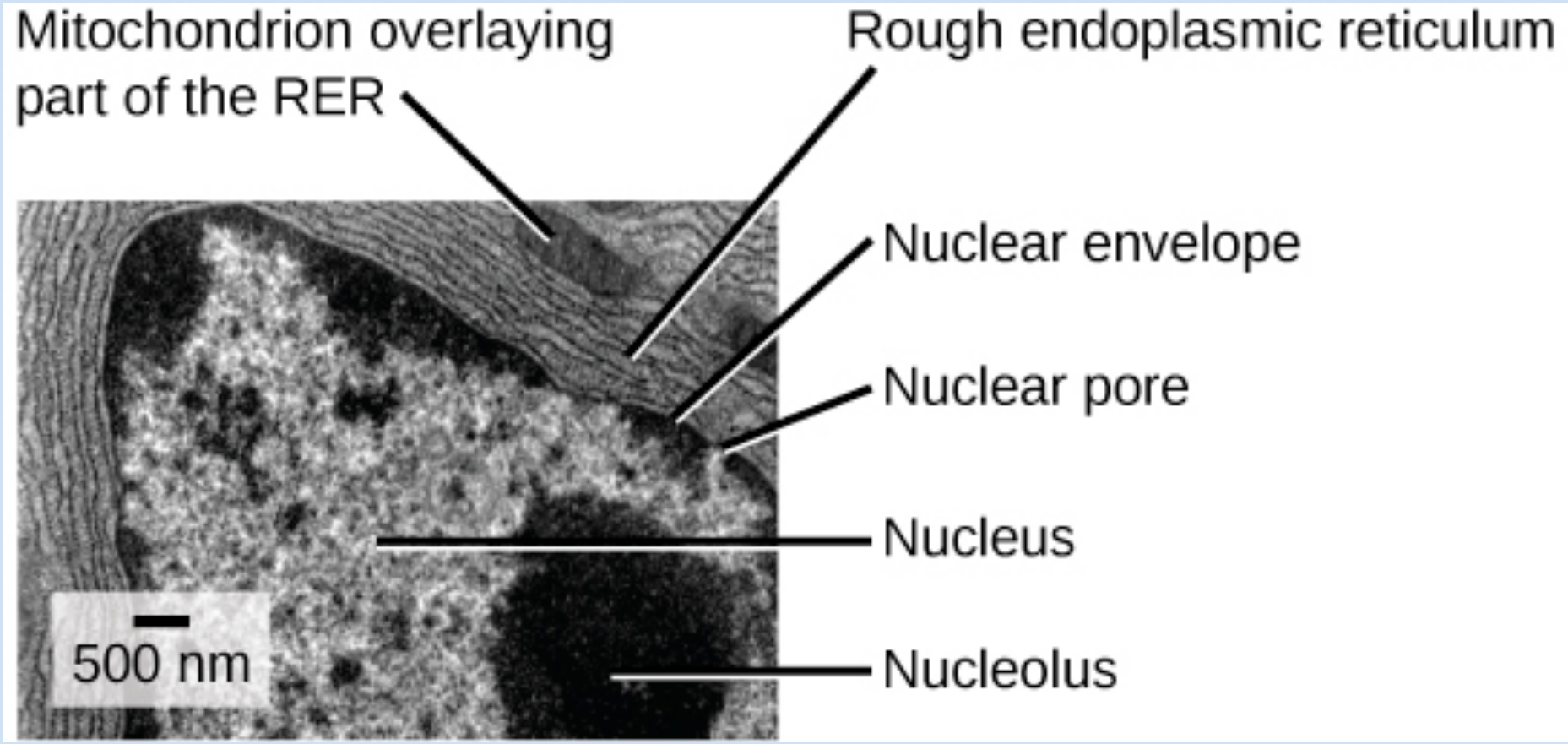
Mitochondrion overlaying part of the RER
Rough endoplasmic reticulum
Nuclear envelope
Nuclear pore
Nucleus
Nucleolus
500 nm

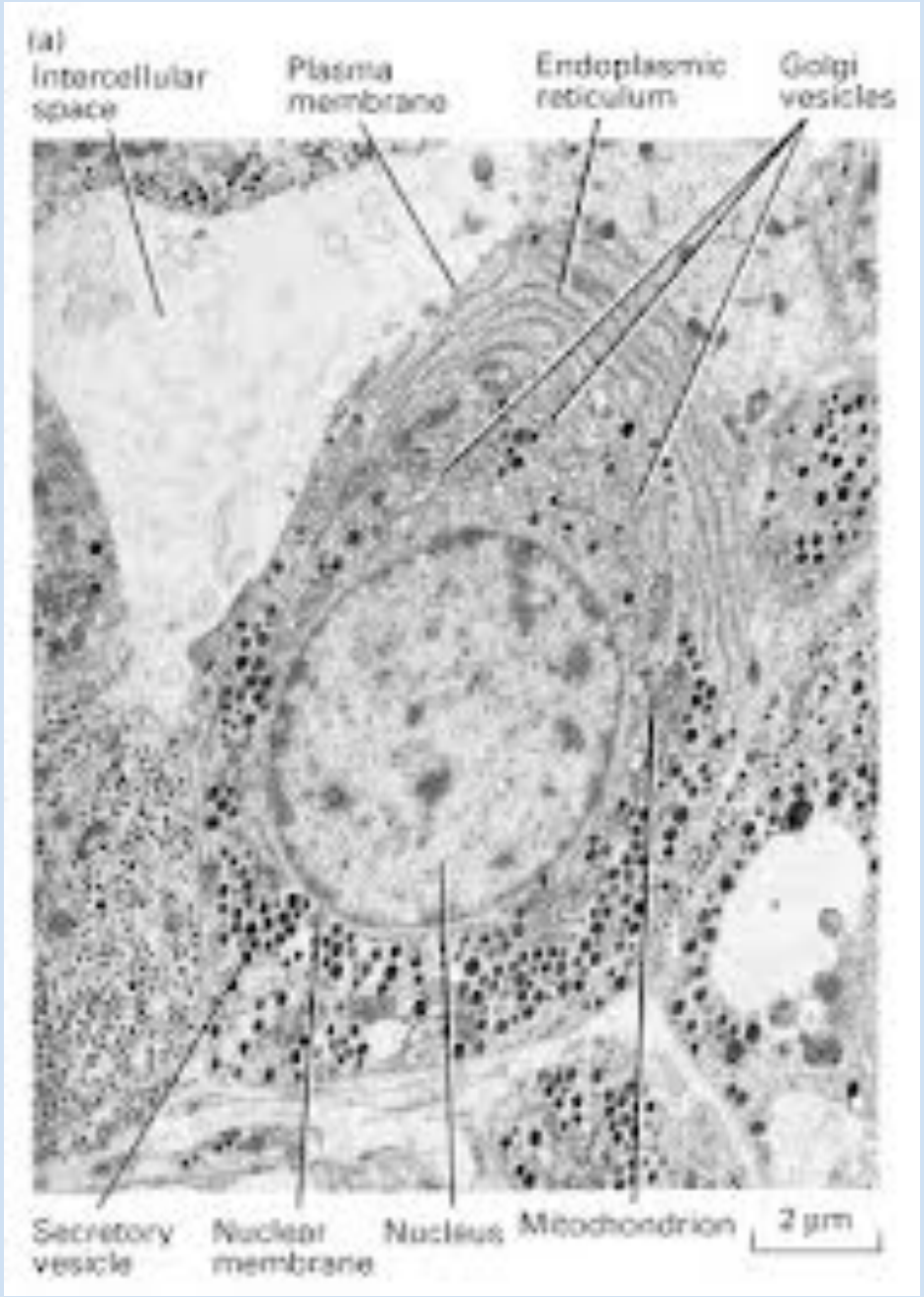
(a)
Intercellular space
Plasma membrane
Endoplasmic reticulum
Golgi vesicles
Secretory vesicle
Nuclear membrane
Nucleus
Mitochondrion
2 μm

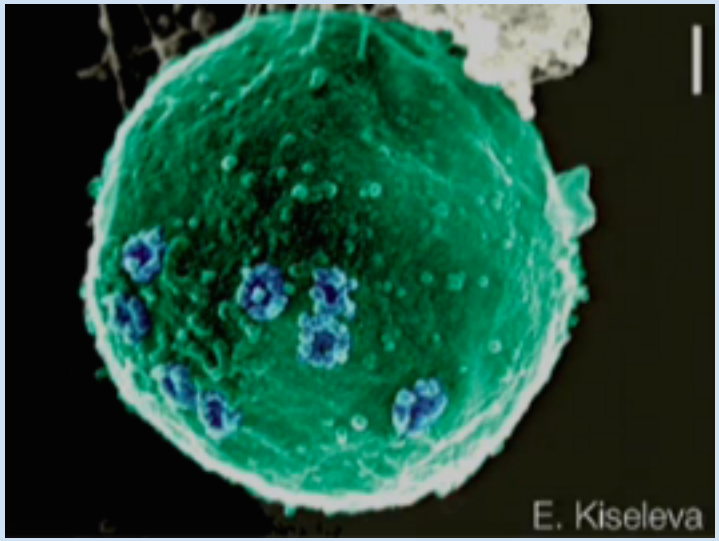

Nuclear pores in a yeast nucleus

Nuclear Pore proteins appear to function as scaffolds for open/active chromatin domains

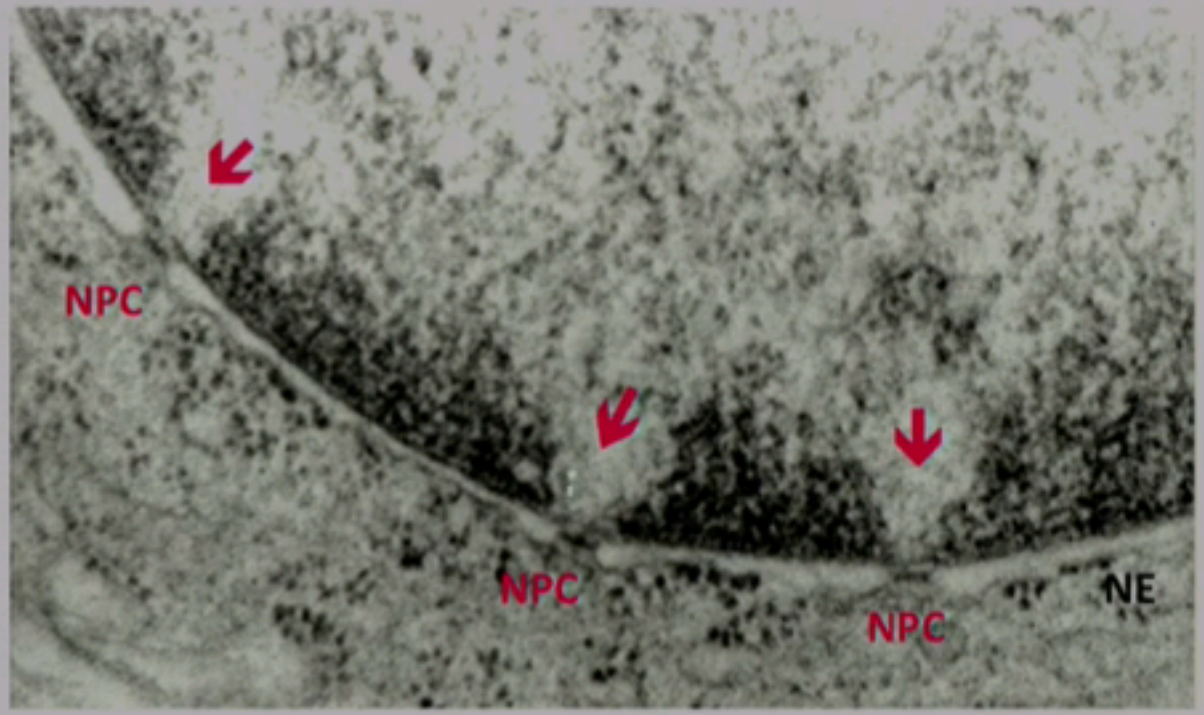

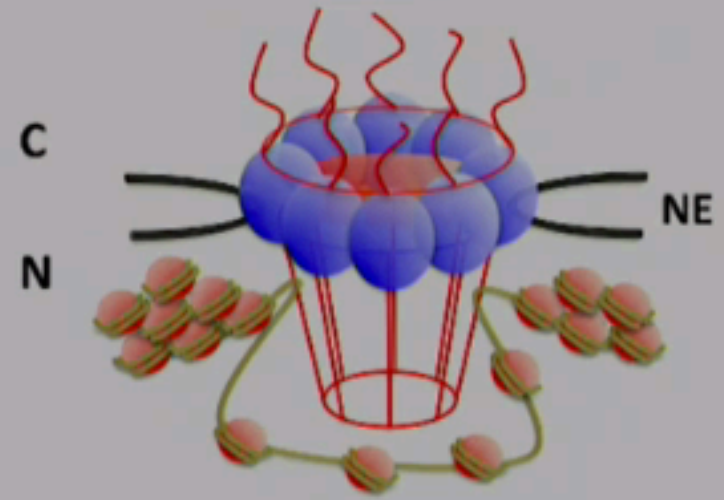

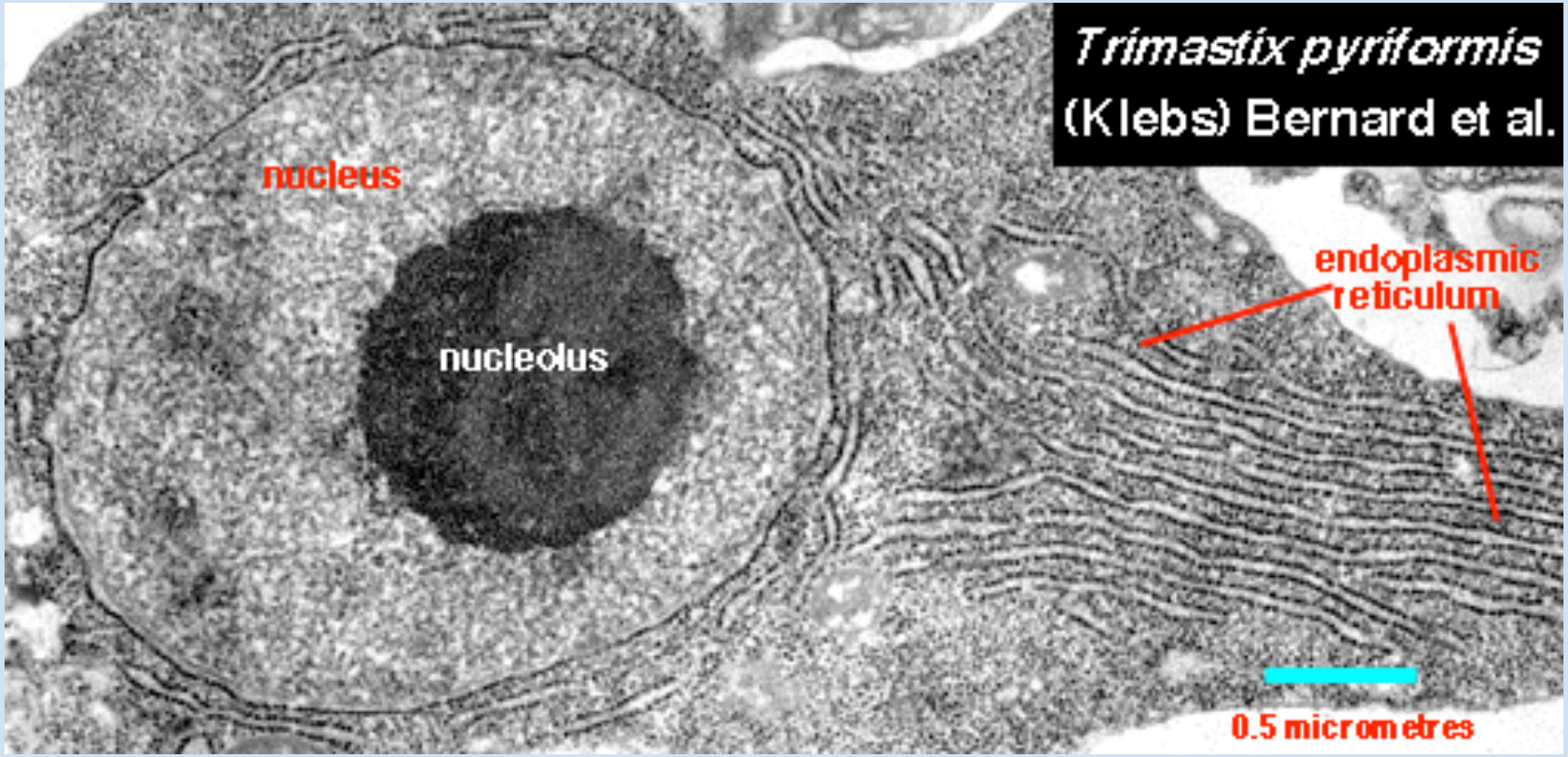

Trimastix pyriformis is a quadriflagellate, free-living, bacterivorous heterotrophic nanoflagellate from anoxic freshwaters that lacks mitochondria

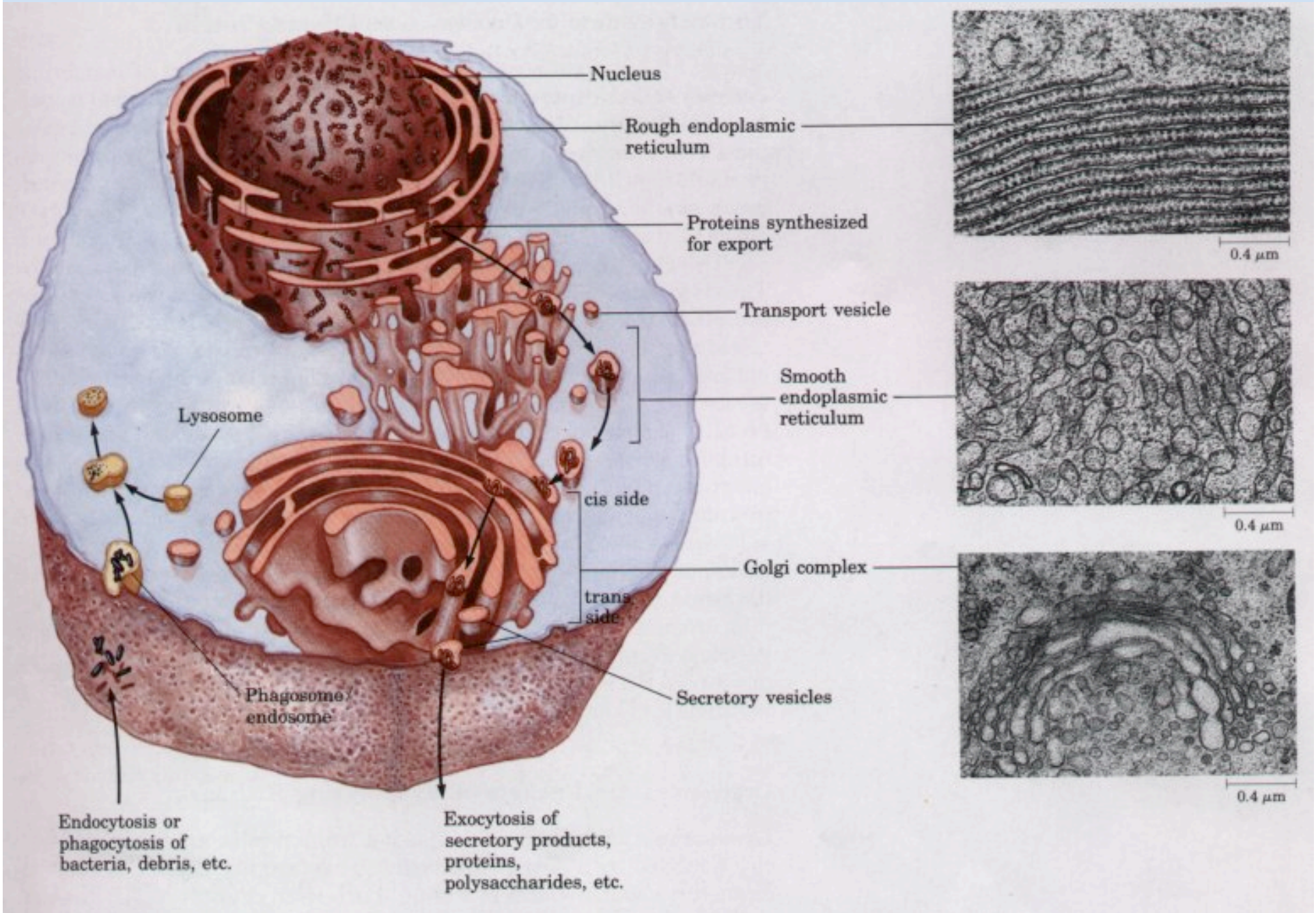
Nucleus
Rough endoplasmic reticulum
Proteins synthesized for export
Transport vesicle
Smooth endoplasmic reticulum
Lysosome
cis side
Golgi complex
trans side
Phagosome endosome
Secretory vesicles
Endocytosis or phagocytosis of bacteria, debris, etc.
Exocytosis of secretory products, proteins, polysaccharides, etc.
0.4 μm
0.4 μm
0.4 μm

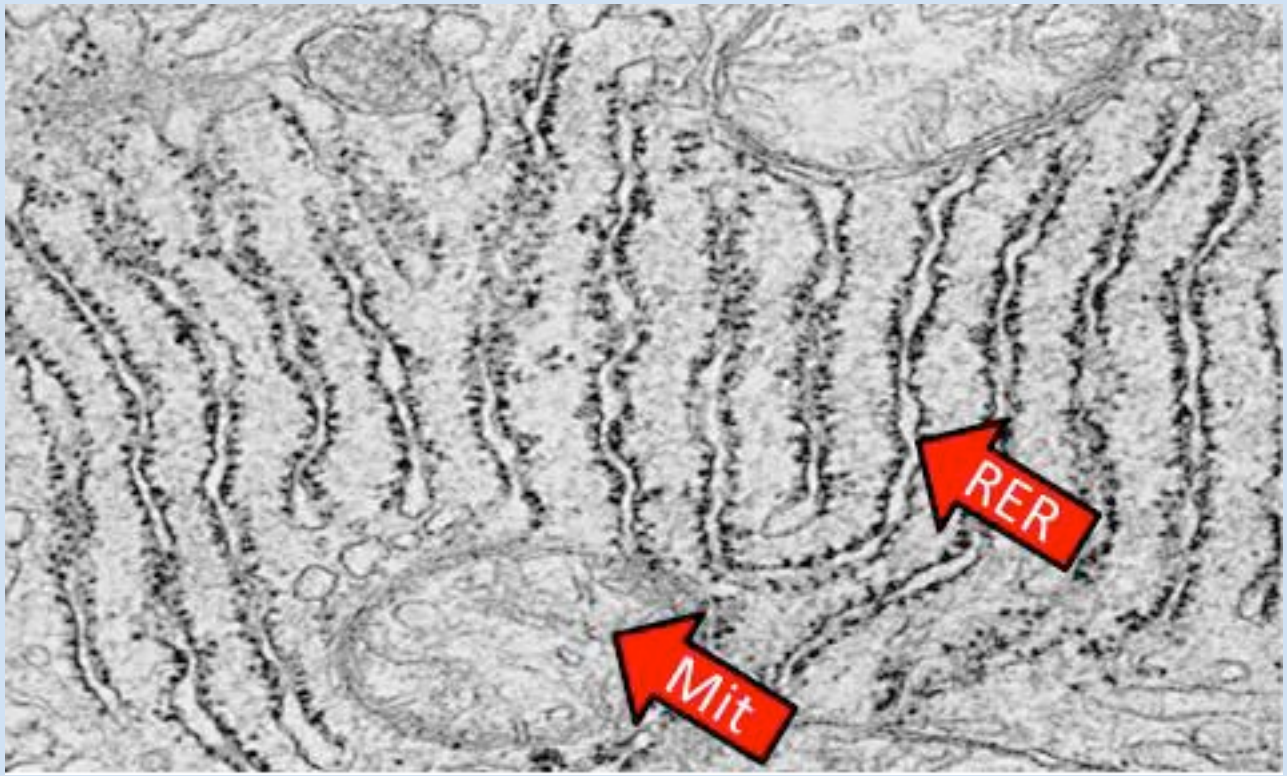
RER
Mit

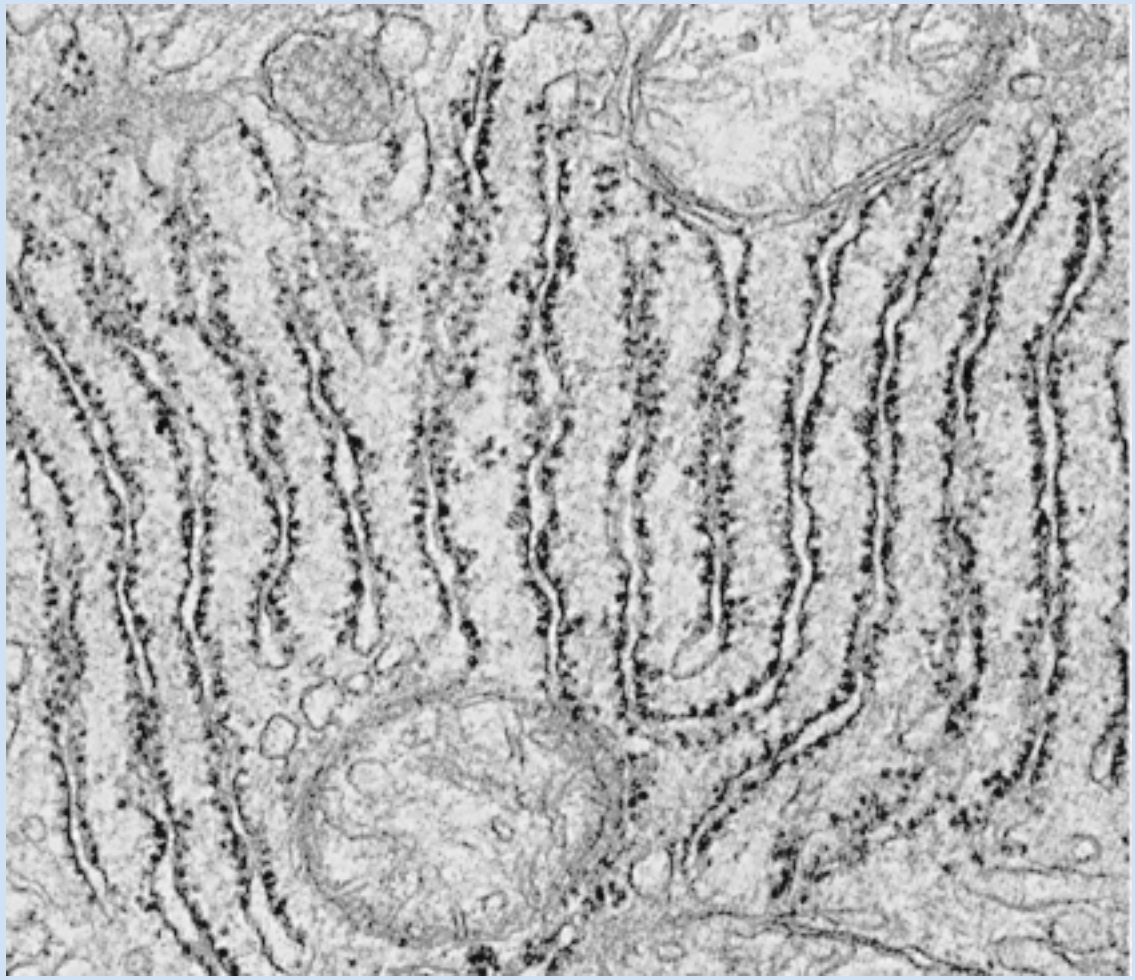

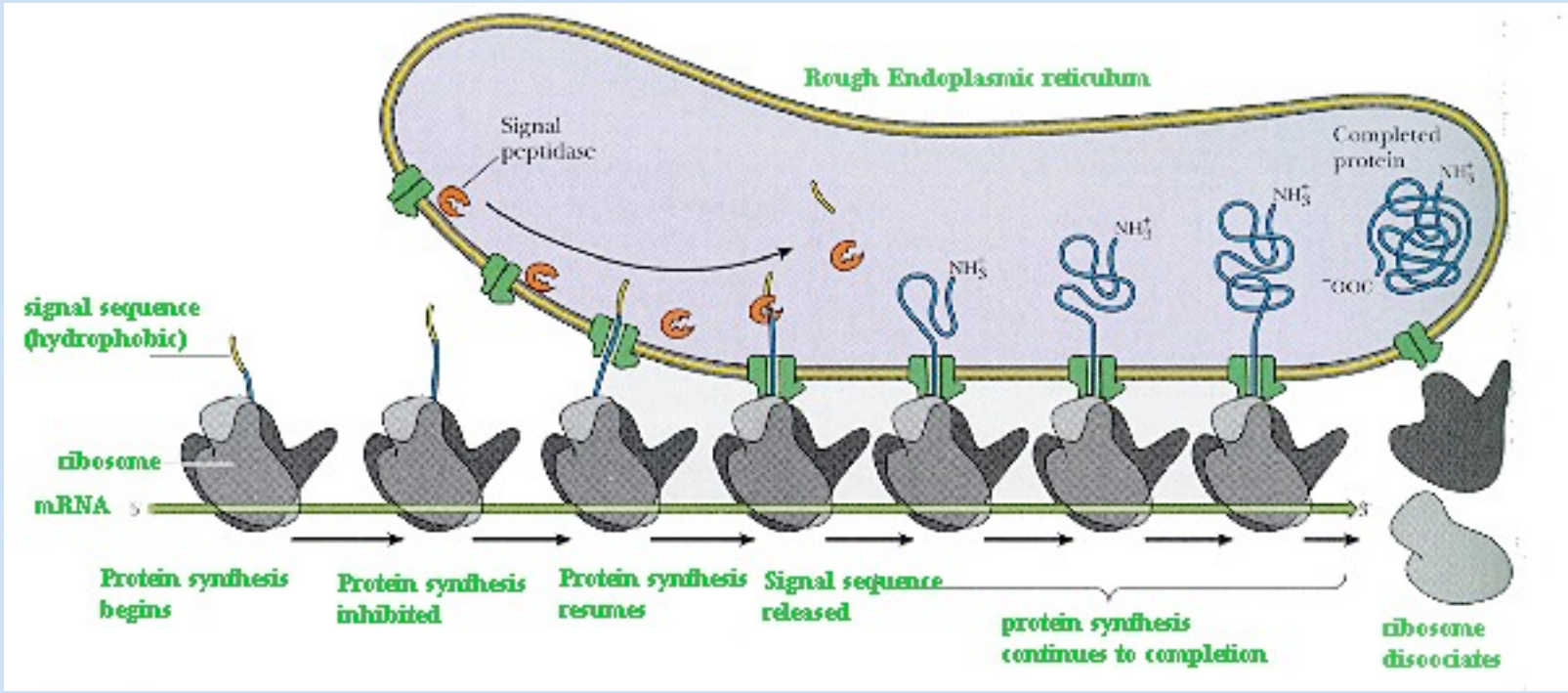
Rough Endoplasmic reticulum
Signal peptidase
Completed protein
signal sequence (hydrophobic)
ribosome
mRNA
Protein synthesis begins
Protein synthesis inhibited
Protein synthesis resumes
Signal sequence released
protein synthesis continues to completion
ribosome dissociates

Mara G. Haseltine is an internationally renowned artist known for her sculptural renditions of microscopic life forms - including the large scale sculpture **Waltz of the Polypeptides** that resides on CSHL grounds near Dolan depicting a ribosome creating a protein.

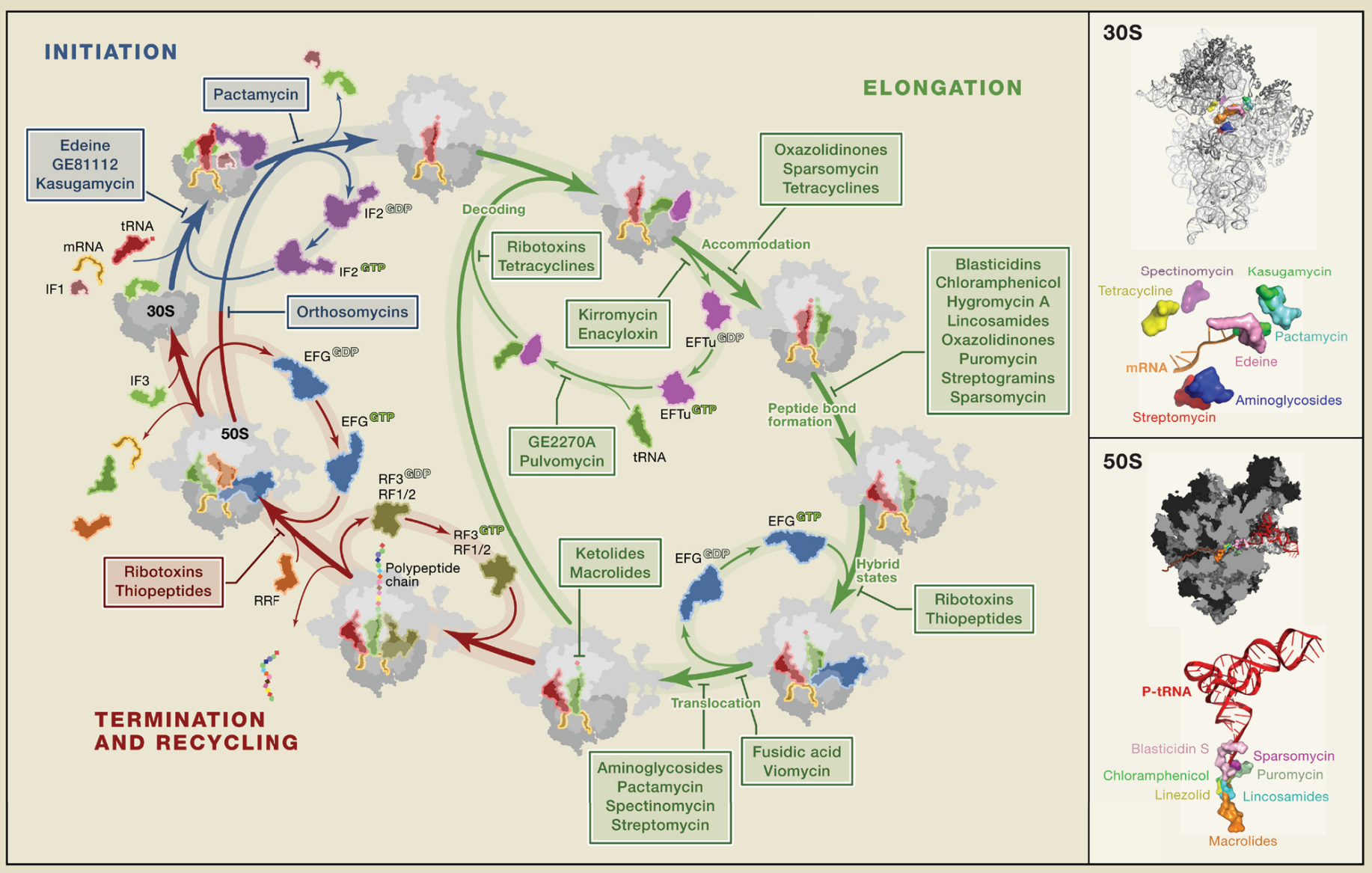
INITIATION
ELONGATION
TERMINATION AND RECYCLING
Pactamycin
Edeine
GE81112
Kasugamycin
tRNA
mRNA
IF1
IF2 GDP
IF2 GTP
30S
Orthosomycins
IF3
EFG GDP
EFG GTP
50S
RF3 GDP
RF1/2
RF3 GTP
RF1/2
Polypeptide chain
RRF
Ribotoxins
Thiopeptides
Decoding
Ribotoxins
Tetracyclines
Kirromycin
Enacyloxin
EFTu GDP
EFTu GTP
GE2270A
Pulvomycin
tRNA
Accommodation
Oxazolidinones
Sparsomycin
Tetracyclines
Blasticidins
Chloramphenicol
Hygromycin A
Lincosamides
Oxazolidinones
Puromycin
Streptogramins
Sparsomycin
Peptide bond formation
Hybrid states
EFG GTP
EFG GDP
Ketolides
Macrolides
Ribotoxins
Thiopeptides
Translocation
Aminoglycosides
Pactamycin
Spectinomycin
Streptomycin
Fusidic acid
Viomycin
30S
Spectinomycin
Kasugamycin
Tetracycline
Pactamycin
mRNA
Edeine
Aminoglycosides
Streptomycin
50S
P-tRNA
Blasticidin S
Sparsomycin
Chloramphenicol
Puromycin
Linezolid
Lincosamides
Macrolides

ENHANCED SnapShot: Antibiotic Inhibition of Protein Synthesis II

Cell

Daniel Sohmen,[1] Joerg M. Harms,[2] Frank Schlünzen,[3] and Daniel N. Wilson[1,4]
[1]University of Munich, Germany; [2]MPSD, University of Hamburg, Germany; [3]DESY, Hamburg, Germany; [4]CiPS-M, Munich, Germany

The translational apparatus is one of the major targets for antibiotics in the bacterial cell. Antibiotics predominantly interact with the functional centers of the ribosome, namely the messenger RNA (mRNA)-transfer RNA (tRNA) decoding region on the 30S subunit, the peptidyltransferase center on the 50S subunit, or the ribosomal exit tunnel through which the nascent polypeptide chain passes during translation. Protein synthesis can be divided into three phases: initiation, elongation, and termination/recycling.

1. Initiation

Translation initiation operates through a 30S initiation complex (30S-IC), consisting of the 30S, mRNA, initiator fMet-tRNA, and three initiation factors, IF1, IF2, and IF3. Subsequently, the 30S-IC associates with the 50S, which releases the initiation factors (IFs) and leaves the initiator-tRNA at the peptidyl-tRNA-binding site (P site), base-paired to the start codon of the mRNA. The antibiotics edeine, GE81112, and kasugamycin interfere with 30S-IC assembly, whereas formation of a functional 70S-IC is blocked by the orthosomycins and pactamycins.

2. Elongation

The elongation phase involves the movement of tRNAs in a cyclic fashion through the three tRNA-binding sites (A→P→E) on the ribosome. The first step in the cycle involves the delivery of the aminoacyl-tRNA (aa-tRNA) to the aa-tRNA-binding site (A site), which is facilitated by the elongation factor EF-Tu•GTP. Hydrolysis of GTP by EF-Tu leads to its dissociation from the ribosome, allowing aa-tRNA accommodation. Peptide-bond formation then proceeds, transferring the entire polypeptide chain from the P-tRNA to the aa-tRNA in the A site. The ribosome now has a peptidyl-tRNA at the A site and an uncharged tRNA at the P site. This ribosomal state is highly dynamic with the tRNAs oscillating between classical (A and P sites) and hybrid states (A/P and P/E sites on 30S/50S). EF-G binds to the ribosome, which stabilizes the tRNAs in hybrid states, hydrolyzes GTP to GDP, and catalyzes the translocation reaction. Translocation shifts the peptidyl-tRNA from the A/P hybrid state to the P site and the deacylated tRNA from the P/E to the exit site (E site). EF-G•GDP dissociates leaving the A site vacant for the next incoming aa-tRNA. The majority of antibiotics targeting translation inhibit a step associated with the elongation phase. Most antibiotics binding to the 30S perturb either tRNA binding, decoding, or translocation, whereas antibiotics targeting the 50S inhibit peptide-bond formation, extension of the polypeptide chain, or stable binding of translation factors. In contrast, some antibiotics interact directly with elongation factors and prevent them from dissociating from the ribosome.

3. Termination/Recycling

Arrival of an mRNA stop codon in the A site of the ribosome signals the termination of protein synthesis. Release factor 1 (RF1) or RF2 binds to the ribosome and hydrolyzes the peptidyl-tRNA bond, releasing the translated polypeptide chain from the ribosome. RF1/2 is recycled from the ribosome by RF3 in a GTP-dependent fashion. The ribosome is then split into subunits by the concerted action of EF-G and ribosome recycling factor (RRF), thus recycling the components for the next round of translation. There are no antibiotics that specifically inhibit termination and ribosome recycling; however antibiotics that target EF-G, such as α-sarcin, fusidic acid, and thiopeptides, also inhibit ribosome recycling.

Abbreviations

30S, small ribosomal subunit; 50S, large ribosomal subunit; aa-tRNA, aminoacyl-tRNA; A site, aa-tRNA-binding site; E site, exit site for tRNA; EF, elongation factor; IF, initiation factor; mRNA, messenger RNA; P-tRNA, peptidyl-tRNA; P site, P-tRNA-binding site; PTC, peptidyltransferase center; RRF, ribosome recycling factor; RF, release factor; tRNA, transfer RNA.

	Class	Name	Target	Mechanism
Small (30S) Ribosomal Subunit	Aminoglycosides	Apramycin, gentamycin, hygromycin B, kanamycin, neomycin, paromomycin, tobramycin	Elongation (translocation)	Most aminoglycoside antibiotics induce translational misreading by promoting binding of near-cognate tRNAs, but the biological effect is probably due to inhibition of the translocation reaction and promotion of back-translocation.
	Edeine	Edeine A	Initiation (fMet-tRNA binding)	Edeine prevents binding of the initiator tRNA to the 30S subunit in an mRNA-dependent manner.
	GE81112	GE81112	Initiation (fMet-tRNA binding)	GE81112 inhibits binding of the initiator tRNA to the 30S subunit in an mRNA-independent manner.
	Kasugamycin	Kasugamycin	Initiation (fMet-tRNA binding)	Kasugamycin inhibits translation initiation of canonical mRNAs by binding in the path of the mRNA and preventing stable interaction of the initiator tRNA with the start codon.
	Pactamycin	Pactamycin	Initiation, elongation (translocation)	Early data suggest that pactamycin allows 30S but not 70S initiation complex formation, whereas recently pactamycin was shown to inhibit translocation in a tRNA-mRNA-dependent manner.
	Spectinomycin	Spectinomycin	Elongation (translocation)	Spectinomycin binds to the neck of the small subunit and prevents the relative movement of the head and body that is needed for the completion of translocation.
	Streptomycin	Streptomycin	Elongation (misreading)	Streptomycin increases affinity of tRNA for the A site, has a modest inhibitory effect on translocation, promotes back-translocation, and induces high-level translational misreading.
	Tetracyclines/glycylcyclines	Doxycycline, minocycline, tetracycline/ tigecycline	Elongation (tRNA delivery)	Tetracyclines prevent stable binding of the EF-Tu-tRNA-GTP ternary complex to the ribosome and inhibit accommodation of A-tRNAs upon EF-Tu-dependent GTP hydrolysis.
	Viomycin	Capreomycin, viomycin	Elongation (translocation)	Viomycin locks tRNAs in a hybrid-site translocation intermediate state, preventing conversion by EF-G into a posttranslocation state.
Large (50S) Ribosomal Subunit	Blasticidins	Blasticidin S	Elongation (peptidyltransferase)	Two molecules of Blasticidin S mimic the C74 and C75 of P-tRNA and in doing so inhibit peptide bond formation by preventing tRNA binding at the P site of the peptidyltransferase center (PTC).
	Chloramphenicols	Chloramphenicol	Elongation (peptidyltransferase)	Chloramphenicol binds at the A site of the PTC where it perturbs placement of A site tRNA and thus prevents peptide bond formation.
	Hygromycin A	Hygromycin A	Elongation (peptidyltransferase)	Hygromycin A overlaps in its binding site with chloramphenicol and inhibits peptide bond formation by inhibiting the placement of the A site tRNA at the PTC.
	Ketolides	Cethromycin (ABT-773), telithromycin	Elongation (nascent chain egress)	Ketolides are derivatives of macrolides where the ketone group replaces the C3 sugar. Ketolides exhibit the same mechanism of action as macrolides by blocking the ribosomal tunnel and inducing peptidyl-tRNA drop-off.
	Lincosamides	Clindamycin, lincomycin	Elongation (peptidyltransferase)	Lincosamides span across both A and P sites of the PTC and inhibit binding of tRNA substrates at both these sites.
	Macrolides	Azithromycin, carbomycin A, clarithromycin, erythromycin, spiramycin, troleandomycin, tylosin	Elongation (nascent chain egress)	Macrolides bind within the ribosomal tunnel and prevent elongation of the nascent polypeptide chain, which leads to peptidyl-tRNA drop-off. Some macrolides, such as carbomycin A and tylosin, also directly inhibit peptide bond formation.
	Orthosomycins	Avilamycin, evernimicin	Initiation (70S-IC formation)	Orthosomycins interact with the large subunit and prevent the joining of the 30S-IC with the large subunit to form the 70S-IC in an IF2-dependent manner.
	Oxazolidinones	Eperezolid, linezolid	Elongation (peptidyltransferase)	Linezolid binds at the PTC in a position overlapping the aminoacyl moiety of A-tRNA, preventing tRNA accommodation and peptide bond formation.
	Puromycin	Puromycin	Elongation (peptidyltransferase)	Puromycin is a structural analog of the 3′ end of a tRNA, which binds at the A site of the PTC and triggers premature release of the nascent polypeptide chain.
	Ribotoxins	α-sarcin	Elongation (translocation), recycling	α-sarcin cleaves the *E. coli* 23S rRNA on the 3′ side of G2661, abolishing the ribosome's ability to stimulate the GTP hydrolysis activity of translation factors, such as EF-G.
	Sparsomycin	Sparsomycin	Elongation (peptidyltransferase)	Sparsomycin binds at the PTC where it blocks tRNA binding at the A site, while promoting translocation and stabilization of tRNA at the P site.
	Streptogramins A/B	Dalfopristin/quinupristin, virginiamycin M/S	Elongation (peptidyltransferase)	Streptogramins A and B act synergistically to inhibit translation. S_A compounds bind at the PTC overlapping A and P sites, whereas S_B compounds bind within the tunnel in a similar location to macrolides.
	Thiopeptides	Micrococcin, nocathiacin, nosiheptide, thiazomycin, thiostrepton	Elongation (translocation), Recycling	Thiopeptide antibiotics inhibit translocation by blocking the stable binding of EF-G to the ribosome. Thiopeptides also inhibit the action of translational GTPases, such IF2 and EF-Tu.
Elongation Factors	Fusidic acid	Fusidic acid	Elongation (translocation)	Fusidic acid stabilizes EF-G on the ribosome by allowing binding and GTP hydrolysis, but not Pi release, nor the associated conformational changes in EF-G necessary for dissociation.
	GE2270A-like thiopeptides	Amythiamicins, GE2270A, thiomuracins	Elongation (tRNA delivery)	The GE2270A-like thiopeptides, like pulvomycin, prevent ternary complex formation by binding to EF-Tu and blocking interaction of EF-Tu with aminoacyl-tRNAs. GE2270A and pulvomycin have distinct but overlapping binding sites on EF-Tu.
	Kirromycins and enacyloxins	Aurodox, kirromycin, and enacyloxin IIa	Elongation (tRNA delivery)	These drugs trap EF-Tu on the ribosome by allowing GTP hydrolysis but preventing Pi release and the conformational changes in EF-Tu that are necessary for tRNA release and EF-Tu dissociation.
	Pulvomycin	Pulvomycin	Elongation (tRNA delivery)	Pulvomycin prevents ternary complex formation by binding to EF-Tu and blocking interaction of EF-Tu with aminoacyl-tRNAs.

Insertion of Polypeptide Chains into the Endoplasmic Reticulum

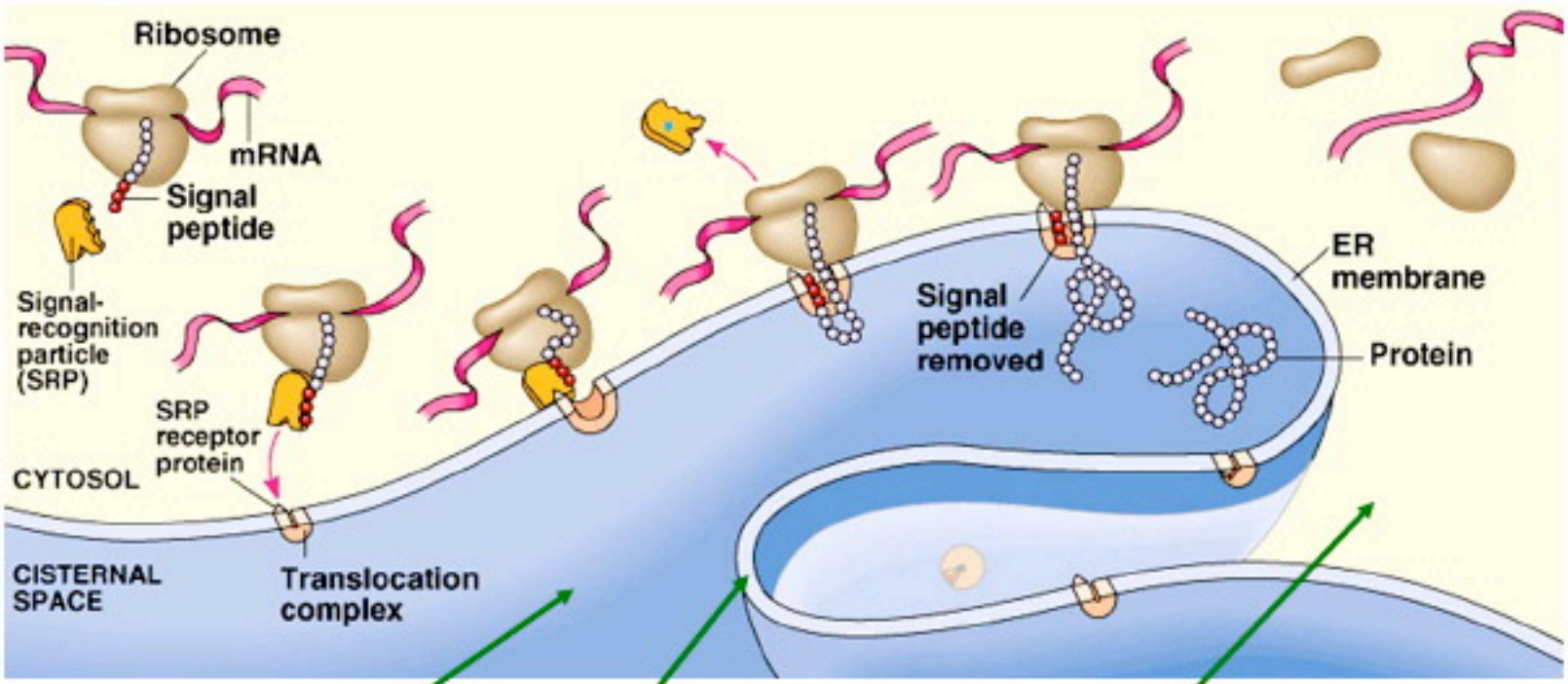

lumen

membrane of rough e.r.

cytoplasmic matrix

*

Endoplasmic Reticulum

- interconnected flattened tubular tunnels continuous with outer membrane of nucleus
- all eukaryotic cells contain ER
- responsible for communication in cell
- part of ***endomembrane system***
- all membranous organelles belong to system
- ***Rough***
  - attached ribosomes
  - makes appear spotty
  - takes in proteins made on ribosomes so cannot escape into cytoplasm
- ***Smooth***
  - no attached ribosomes→ smooth
  - not involved in protein synthesis
  - ***steroid production***
- contains enzymes required to detoxify wide variety of organic molecules
- storage site for calcium

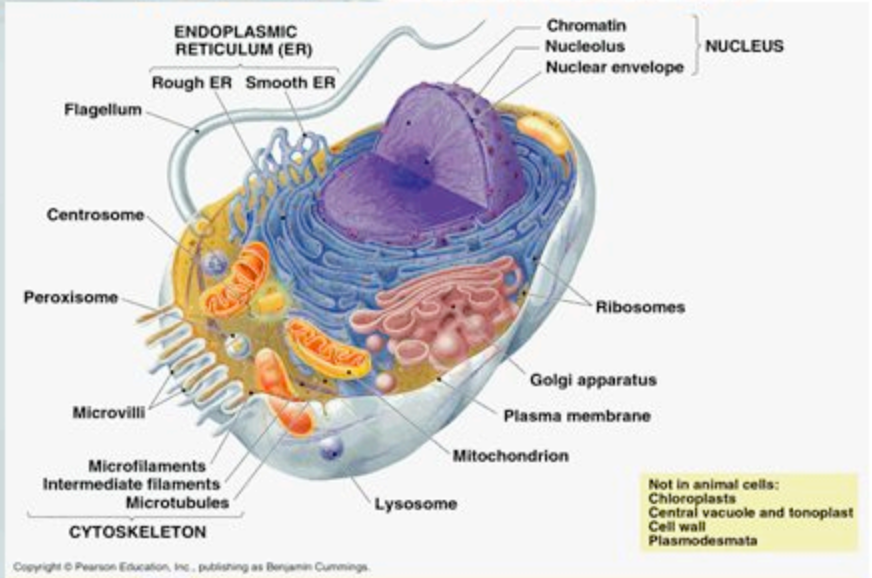

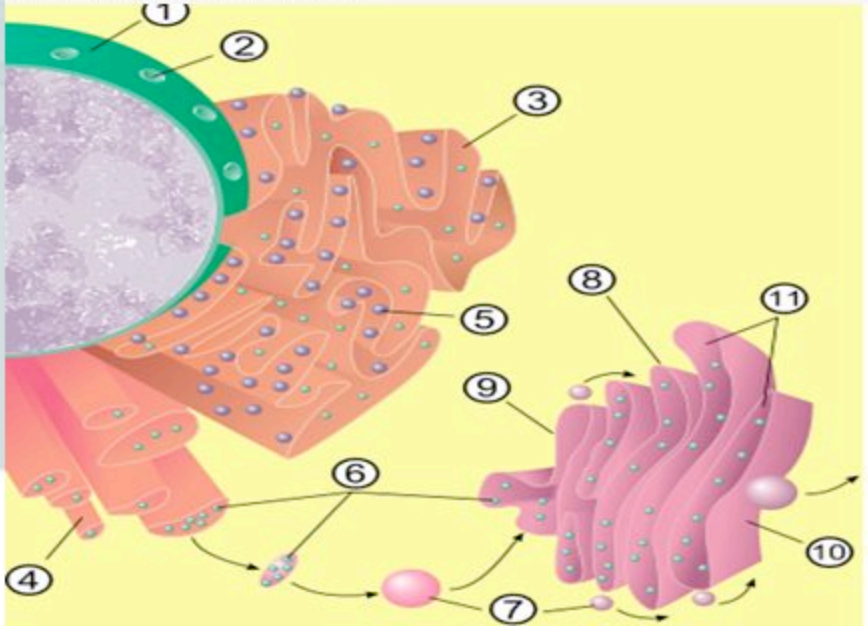

A new system for naming ribosomal proteins

Nenad Ban[1], Roland Beckmann[2], Jamie HD Cate[3], Jonathan D Dinman[4], François Dragon[5], Steven R Ellis[6], Denis LJ Lafontaine[7], Lasse Lindahl[8], Anders Liljas[9], Jeffrey M Lipton[10,11], Michael A McAlear[12], Peter B Moore[13], Harry F Noller[14], Joaquin Ortega[15], Vikram Govind Panse[16], V Ramakrishnan[17], Christian MT Spahn[18], Thomas A Steitz[19], Marek Tchorzewski[20], David Tollervey[21], Alan J Warren[17], James R Williamson[22], Daniel Wilson[23], Ada Yonath[24] and Marat Yusupov[25]

Current Opinion in Structural Biology 2014, **24**:165–169

This review comes from a themed issue on **Nucleic acids and their protein complexes**

Edited by **Karolin Luger** and **Simon EV Phillips**

For a complete overview see the Issue and the Editorial

Available online 10th February 2014

0959-440X/$ – see front matter,

http://dx.doi.org/10.1016/j.sbi.2014.01.002

Table 1

New nomenclature for proteins from the small ribosomal subunit.

New name[#]	Taxonomic range[*]	Bacteria name	Yeast name	Human name
bS1	B	S1	–	–
eS1	A E	–	S1	S3A
uS2	B A E	S2	S0	SA
uS3	B A E	S3	S3	S3
uS4	B A E	S4	S9	S9
eS4	A E	–	S4	S4
uS5	B A E	S5	S2	S2
bS6	B	S6	–	–
eS6	A E	–	S6	S6
uS7	B A E	S7	S5	S5
eS7	E	–	S7	S7
uS8	B A E	S8	S22	S15A
eS8	A E	–	S8	S8
uS9	B A E	S9	S16	S16
uS10	B A E	S10	S20	S20
eS10	E	–	S10	S10
uS11	B A E	S11	S14	S14
uS12	B A E	S12	S23	S23
eS12	E	–	S12	S12
uS13	B A E	S13	S18	S18
uS14	B A E	S14	S29	S29
uS15	B A E	S15	S13	S13
bS16	B	S16	–	–
uS17	B A E	S17	S11	S11
eS17	A E	–	S17	S17
bS18	B	S18	–	–
uS19	B A E	S19	S15	S15
eS19	A E	–	S19	S19
bS20	B	S20	–	–
bS21	B	S21	–	–
bTHX	B	THX	–	–
eS21	E	–	S21	S21
eS24	A E	–	S24	S24
eS25	A E	–	S25	S25
eS26	E	–	S26	S26
eS27	A E	–	S27	S27
eS28	A E	–	S28	S28
eS30	A E	–	S30	S30
eS31	A E	–	S31	S27A
RACK1	E	–	Asc1	RACK1

[#] b: bacterial, e: eukaryotic, u: universal.
[*] B: bacteria, A: archaea, E: eukaryotes.

Table 2

Nomenclature for proteins from the large ribosomal subunit.

New name[#]	Taxonomic range[*]	Bacteria name	Yeast name	Human name
uL1	B A E	L1	L1	L10A
uL2	B A E	L2	L2	L8
uL3	B A E	L3	L3	L3
uL4	B A E	L4	L4	L4
uL5	B A E	L5	L11	L11
uL6	B A E	L6	L9	L9
eL6	E	–	L6	L6
eL8	A E	–	L8	L7A
bL9	B	L9	–	–
uL10	B A E	L10	P0	P0
uL11	B A E	L11	L12	L12
bL12	B	L7/L12	–	–
uL13	B A E	L13	L16	L13A
eL13	A E	–	L13	L13
uL14	B A E	L14	L23	L23
eL14	A E	–	L14	L14
uL15	B A E	L15	L28	L27A
eL15	A E	–	L15	L15
uL16	B A E	L16	L10	L10
bL17	B	L17	–	–
uL18	B A E	L18	L5	L5
eL18	A E	–	L18	L18
bL19	B	L19	–	–
eL19	A E	–	L19	L19
bL20	B	L20	–	–
eL20	E	–	L20	L18A
bL21	B	L21	–	–
eL21	A E	–	L21	L21
uL22	B A E	L22	L17	L17
eL22	E	–	L22	L22
uL23	B A E	L23	L25	L23A
uL24	B A E	L24	L26	L26
eL24	A E	–	L24	L24
bL25	B	L25	–	–
bL27	B	L27	–	–
eL27	E	–	L27	L27
bL28	B	L28	–	–
eL28	E	–	–	L28
uL29	B A E	L29	L35	L35
eL29	E	–	L29	L29
uL30	B A E	L30	L7	L7
eL30	A E	–	L30	L30
bL31	B	L31	–	–
eL31	A E	–	L31	L31
bL32	B	L32	–	–
eL32	A E	–	L32	L32
bL33	B	L33	–	–
eL33	A E	–	L33	L35A
bL34	B	L34	–	–
eL34	A E	–	L34	L34
bL35	B	L35	–	–
bL36	B	L36	–	–
eL36	E	–	L36	L36
eL37	A E	–	L37	L37
eL38	A E	–	L38	L38
eL39	A E	–	L39	L39
eL40	A E	–	L40	L40
eL41	A E	–	L41	L41
eL42	A E	–	L42	L36A
eL43	A E	–	L43	L37A
P1/P2	A E	–	P1/P2 (AB)	P1/P2 ($\alpha\beta$)

[#] b: bacterial, e: eukaryotic, u: universal.
[*] B: bacteria, A: archaea, E: eukaryotes.

Structure of the Mammalian Ribosome-Sec61 Complex to 3.4 Å Resolution

Rebecca M. Voorhees,[1,2,*] Israel S. Fernández,[1,2] Sjors H.W. Scheres,[1] and Ramanujan S. Hegde[1,*]
[1]MRC Laboratory of Molecular Biology, Francis Crick Avenue, Cambridge, CB2 0QH, UK
[2]Co-first authors
*Correspondence: voorhees@mrc-lmb.cam.ac.uk (R.M.V.), rhegde@mrc-lmb.cam.ac.uk (R.S.H.)
http://dx.doi.org/10.1016/j.cell.2014.05.024

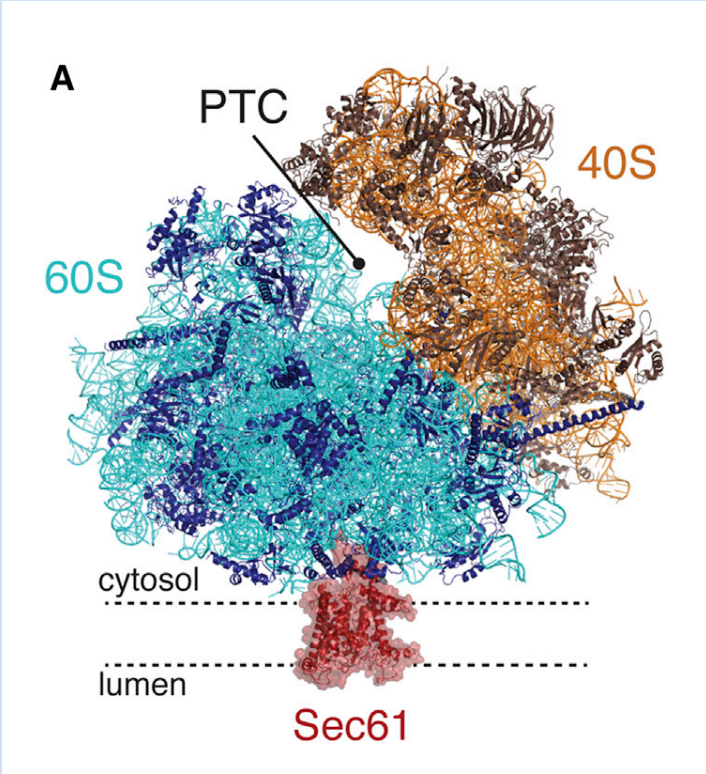

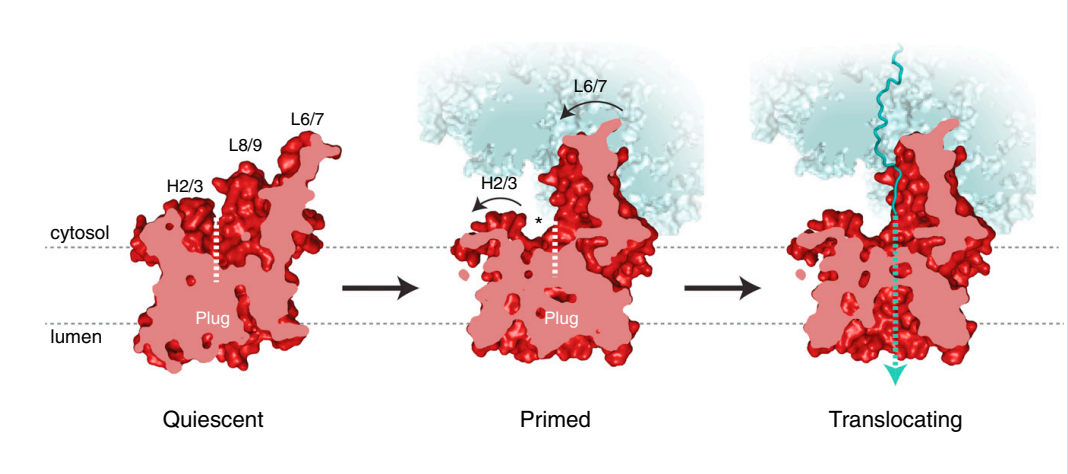

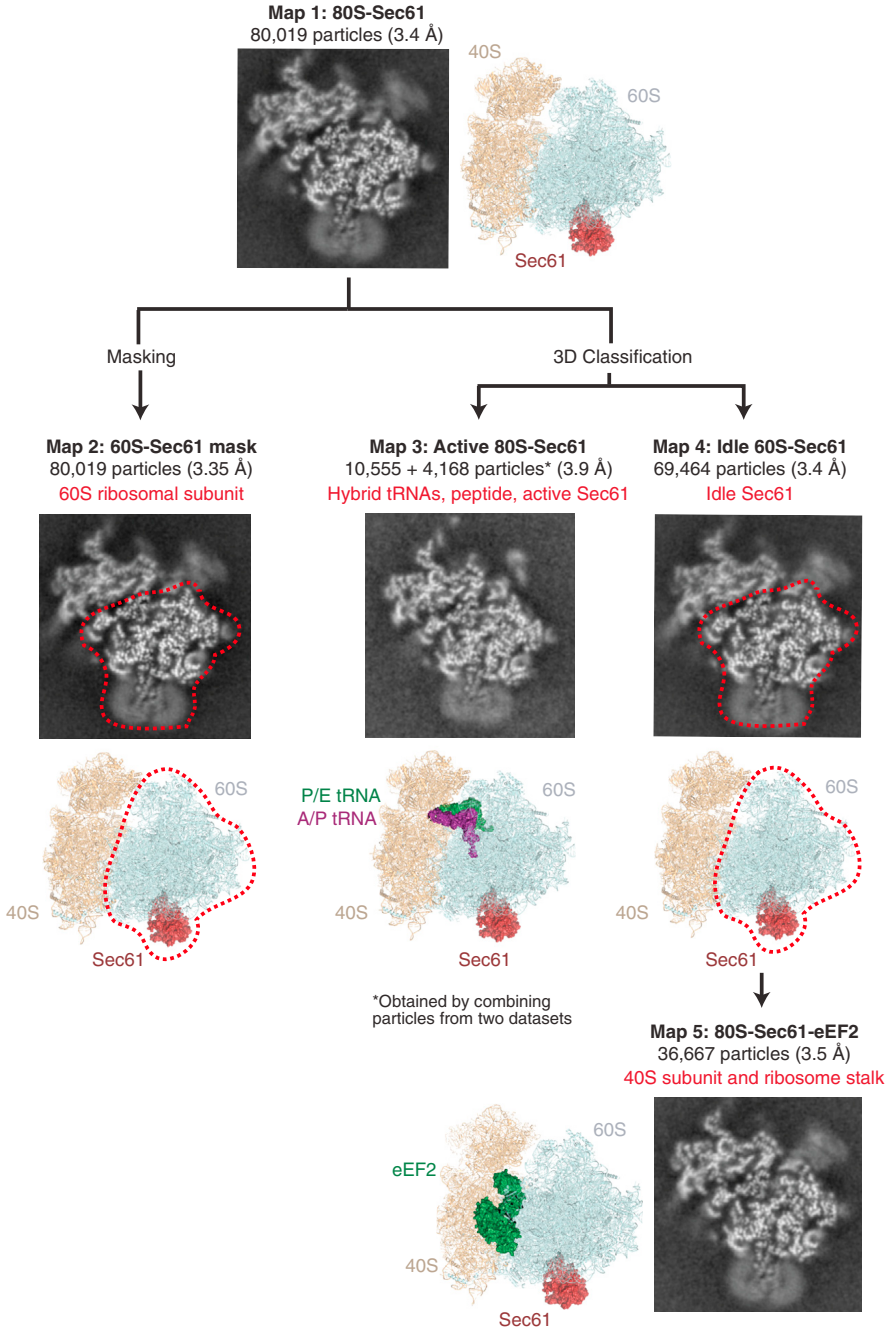
Map 1: 80S-Sec61
80,019 particles (3.4 Å)
40S
60S
Sec61
Masking
3D Classification
Map 2: 60S-Sec61 mask
80,019 particles (3.35 Å)
60S ribosomal subunit
Map 3: Active 80S-Sec61
10,555 + 4,168 particles* (3.9 Å)
Hybrid tRNAs, peptide, active Sec61
Map 4: Idle 60S-Sec61
69,464 particles (3.4 Å)
Idle Sec61
60S
40S
Sec61
P/E tRNA
A/P tRNA
60S
40S
Sec61
60S
40S
Sec61
*Obtained by combining particles from two datasets
Map 5: 80S-Sec61-eEF2
36,667 particles (3.5 Å)
40S subunit and ribosome stalk
eEF2
60S
40S
Sec61

Figure S2. Refinement and 3D Classification Strategy, Related to Experimental Procedures

Each class in the displayed flowchart shows a cross section image of the respective map, the derived model, any mask that was applied (red dashed line), and the structure (s) derived from that class (red text). The complete data set containing 80,019 particles was refined using RELION (Scheres, 2012a, 2012b), resulting in an initial reconstruction calculated to 3.4 Å resolution (Map 1). As the 40S subunit was in a variety of distinct conformations, a soft mask for the 60S subunit was used throughout the refinement procedure (Map 2). Although this only resulted in a modest nominal increase in resolution (3.35 Å), the observed density for the 60S subunit was improved compared to the complete refinement, and was used to build the 60S ribosomal proteins and RNA. In parallel, 3D classification of the entire data set identified 13% of particles containing hybrid A/P- and P/E-site tRNAs and a nascent peptide. In order to supplement this relatively small class, an additional data set was collected, resulting in a combined14,723 particles used to build the translating ribosome-Sec61 complex to 3.9 Å resolution (Map 3). The remaining 87% of particles (69,464) were used to model the idle ribosome-Sec61 complex, lacking a nascent chain and tRNAs, to 3.4 Å resolution (Map 4). Within this idle class, 36,667 particles containing eEF2, which stabilized both the stalk base proteins and the orientation of the 40S subunit relative to the 60S (Map 5). This class of particles was used to build a model for the 40S ribosomal proteins and RNA at 3.5 Å resolution. The remaining idle particles either contained eEF2 bound in different ratcheted conformations (19%) or were devoid of tRNAs or factors (22%). All reported resolutions are determined using the gold-standard Fourier Shell Correlation (FSC = 0.143) criterion (Scheres and Chen, 2012), and are shown in Figure S3.

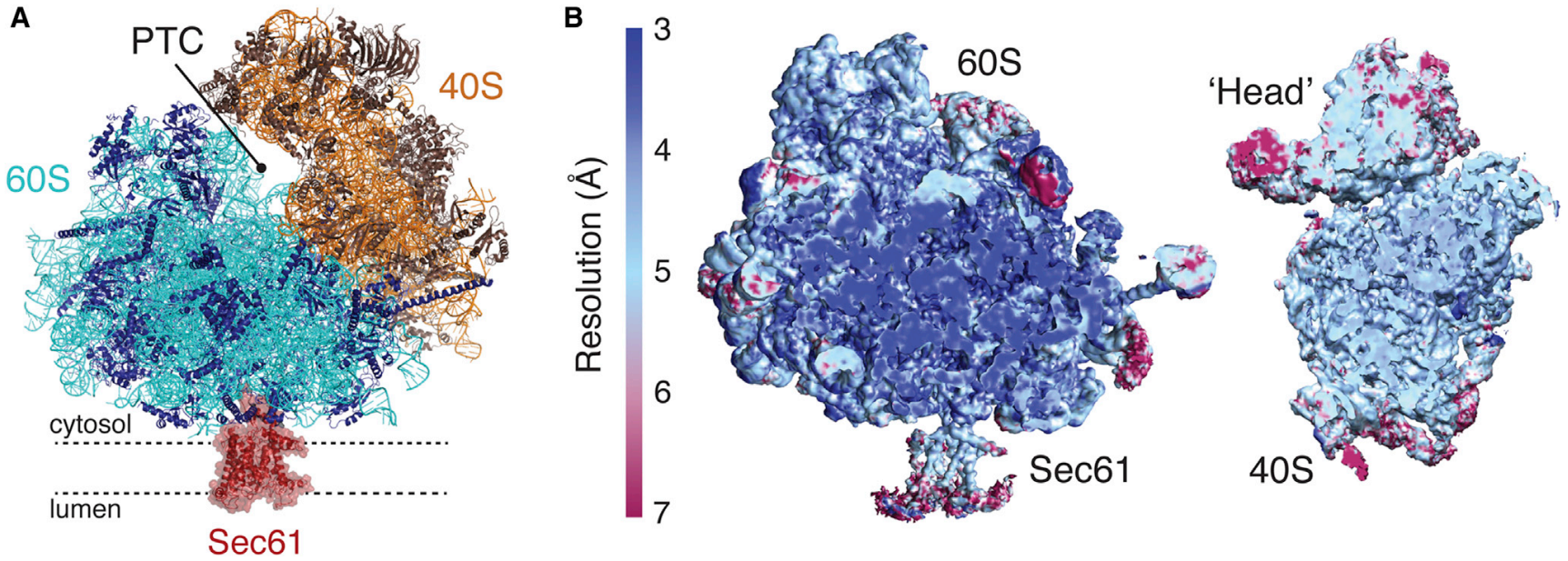

Figure 1. The Structure of a Mammalian Ribosome-Translocon Complex

(A) Model of the idle 80S ribosome in complex with Sec61, shown in red. The color scheme shown here is used throughout the manuscript: 40S rRNA is displayed in orange, the 40S ribosomal proteins in brown, the 60S rRNA in cyan, and the 60S ribosomal proteins in dark blue. The region of the peptidyl transferase center (PTC) is indicated.

(B) Cut view of the final unsharpened cryo-EM density map for both the idle 60S-Sec61 complex and the 40S subunit, colored by local resolution in Å (Kucukelbir et al., 2014). Also see Figure S3.

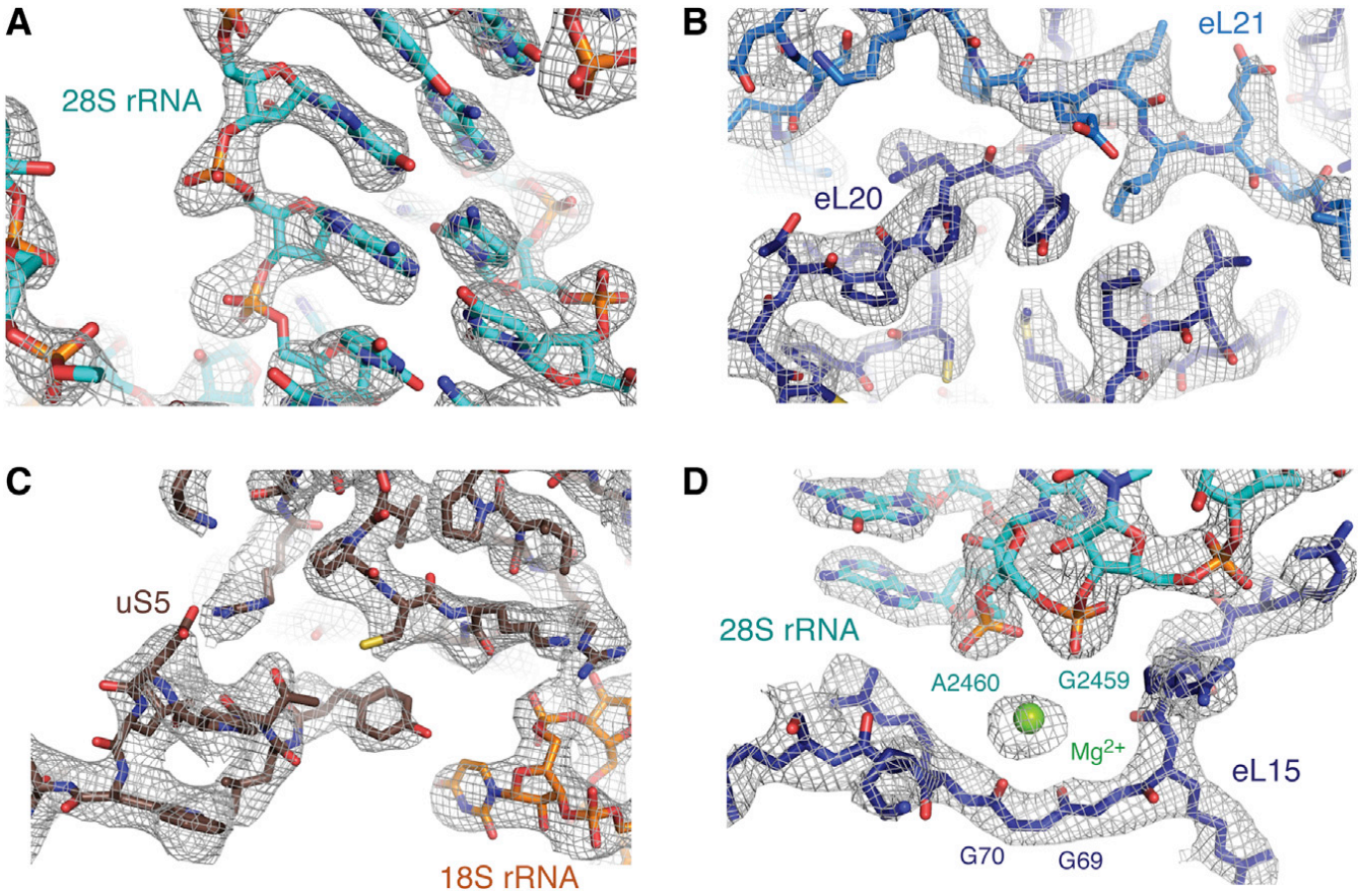

Figure 2. Representative Density for the Ribosomal Proteins and rRNA

(A–D) Cryo-EM density for the 60S subunit and the body of the 40S was sufficient to allow unambiguous placement of rRNA bases (A, C, D) amino acid side chains (B, C, D), and many ions (D). Also see Figure S4.

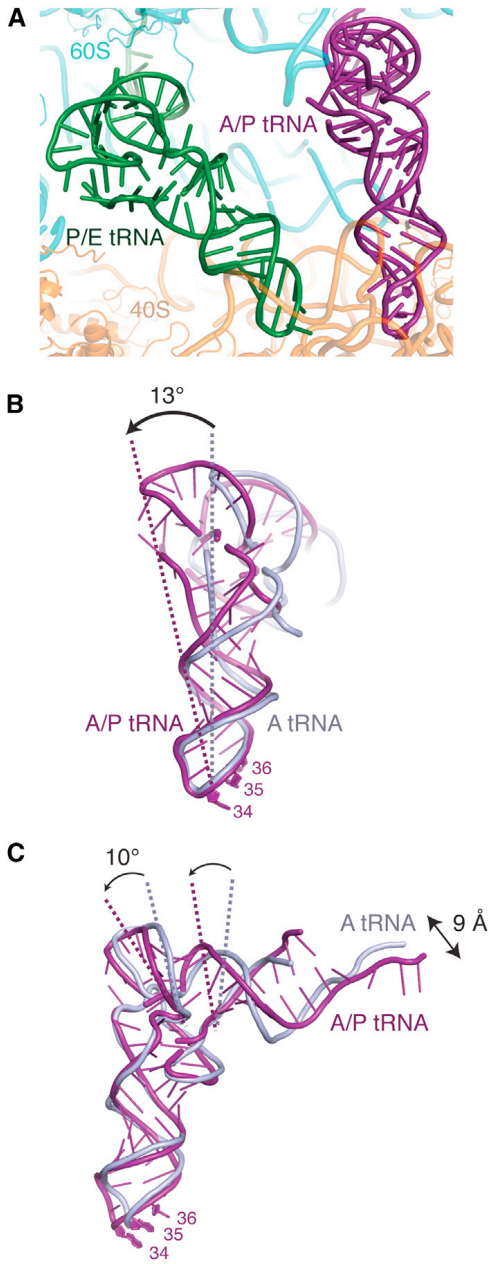

Figure 3. An A/P Hybrid State tRNA

(A) Overview of the hybrid A/P (purple) and P/E tRNAs (green) visualized in the translating ribosome-Sec61 structure.

(B and C) Adoption of the hybrid A/P conformation (purple) relative to the canonical A-site tRNA (gray) requires a ~13° rotation in the backbone of the tRNA just above the anticodon stem loop, as well as a 10° rotation in the acceptor/T-stem stack and a 9 Å displacement of the 3′ tail.

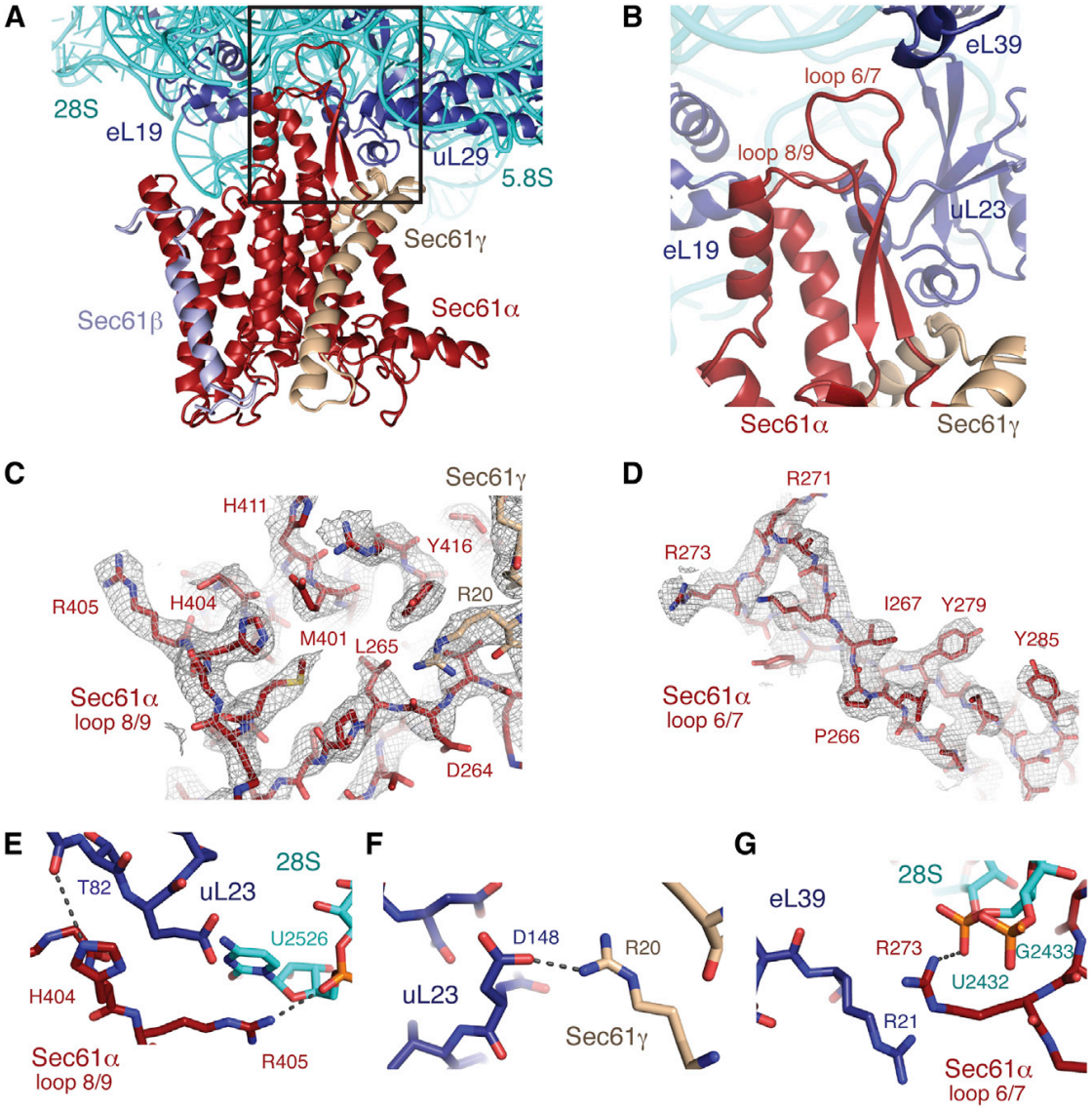

Figure 4. Interaction of Sec61 with the Ribosome

(A) Overview of the region of the ribosome surrounding the Sec61 complex, including the cytosolic loops 6/7 and 8/9. Sec61α is displayed in red, γ in tan, and β in light blue.

(B) Close-up of the cytosolic loops of Sec61 and the surrounding ribosomal proteins and RNA.

(C and D) Representative density for the cytosolic loops of Sec61α, regions of Sec61γ, and their corresponding helices.

(E) Hydrogen bonding interactions between residues H404 and R405 in loop 8/9 of Sec61α and ribosomal protein uL23 and the 28S rRNA.

(F) Visualization of a salt bridge between R20 in the N-terminal helix of Sec61γ and D148 in υΛ23.

(G) An arginine stack between residue R273 in loop 6/7 and R21 in eL39 is stabilized by interaction with the backbone of the 28S rRNA.

See also Figure S5.

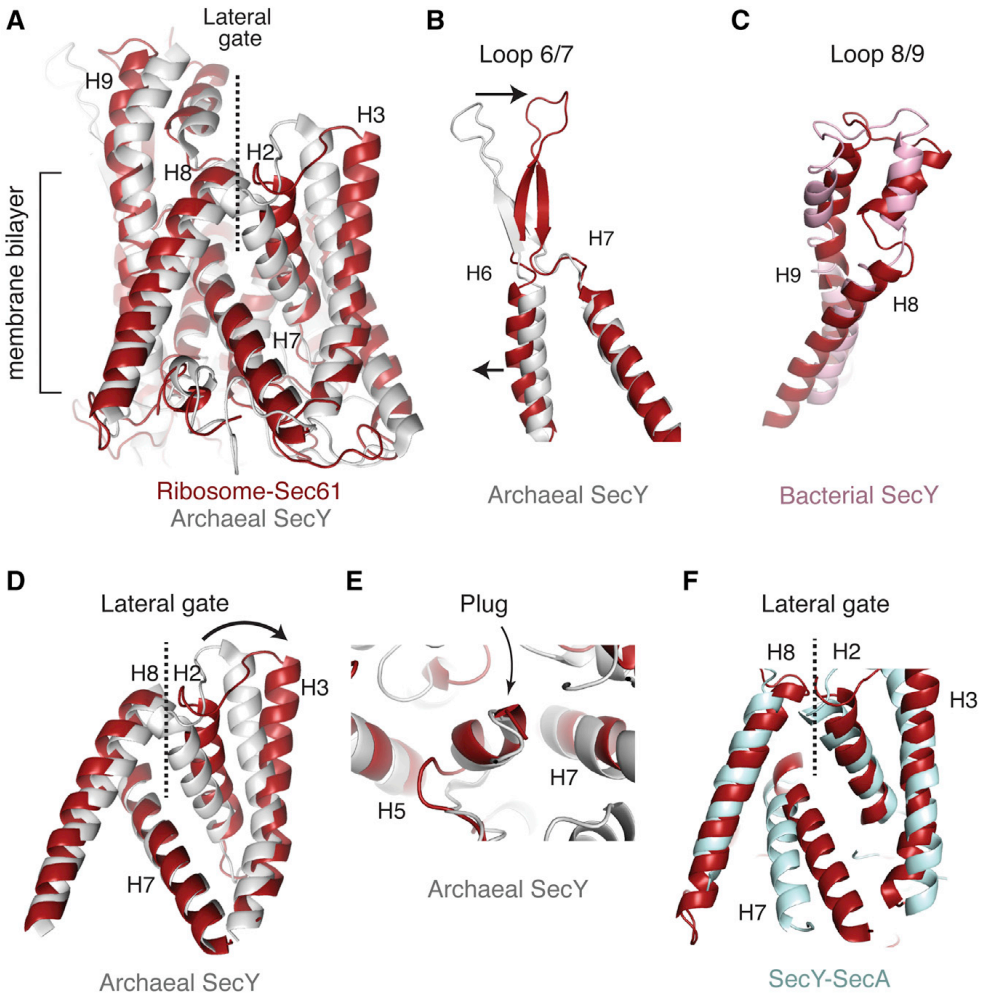

Figure 5. Conformation of Ribosome-Bound Sec61α

(A) Overview of the lateral gate of the ribosome-bound Sec61α in red, compared to the isolated crystal structure of the archaeal SecY in gray (Park et al., 2014).

(B) Cytosolic loop 6/7 shifts by 11 Å relative to the the archaeal SecY structure.

(C) Cytosolic loop 8/9 shifts by 6 Å relative to the bacterial SecY structure shown in pink (Tsukazaki et al., 2008). The bacterial structure is used for comparison here because loop 8/9 is disordered in the archaeal structure.

(D) Close-up of the lateral gate (helices 2 and 3 with helices 7 and 8), highlighting the opening of the cytosolic region between helices 8 and 2 in the ribosome-bound state.

(E) Close-up of the plug region, which is unaltered in the ribosome-bound state.

(F) Comparison of the lateral gate in the Sec61-ribosome structure relative to that observed in the SecY-SecA complex (light blue; Zimmer et al., 2008).

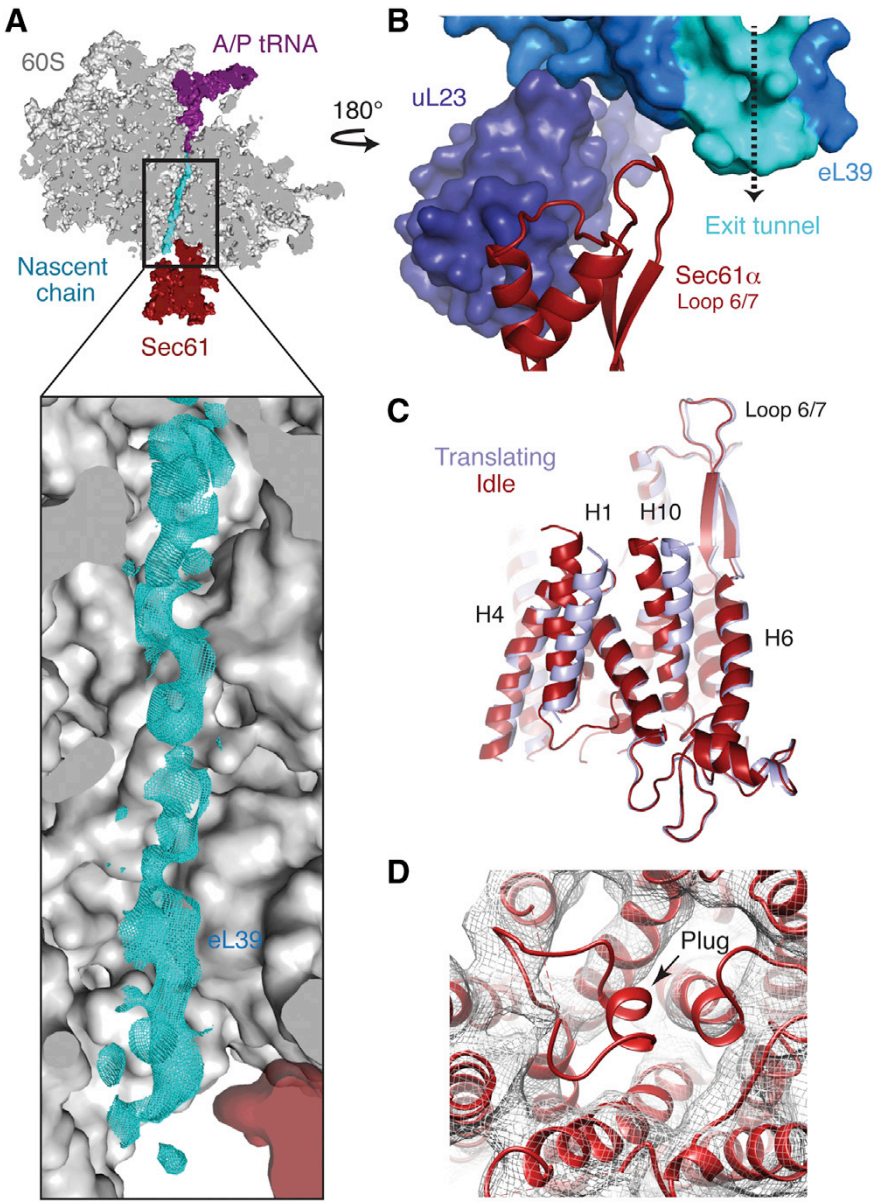

Figure 6. The Translating Ribosome-Sec61 Complex

(A) Cryo-EM density within the ribosomal exit tunnel for the nascent peptide (cyan), which spans from the A/P tRNA to Sec61. The location of ribosomal protein eL39, which lines the exit tunnel, is indicated.

(B) Ribosomal protein eL39 (bright blue) forms part of the exit tunnel (highlighted in cyan) and interacts with loop 6/7 of Sec61. Ribosomal protein uL23 (dark blue) contacts both eL39 and loop 8/9 of Sec61.

(C) Comparison of the Sec61 channel structures bound to idle or translating ribosome, showing movements in helices 1 and 10, which may be important for allowing translocation of the nascent polypeptide. Also see Figure S6.

(D) Rigid-body fitting of the idle Sec61 model (red) into the density for the translating Sec61-ribosome complex demonstrates that the plug is not visible in its canonical location. Displayed is an unsharpened map in which the disordered density for the detergent micelle has been removed using Chimera (Goddard et al., 2007).

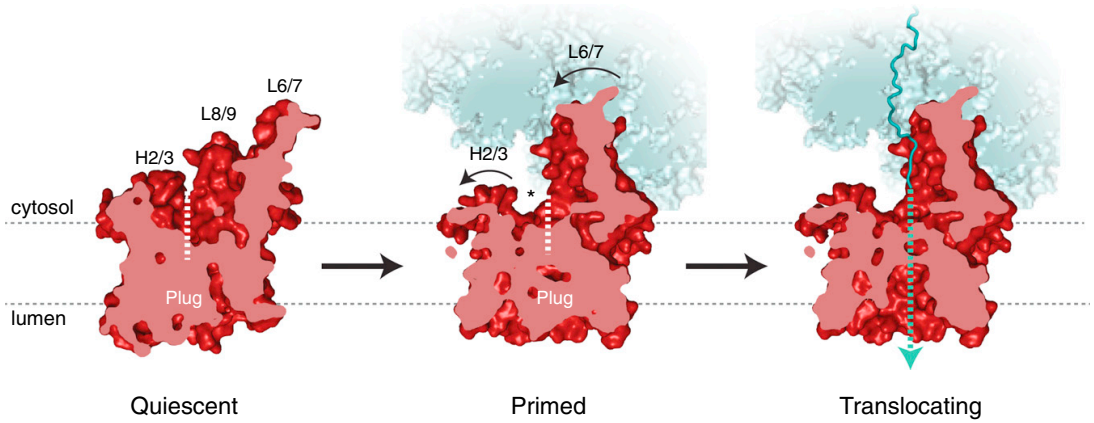

Figure 7. A Two-Step Model for Activation of Sec61

Displayed here is a cut-away view of the model for the Sec channel from the central pore toward the lateral gate (dashed line). In the quiescent state (left), approximated by a crystal structure of the archaeal SecY complex (Van den Berg et al., 2004), the Sec channel is closed to both the lumen and lipid bilayer. The channel becomes primed for protein translocation upon ribosome binding (middle), triggering conformational changes in Sec61 that crack the cytosolic side of the lateral gate (demarcated by an asterisk). The movements of helices 2 and 3 in this region may create an initial binding site for signal peptide recognition. Engagement of the lateral gate by the signal peptide would open the channel toward the membrane and initiate translocation (not depicted; Park et al., 2014). The translocating state of the active ribosome-Sec61 complex (right) contains a nascent polypeptide (teal) and is characterized by a dynamic plug domain and an open conduit between the cytosol and lumen (teal dotted line).

The Structure and Function of the Eukaryotic Ribosome

Daniel N. Wilson[1,2] and Jamie H. Doudna Cate[3,4]

[1]Center for Integrated Protein Science Munich (CiPSM), 81377 Munich, Germany

[2]Gene Center and Department of Biochemistry, Ludwig-Maximilians-Universität München, 81377 Munich, Germany

[3]Departments of Molecular and Cell Biology and Chemistry, University of California at Berkeley, Berkeley, California 94720

[4]Physical Biosciences Division, Lawrence Berkeley National Laboratory, Berkeley, California 94720

Correspondence: wilson@lmb.uni-muenchen.de and jcate@lbl.gov

Cite this article as *Cold Spring Harb Perspect Biol* 2012;4:a011536

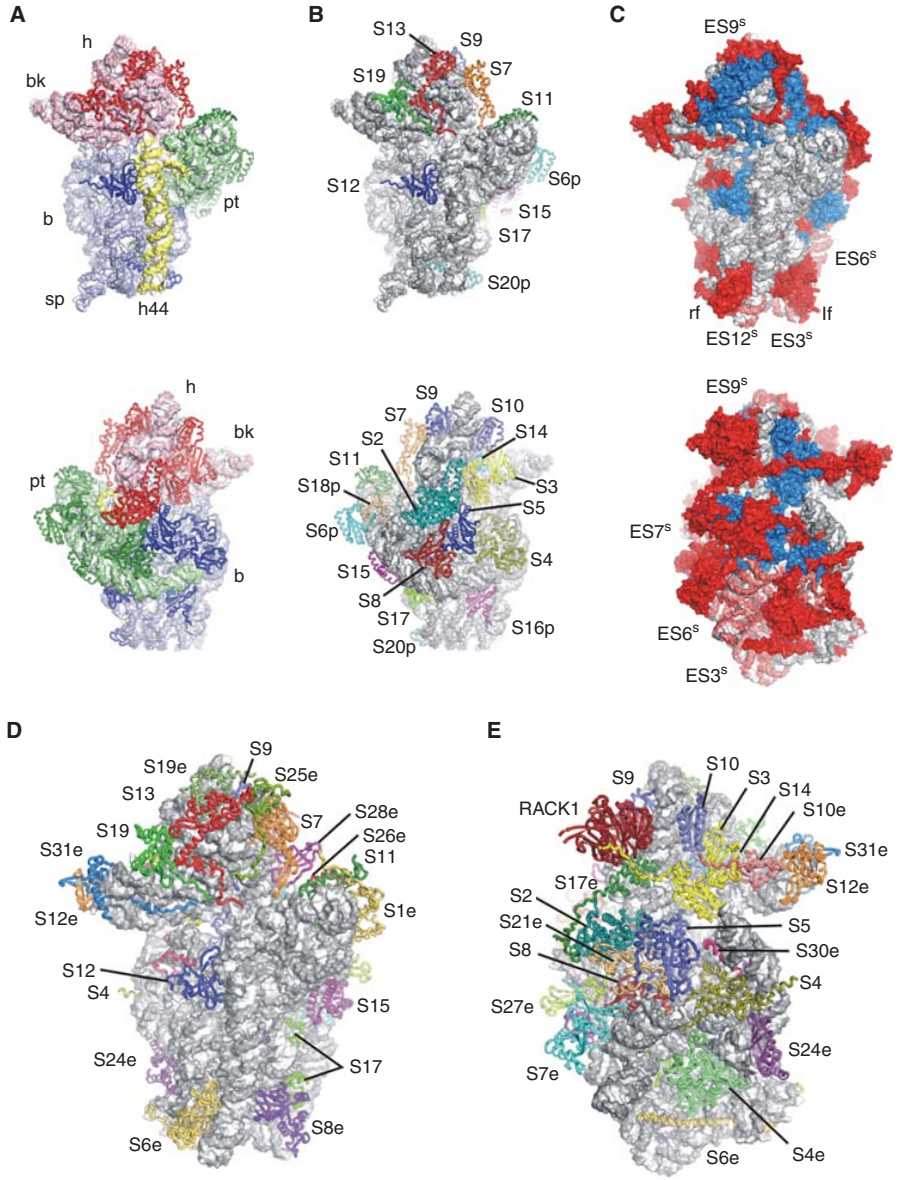

Figure 1. The bacterial and eukaryotic small ribosomal subunit. (*A,B*) Interface (*upper*) and solvent (*lower*) views of the bacterial 30S subunit (Jenner et al. 2010a). (*A*) 16S rRNA domains and associated r-proteins colored distinctly: b, body (blue); h, head (red); pt, platform (green); and h44, helix 44 (yellow). (*B*) 16S rRNA colored gray and r-proteins colored distinctly and labeled. (*C–E*) Interface and solvent views of the eukaryotic 40S subunit (Rabl et al. 2011), with (*C*) eukaryotic-specific r-proteins (red) and rRNA (pink) shown relative to conserved rRNA (gray) and r-proteins (blue), and with (*D,E*) 18S rRNA colored gray and r-proteins colored distinctly and labeled.

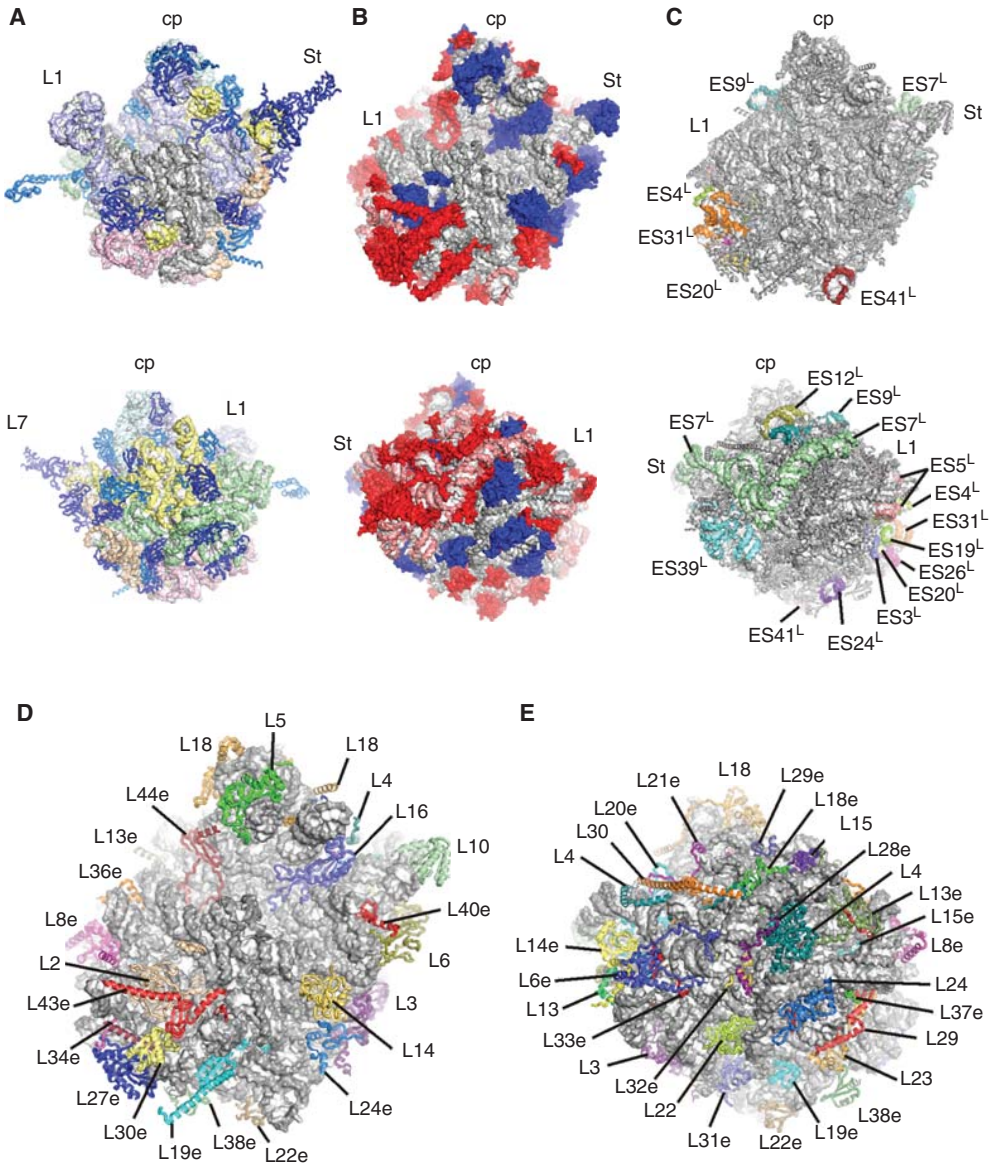

Figure 2. The bacterial and eukaryotic large ribosomal subunit. (*A*) Interface (*upper*) and solvent (*lower*) views of the bacterial 50S subunit (Jenner et al. 2010b), with 23S rRNA domains and bacterial-specific (light blue) and conserved (blue) r-proteins colored distinctly: cp, central protuberance; L1, L1 stalk; and St, L7/L12 stalk (or P-stalk in archeaa/eukaryotes). (*B–E*) Interface and solvent views of the eukaryotic 60S subunit (Klinge et al. 2011), with (*B*) eukaryotic-specific r-proteins (red) and rRNA (pink) shown relative to conserved rRNA (gray) and r-proteins (blue), (*C*) eukaryotic-specific expansion segments (ES) colored distinctly, and (*D*,*E*) 28S rRNA colored gray and r-proteins colored distinctly and labeled.

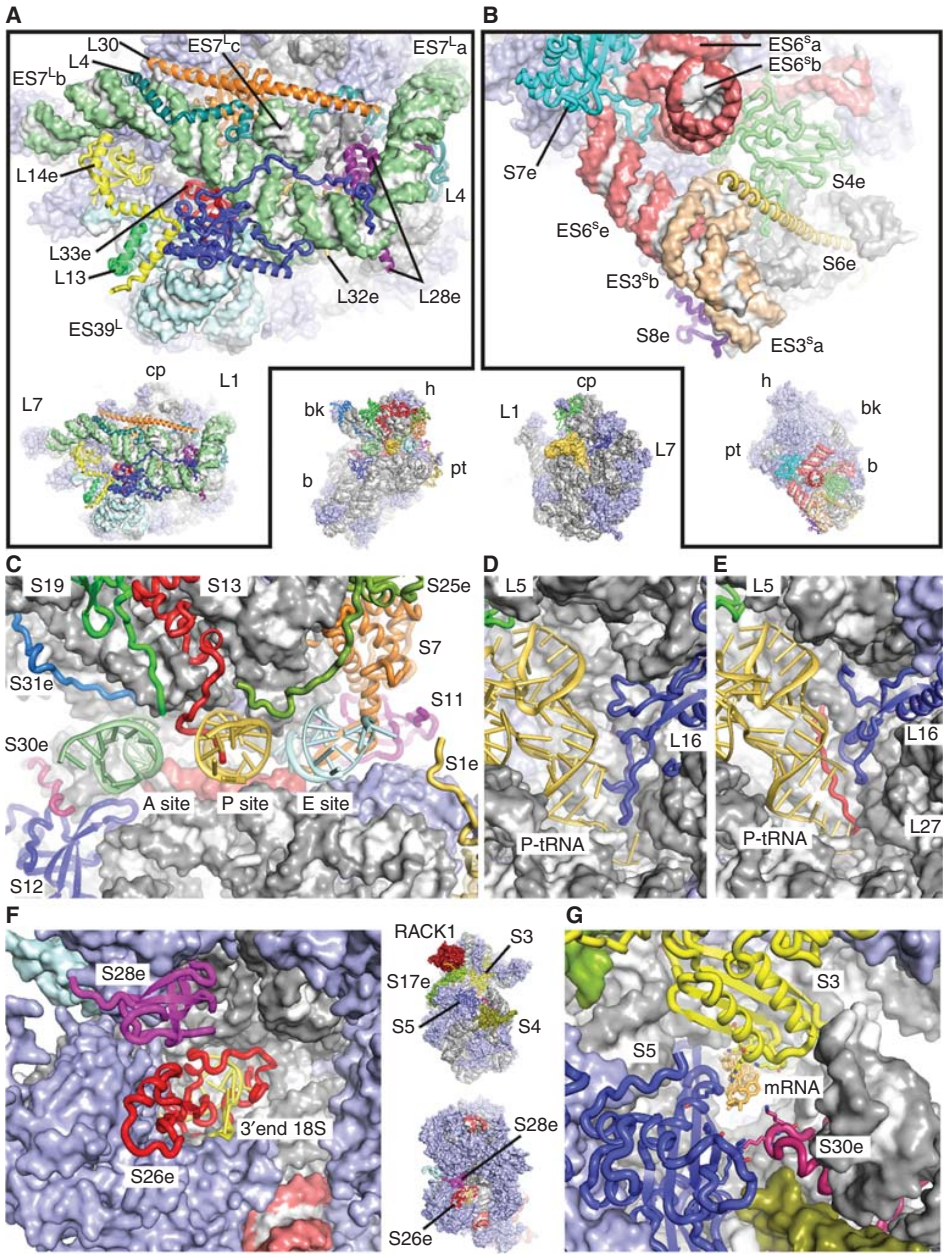

Figure 3. Structural and functional aspects of the eukaryotic ribosome. Interweaving of rRNA and r-proteins on the (*A*) LSU near ES7^{L} and ES39^{L} (Klinge et al. 2011), and (*B*) SSU near ES3 and ES6 (Rabl et al. 2011). Extension of r-proteins at the tRNA-binding sites on the (*C*) SSU (Armache et al. 2010b; Rabl et al. 2011), LSU of the (*D*) bacterial (Jenner et al. 2010b), and (*E*) eukaryotic (Armache et al. 2010b) peptidyltransferase centers. R-proteins located at the mRNA (*F*) exit, and (*G*) entry sites (Klinge et al. 2011).

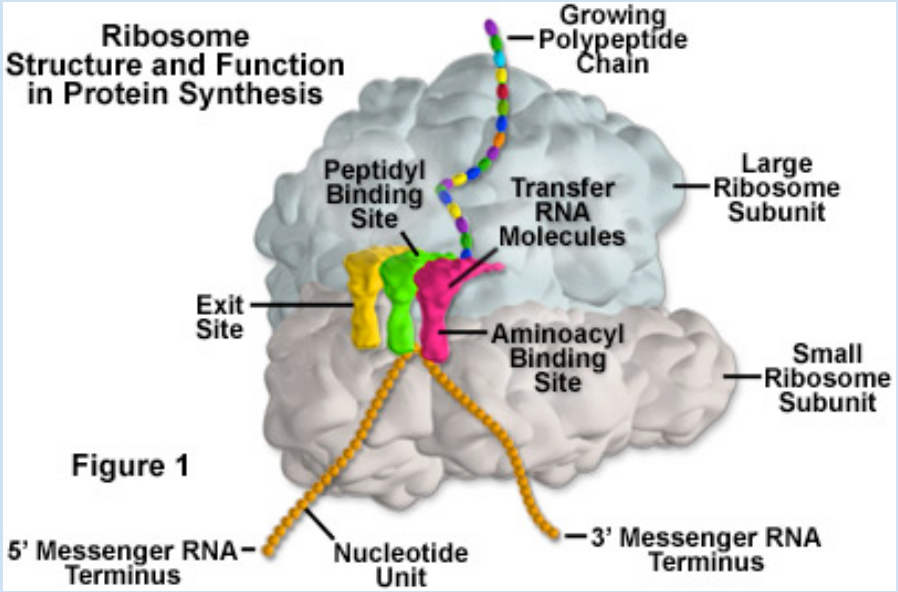

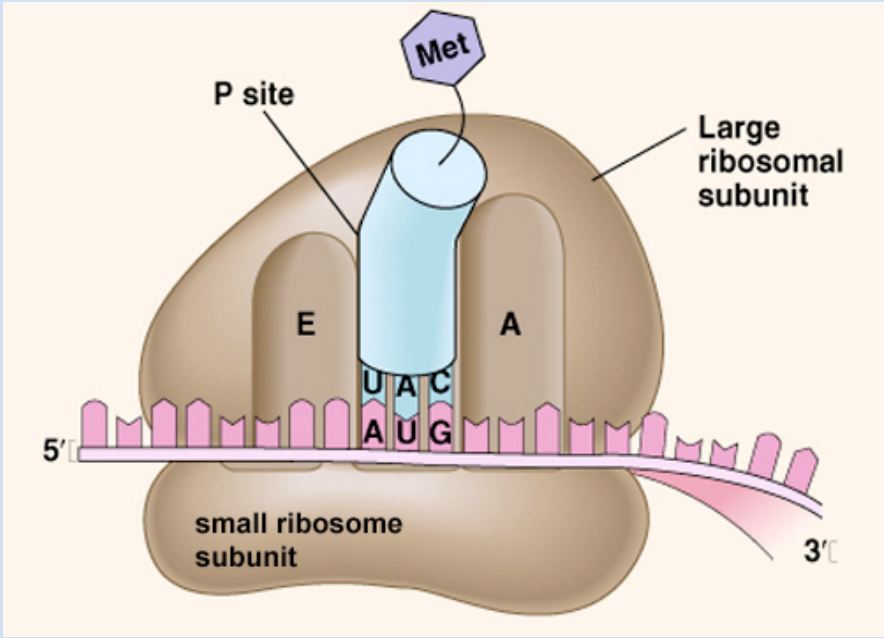

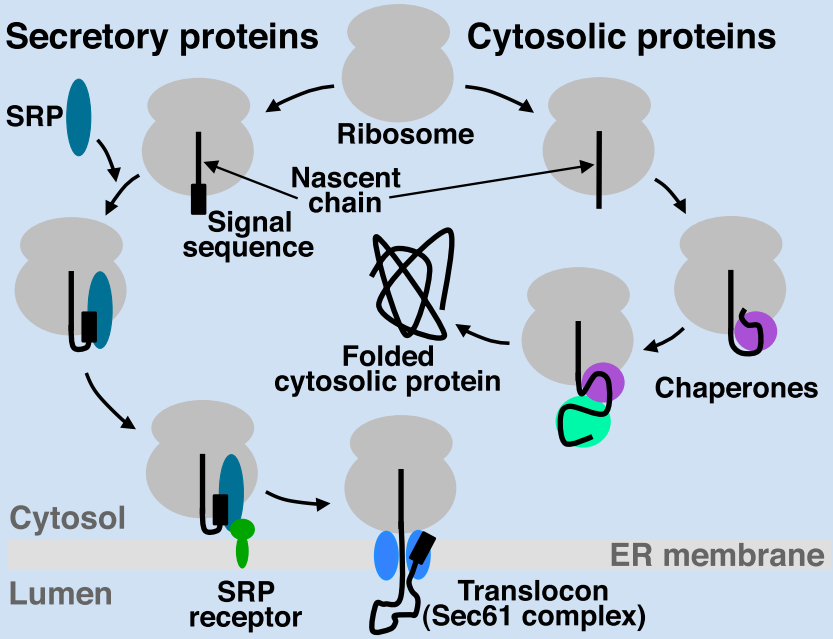

Inefficient SRP Interaction with a Nascent Chain Triggers a mRNA Quality Control Pathway

Andrey L. Karamyshev,[1,*] Anna E. Patrick,[1,9] Zemfira N. Karamysheva,[1] Dustin S. Griesemer,[1,10] Henry Hudson,[1] Sandra Tjon-Kon-Sang,[1] IngMarie Nilsson,[3] Hendrik Otto,[5] Qinghua Liu,[2] Sabine Rospert,[5] Gunnar von Heijne,[3,4] Arthur E. Johnson,[6,7,8] and Philip J. Thomas[1,*]

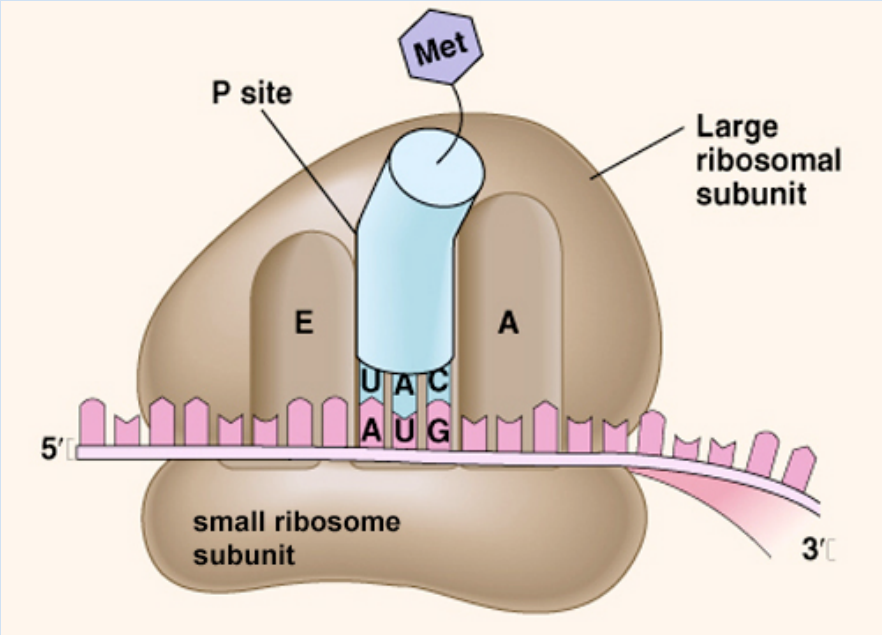
Met
P site
Large ribosomal subunit
E
A
U A C
A U G
5′
3′
small ribosome subunit

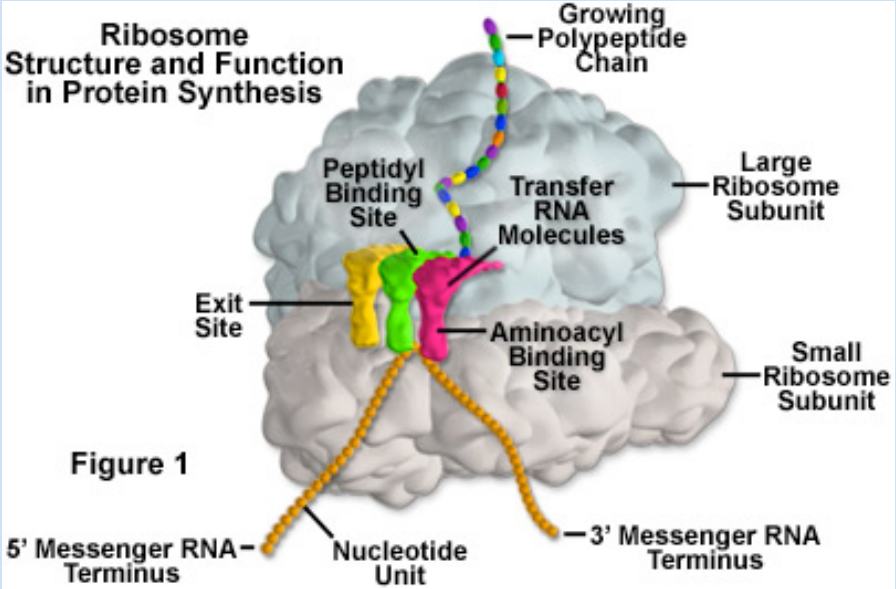
Ribosome Structure and Function in Protein Synthesis
Growing Polypeptide Chain
Peptidyl Binding Site
Transfer RNA Molecules
Large Ribosome Subunit
Exit Site
Aminoacyl Binding Site
Small Ribosome Subunit
Figure 1
5' Messenger RNA Terminus
Nucleotide Unit
3' Messenger RNA Terminus

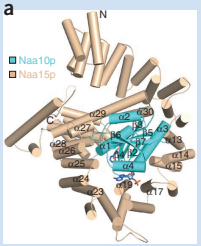
a
N
Naa10p
Naa15p
C

NAA10 + NAA15

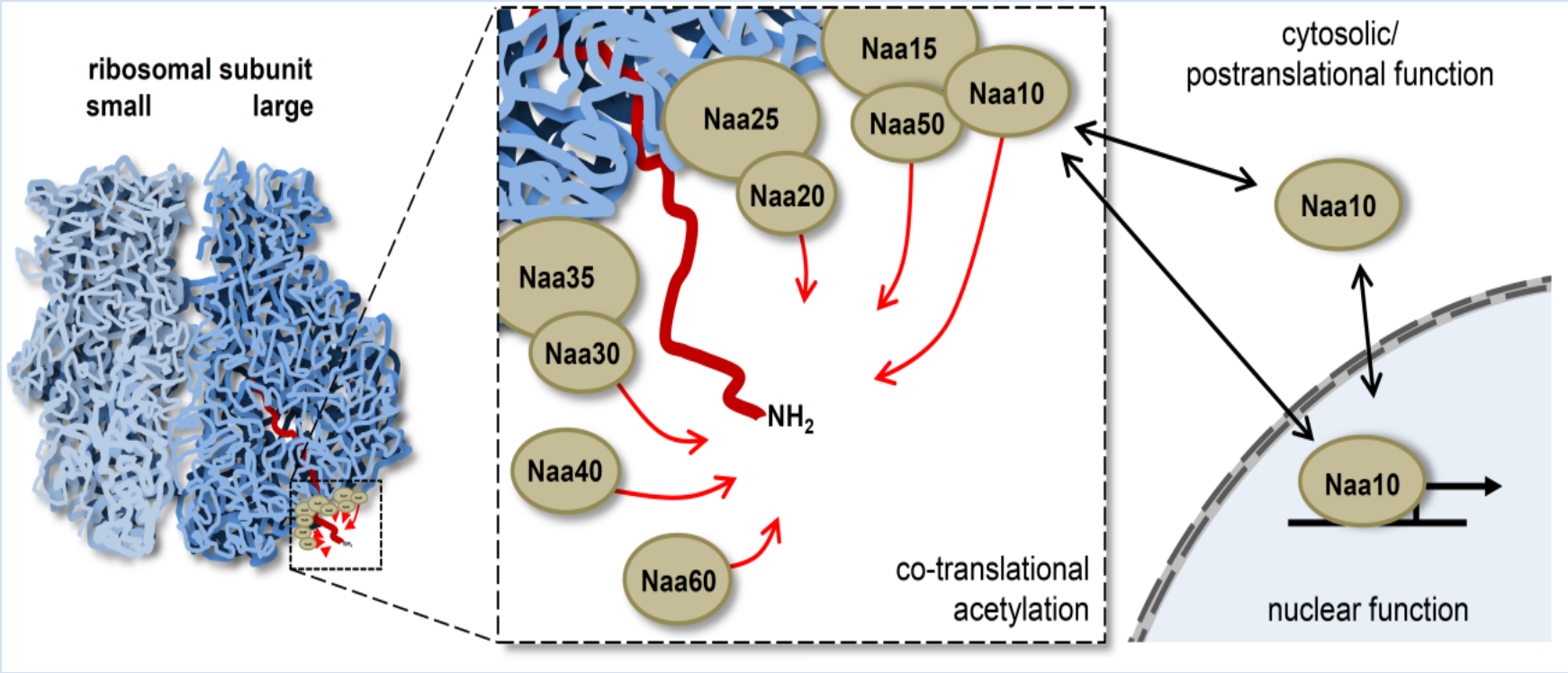

- Naa10 co-translationally acetylates the N^{α}-terminal amino group of the nascent polypeptide chains of classical substrates as they emerge from the ribosome.

CHEMBIOCHEM

DOI: 10.1002/cbic.201000558

Chemical Approaches for the Detection and Synthesis of Acetylated Proteins

Yu-Ying Yang and Howard C. Hang*[a]

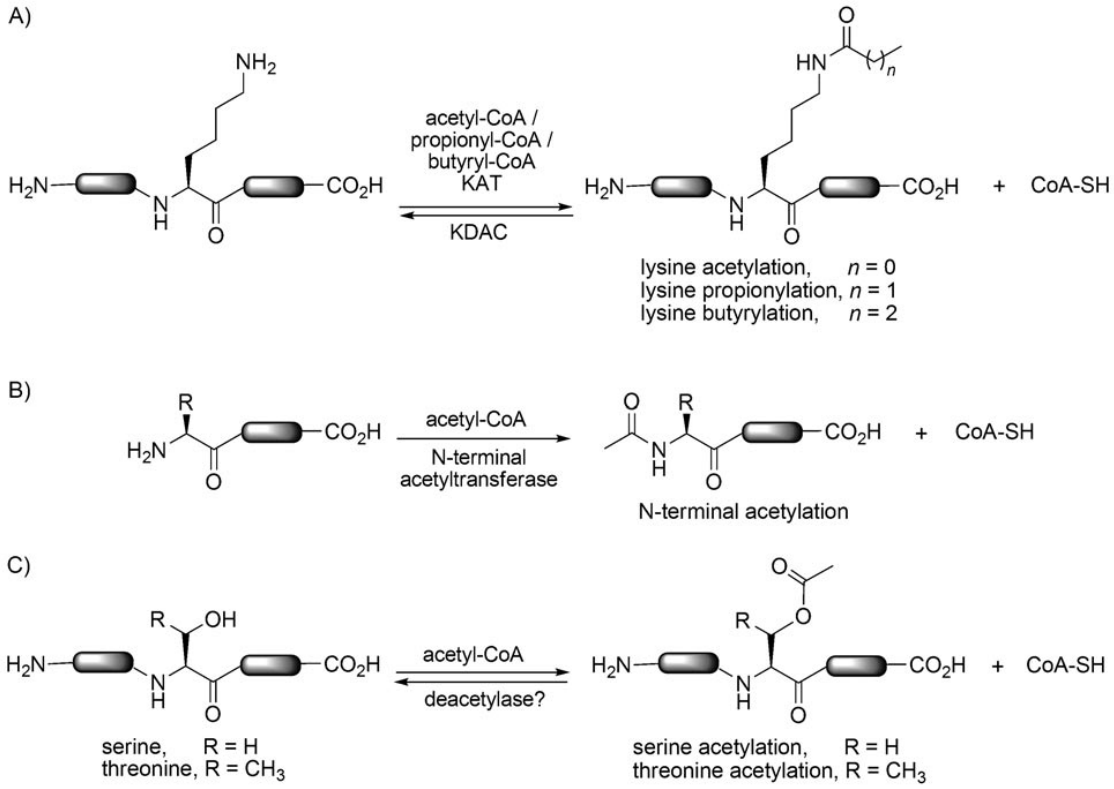

Scheme 1. Different classes of protein acetylation. A) Lysine acetylation is a reversible PTM that is tightly regulated by KATs and KDACs. Propionylation and butyrylation have also been described on lysine residues. B) N-terminal acetylation is regulated by N-acetyltransferases. C) Serine and threonine acetylation are executed by secreted bacterial effector proteins during infection of eukaryotic cells.

NatA (Naa10/Naa15)

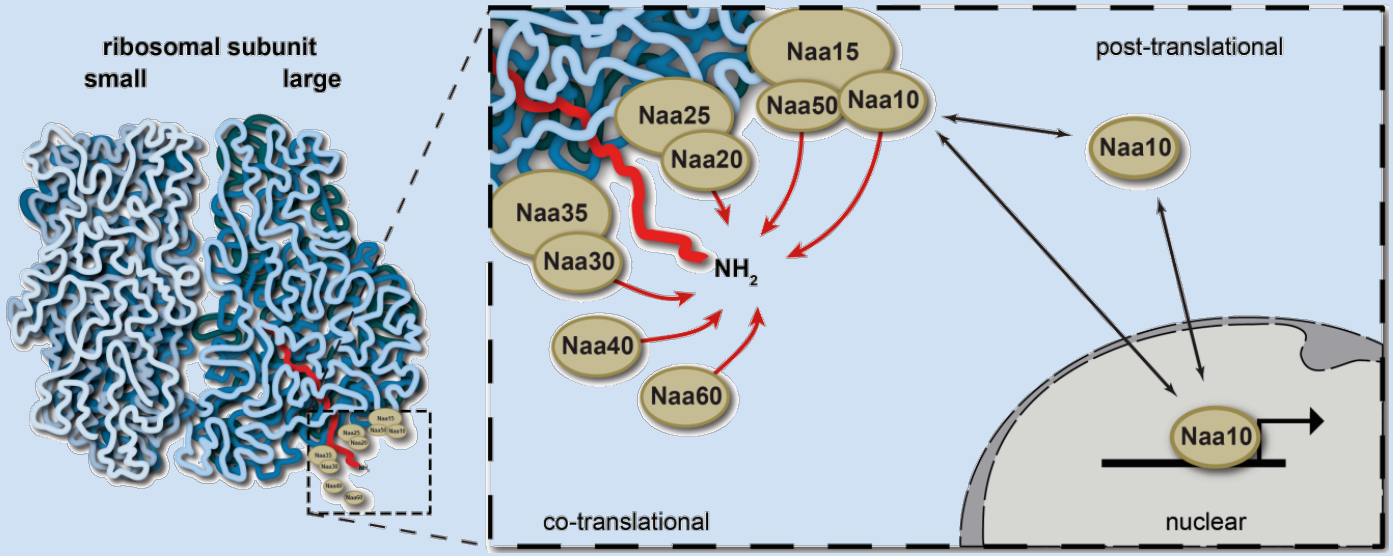

NatA consists of

- Naa15 (auxiliary subunit;100 kDa)
- Naa10 (catalytical subunit; 26 kDa)
- Naa50 (catalytical subunit NatE)
- HYPK
- others?

NatA function

- generation and differentiation of neurons
- β-Catenin transcriptional activity
- cyclin D1 regulation
- NF- κB /DNA-damage response pathways
- cellular hypoxia
- apoptosis & cancer

NAA10 + NAA15
And MAPs and SRP and chaperones

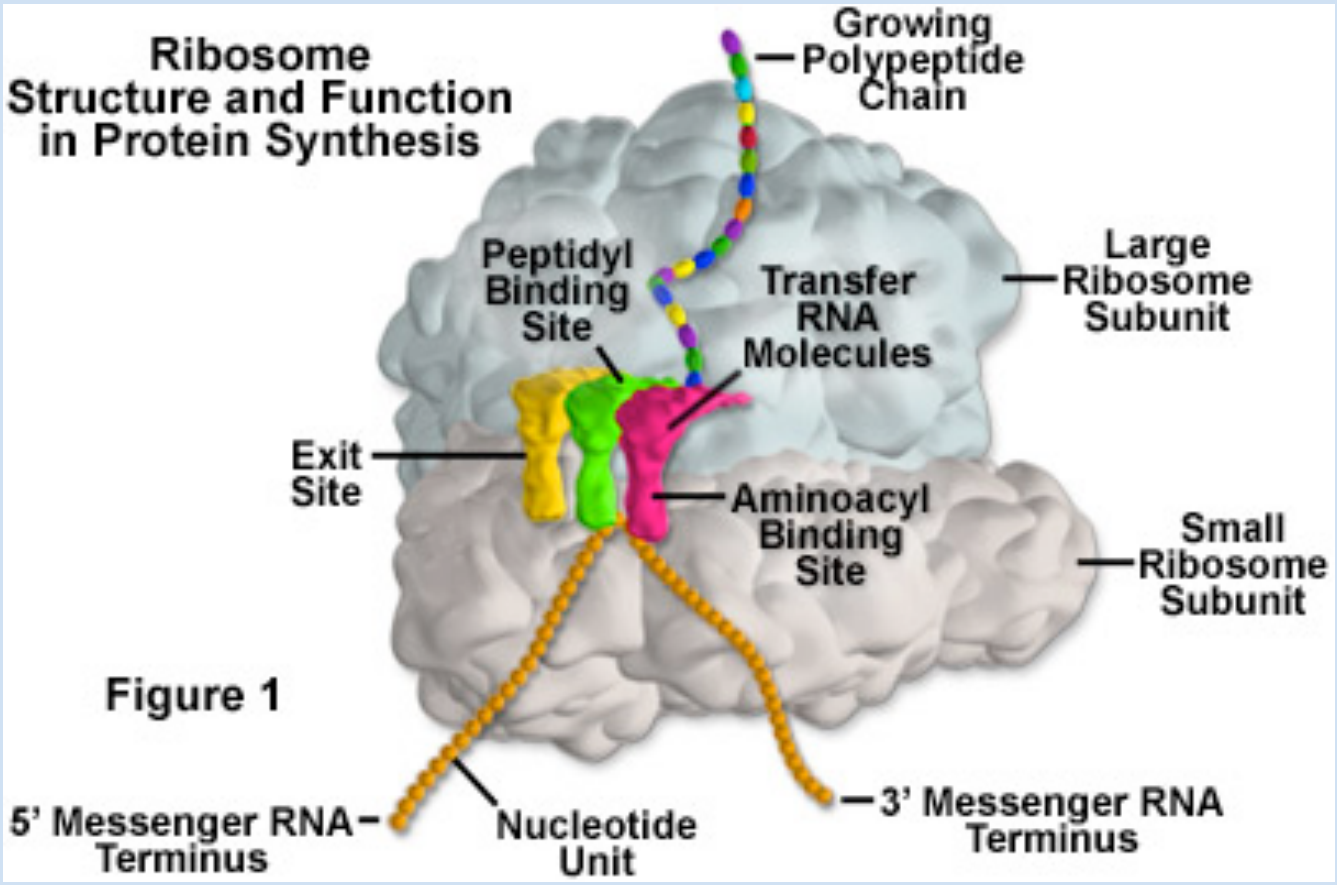

N-terminal acetylation machinery (NatA) in human cells.

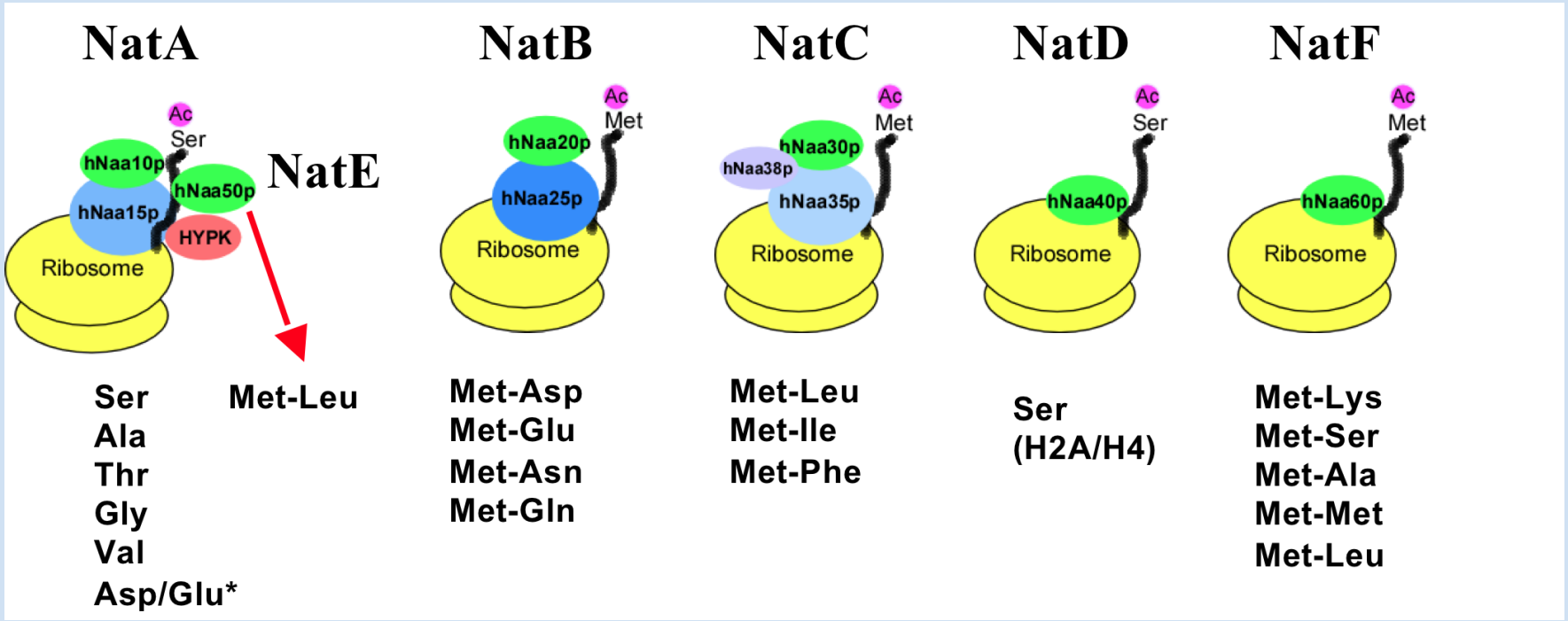

Slide courtesy of Thomas Arnesen

N$^{\alpha}$-terminal acetyltransferases

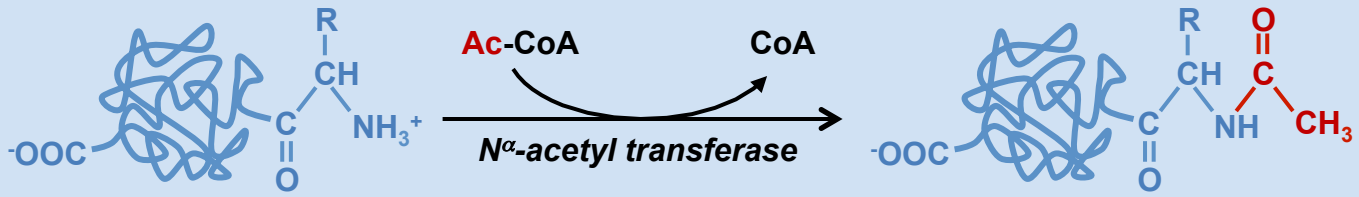

human NATs

- NatA-NatF
- associated with ribosome
- act co-translationally
- distinct substrate specificity

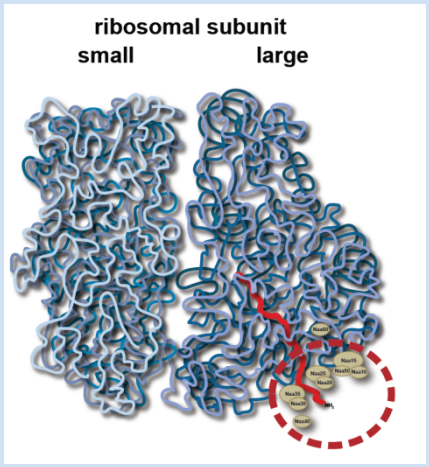

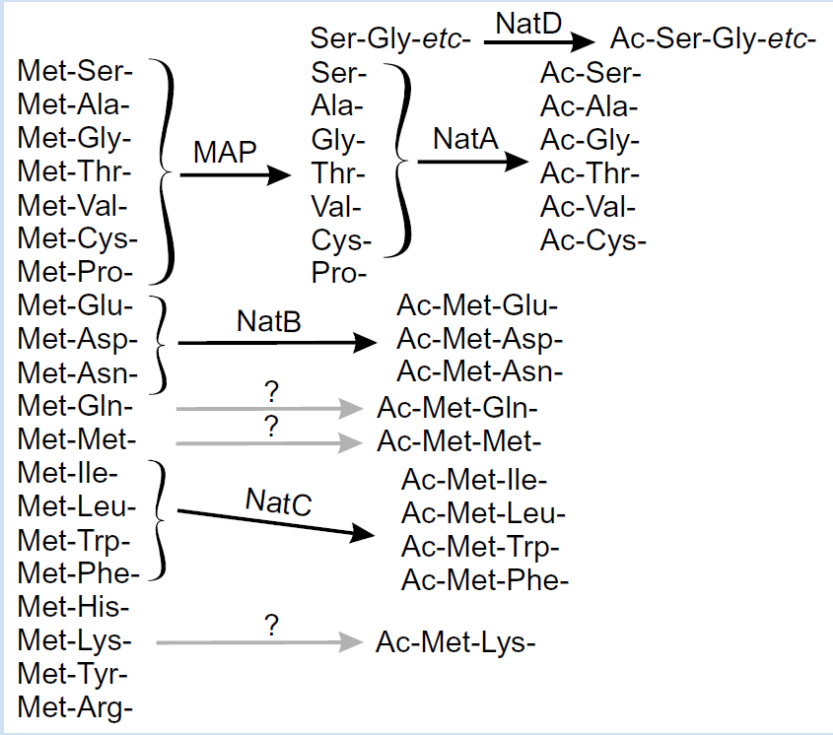

BMC Proceedings 2009, **3**(Suppl 6):S2

Crystal Structure of NAA50

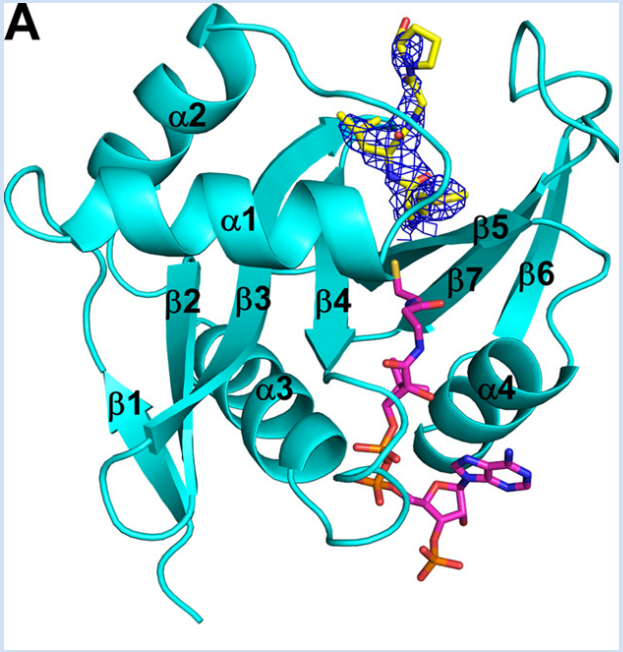

FIGURE 1. **Overall structure of the ternary Naa50p·CoA·peptide complex.** *A*, structure of the ternary complex showing Naa50p in *teal*; CoA as *magenta sticks* with carbon, nitrogen, and sulfur atoms in Corey-Pauling-Koltun coloring; and the substrate peptide as *yellow sticks* with carbon, nitrogen, and sulfur atoms in Corey-Pauling-Koltun coloring. Substrate peptide electron density obtained from a composite omit map (*blue*) is shown contoured to 1.5σ. *B*, superposition of the ternary Naa50p complex with the ternary Gcn5

Glen Liszczak[‡§], Thomas Arnesen[¶‖], and Ronen Marmorstein[‡§1]

THE JOURNAL OF BIOLOGICAL CHEMISTRY VOL. 286, NO. 42, pp. 37002–37010, October 21, 2011

Molecular basis for N-terminal acetylation by the heterodimeric NatA complex

Glen Liszczak[1,2], Jacob M Goldberg[2], Håvard Foyn[3], E James Petersson[2], Thomas Arnesen[3,4] & Ronen Marmorstein[1,2]

VOLUME 20 NUMBER 9 SEPTEMBER 2013 NATURE STRUCTURAL & MOLECULAR BIOLOGY

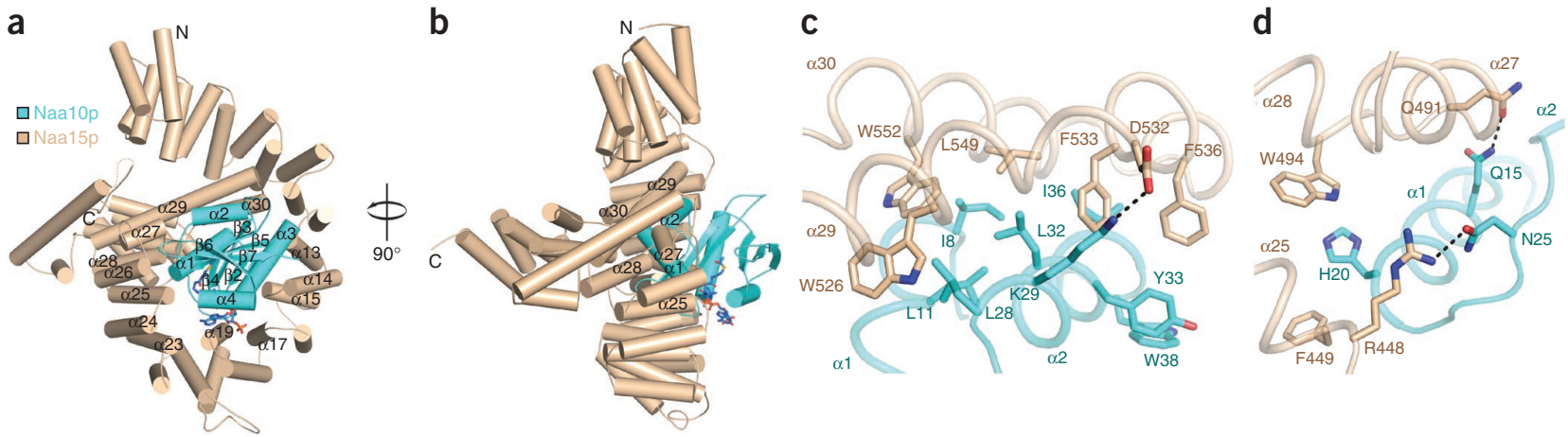

Figure 1 Overall structure of the NatA complex bound to acetyl CoA. (**a**) Naa10p (teal) and Naa15p (brown) subunits, shown in cartoon, bound to acetyl CoA (CPK coloring and stick format). Only Naa15p helices that contact Naa10p are labeled. The dashed brown line represents a disordered loop region in Naa15p. The dimensions of the complex are 107 Å × 85 Å × 70 Å. (**b**) A 90° rotation of the view in **a**. Helices that are depicted in **c** and **d** are labeled. (**c**) Zoom view highlighting key residues that compose the predominantly hydrophobic interface between Naa10p α1–α2 and Naa15p α29–α30. (**d**) Zoom view of the intersubunit interface at the C-terminal region of Naa10p α1 and the Naa15p α25–α27–α28 helices.

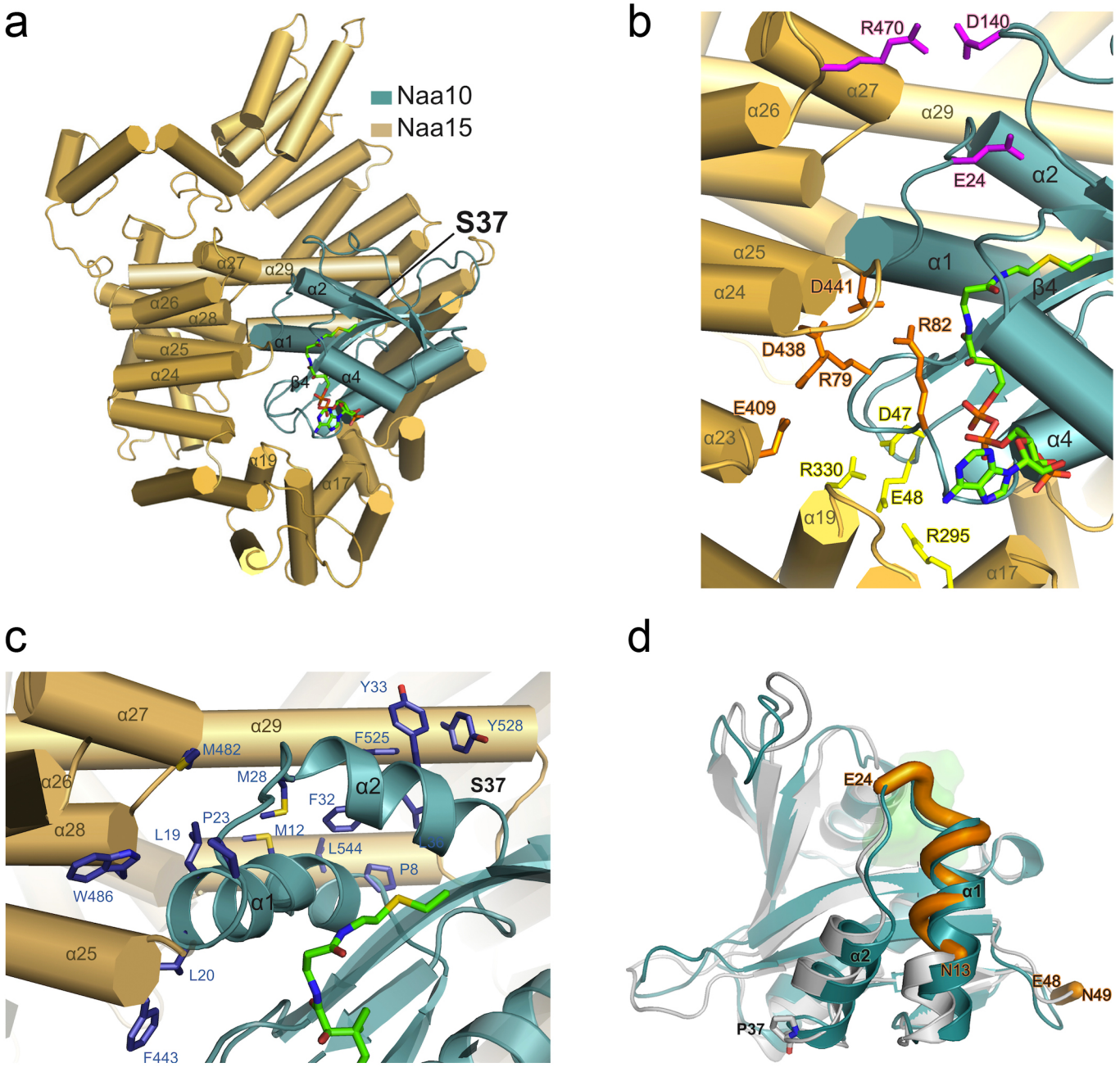
a
Naa10
Naa15
S37
α27
α29
α2
α26
α28
α25
α24
α1
β4
α4
α19
α17
b
R470
D140
α27
α26
α29
E24
α2
α25
α1
α24
D441
β4
R82
D438
R79
E409
D47
α23
α4
R330
E48
α19
R295
α17
c
Y33
α27
α29
Y528
F525
M482
M28
α26
α2
S37
F32
P23
α28
L19
M12
L544
P8
W486
α1
α25
L20
F443
d
E24
α1
α2
N13
E48
N49
P37

function of N$^{\alpha}$-terminal acetylation

general

- most abundant protein modification in eukaryotes
- NatA is the major NAT

NAT function

- protein function (hemoglobin, actin/tropomyosin…)
- protein stability
- proteasomal degradation via ubiquitin ligase Doa10
- avidity enhancer
- protein targeting to ER

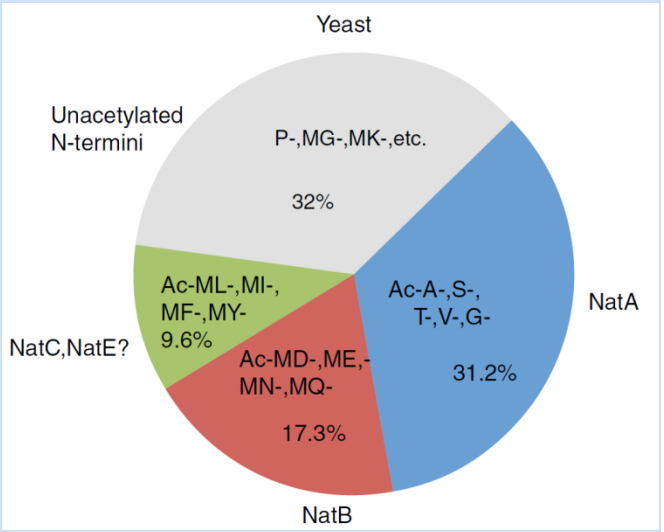

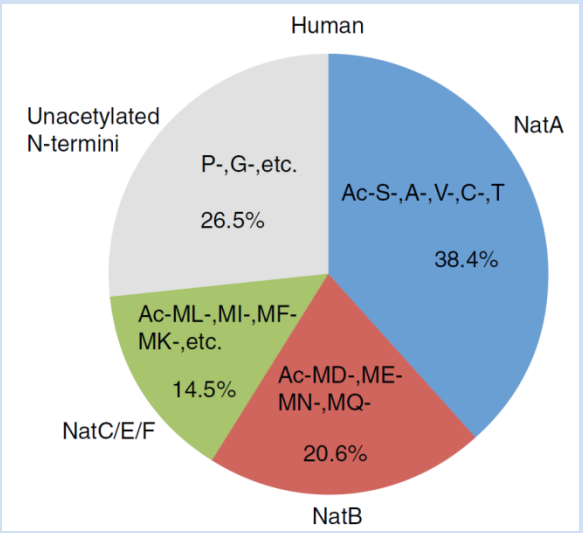

Trends in Biochemical Sciences April 2012, Vol. 37, No. 4

Open question:
Function of N-terminal acetylation?

Protein stability? Protein secretion?

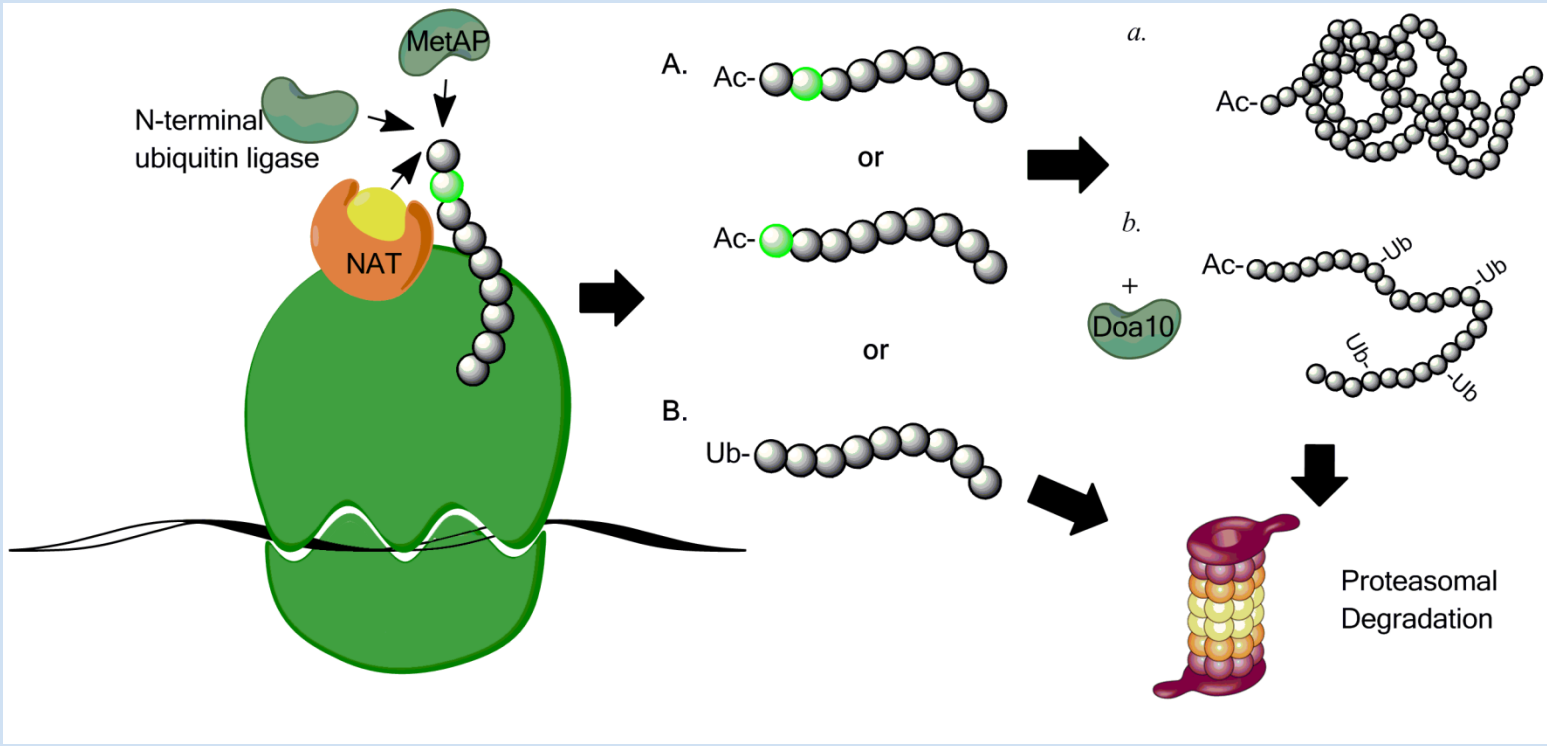

Figure courtesy of Kris Gevaert

N-Terminal Acetylation of Cellular Proteins Creates Specific Degradation Signals

Cheol-Sang Hwang, Anna Shemorry, Alexander Varshavsky*

N-Terminal Acetylation Inhibits Protein Targeting to the Endoplasmic Reticulum

Gabriella M. A. Forte, Martin R. Pool*, Colin J. Stirling*

Faculty of Life Sciences, University of Manchester, Manchester, United Kingdom

Abstract

Amino-terminal acetylation is probably the most common protein modification in eukaryotes with as many as 50%–80% of proteins reportedly altered in this way. Here we report a systematic analysis of the predicted N-terminal processing of cytosolic proteins versus those destined to be sorted to the secretory pathway. While cytosolic proteins were profoundly biased in favour of processing, we found an equal and opposite bias against such modification for secretory proteins. Mutations in secretory signal sequences that led to their acetylation resulted in mis-sorting to the cytosol in a manner that was dependent upon the N-terminal processing machinery. Hence N-terminal acetylation represents an early determining step in the cellular sorting of nascent polypeptides that appears to be conserved across a wide range of species.

interaction partners of Naa10

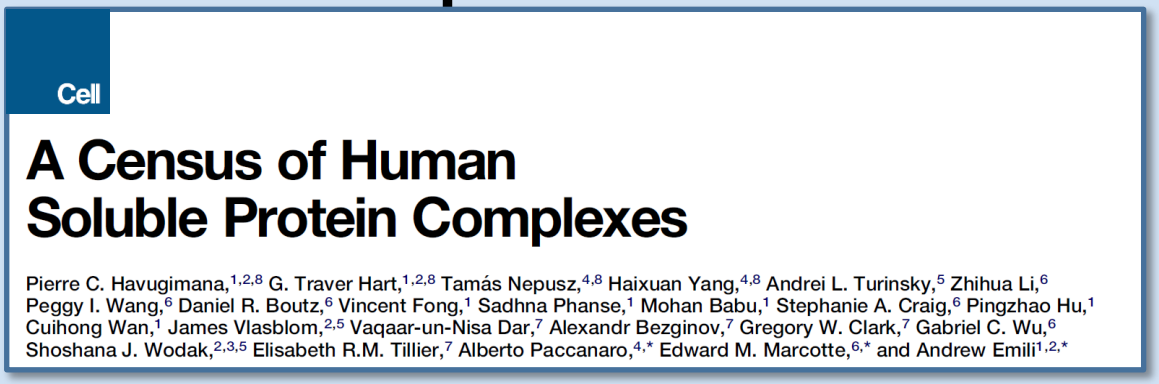
Cell

A Census of Human Soluble Protein Complexes

Pierre C. Havugimana,[1,2,8] G. Traver Hart,[1,2,8] Tamás Nepusz,[4,8] Haixuan Yang,[4,8] Andrei L. Turinsky,[5] Zhihua Li,[6] Peggy I. Wang,[6] Daniel R. Boutz,[6] Vincent Fong,[1] Sadhna Phanse,[1] Mohan Babu,[1] Stephanie A. Craig,[6] Pingzhao Hu,[1] Cuihong Wan,[1] James Vlasblom,[2,5] Vaqaar-un-Nisa Dar,[7] Alexandr Bezginov,[7] Gregory W. Clark,[7] Gabriel C. Wu,[6] Shoshana J. Wodak,[2,3,5] Elisabeth R.M. Tillier,[7] Alberto Paccanaro,[4,*] Edward M. Marcotte,[6,*] and Andrew Emili[1,2,*]

NAA15_HUMAN,NAA10_HUMAN,M89BB_HUMAN

PARP9_HUMAN,NHEJ1_HUMAN,NAA25_HUMAN,NAA20_HUMAN

TCEA1_HUMAN,PLCB3_HUMAN,NAA16_HUMAN,NAA10_HUMAN,MINA_HUMAN

RT21_HUMAN,NAA15_HUMAN,ML12A_HUMAN,HYPK_HUMAN,CAP1_HUMAN

TCEA1_HUMAN,PLCB3_HUMAN,NAA16_HUMAN,NAA10_HUMAN,MINA_HUMAN

WDR44_HUMAN,TF2B_HUMAN,TCEA2_HUMAN,SNAG_HUMAN,RMI2_HUMAN,PYRD1_HUMAN,PRP18_HUMAN,NAA38_HUMAN,METH_HUMAN,LSM7_HUMAN,LSM6_HUMAN,LSM5_HUMAN,LSM4_HUMAN,LSM3_HUMAN,LSM2_HUMAN,HELQ_HUMAN,GON4L_HUMAN,GCC2_HUMAN,EHD2_HUMAN,DHX16_HUMAN

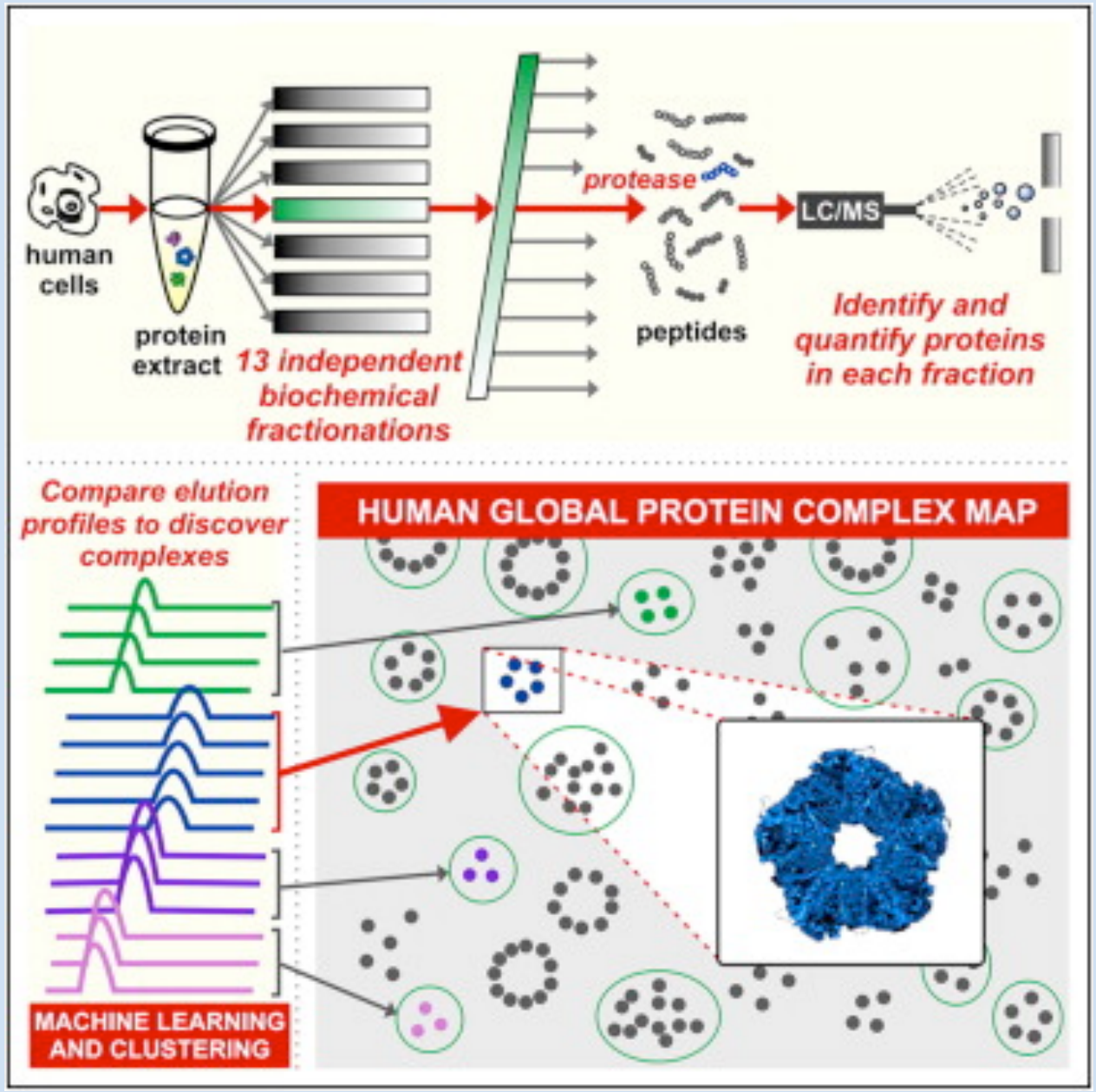
human cells
protein extract
13 independent biochemical fractionations
protease
peptides
LC/MS
Identify and quantify proteins in each fraction
Compare elution profiles to discover complexes
HUMAN GLOBAL PROTEIN COMPLEX MAP
MACHINE LEARNING AND CLUSTERING

interaction partners of Naa10

Cell

A Census of Human Soluble Protein Complexes

Pierre C. Havugimana,[1,2,8] G. Traver Hart,[1,2,8] Tamás Nepusz,[4,8] Haixuan Yang,[4,8] Andrei L. Turinsky,[5] Zhihua Li,[6] Peggy I. Wang,[6] Daniel R. Boutz,[6] Vincent Fong,[1] Sadhna Phanse,[1] Mohan Babu,[1] Stephanie A. Craig,[6] Pingzhao Hu,[1] Cuihong Wan,[1] James Vlasblom,[2,5] Vaqaar-un-Nisa Dar,[7] Alexandr Bezginov,[7] Gregory W. Clark,[7] Gabriel C. Wu,[6] Shoshana J. Wodak,[2,3,5] Elisabeth R.M. Tillier,[7] Alberto Paccanaro,[4,*] Edward M. Marcotte,[6,*] and Andrew Emili[1,2,*]

new interaction partners of NatA?

- TCEA1
- Mina53
- PLCβ3

co-immunoprecipitation assay

- HEK293 cells
- + V5-hNaa10 wt / myc-Naa15
- IP with anti-V5 / myc
- IB: Naa10/Naa15 (control)
  TCEA1
  Mina53
  PLCβ3 (not shown)

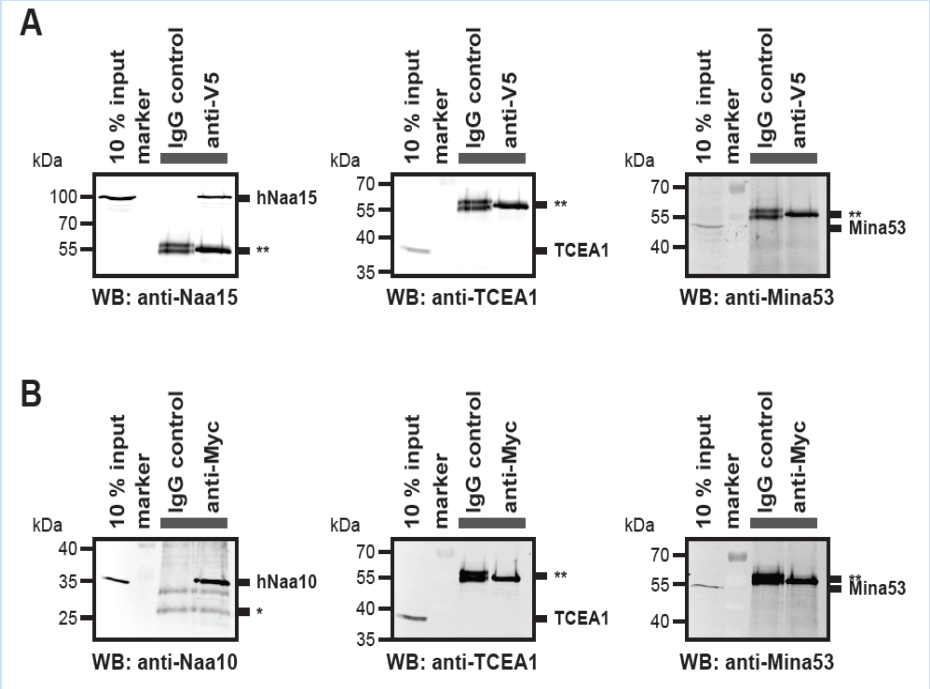

materials/methods IP mass spec

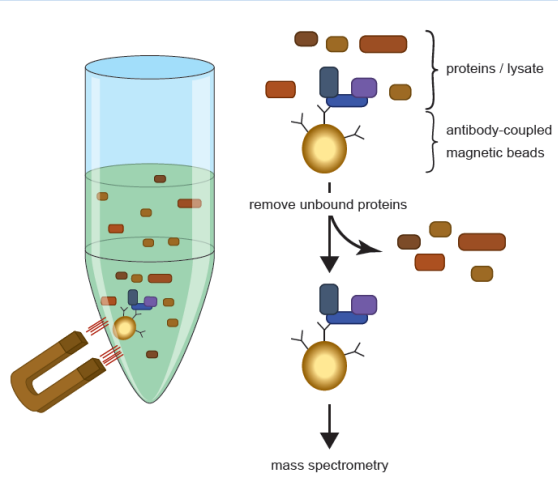

5 x 106 HEK293 cells were seeded in 10 cm dish and transfected after 24 h with pcDNA3.1 V5/His hNaa10 wt, pcDNA3.1 V5/His hNaa10 S37P or corresponding empty vector. Cells were lysed after 48 h in 500 µl lysis buffer (0.2 % Triton X-100, 0.1 % DTT and 1 x Complete protease inhibitor cocktail in PBS) per dish and cellular debris was pelleted at 20,800 g for 10 min. The lysates were pooled and protein concentration was determined using APA protein assay (Cytoskeleton).

For IP, 40 mg total protein were incubated with 400 µl anti-V5-coupled magnetic beads (Invitrogen) for 2 h at 4°C under constant agitation. Beads were washed 3 times with lysis buffer, 1 x with PBS and once with 50 % PBS. **Proteins were digested with trypsin off the beads and labelled with distinct isobaric iTRAQ reagents.** The samples were combined and subjected to standard 2D MudPIT LCMS and analyzed using a Thermo Velos Orbitrap mass spectrometer. Peptides were fragmented using the high-energy collision (HCD) cell to avoid low-mass ejection of iTRAQ reporter ions. The effects of compression of iTRAQ ratio values were procedurally minimized by using narrow precursor selection tolerances (1.2Da) and optimized settings for HCD collision energy and transmission efficiency. iTRAQ labeled peptides remain isobaric in MS but following HCD the iTRAQ reporter ions appear as distinct ions in the range 113 to 121 m/z in each MS/MS spectrum. The relative abundance of the peptides (and thus corresponding proteins) were deduced directly from the relative intensities of the corresponding reporter ions. Peak lists were extracted from instrument raw data files using the MASCOT Distiller software (MatrixScience) and the MASCOT searches were performed on a 64-processor cluster (Perkins et al. 1999). False discovery rates (FDR) were estimated by searching equivalent reversed or randomized sequence databases, typically using a cutoff value of 1% FDR. Protein-abundance ratios were calculated using intensity weighted averages from matching peptides after outlier removal. **The relative enrichment in the samples were calculated as a ratio of the intensities between the samples and the empty-vector control. The whole experiment was done twice.**

slides IP & mass spec

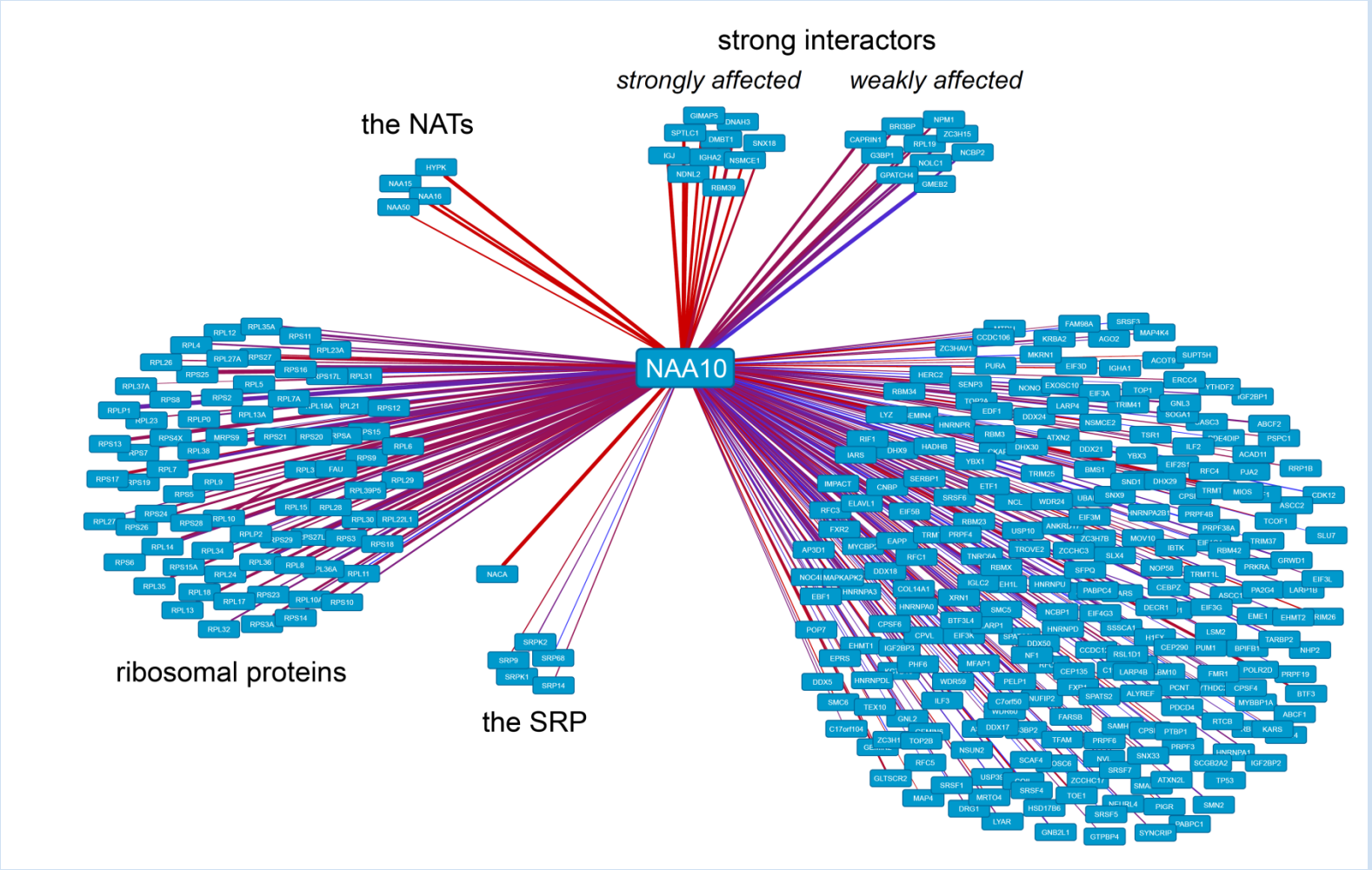

Top 20 hits

Nr.	Name	Description	Enrichment	
			wt	S37P
1	RPLP1*	60S acidic ribosomal protein P1	30.3	23.7
2	RPS25*	40S ribosomal protein S25	29.4	18.1
3	NACA	Nascent polypeptide-associated complex subunit alpha, muscle-specific form (Fragment)	27.5	11.0
4	HYPK	Huntingtin-interacting protein K	27.0	4.3
5	RPL38*	60S ribosomal protein L38	26.8	18.3
6	RPL8*	60S ribosomal protein L8	24.7	14.4
7	RPS13*	40S ribosomal protein S13	24.1	13.5
8	RPS28*	40S ribosomal protein S28	23.8	14.6
9	FAU*	40S ribosomal protein S30	23.7	15.9
10	RPL27A*	60S ribosomal protein L27a	21.9	11.9
11	RPL6*	60S ribosomal protein L6	21.8	13.7
12	CAPRIN1	Caprin-1	21.7	12.4
13	GPATCH4	G patch domain-containing protein 4	21.4	15.3
14	NAA15	N-alpha-acetyltransferase 15, NatA auxiliary subunit	21.2	5.2
15	RPS18*	40S ribosomal protein S18	20.9	12.0
16	RPS14*	40S ribosomal protein S14	20.7	11.6
17	RPS19*	40S ribosomal protein S19	20.3	12.8
18	RPL13*	60S ribosomal protein L13	19.9	11.5
19	NDNL2	Melanoma-associated antigen G1	19.6	4.7
20	RPS16*	40S ribosomal protein S16	19.5	13.6

*ribosomal protein

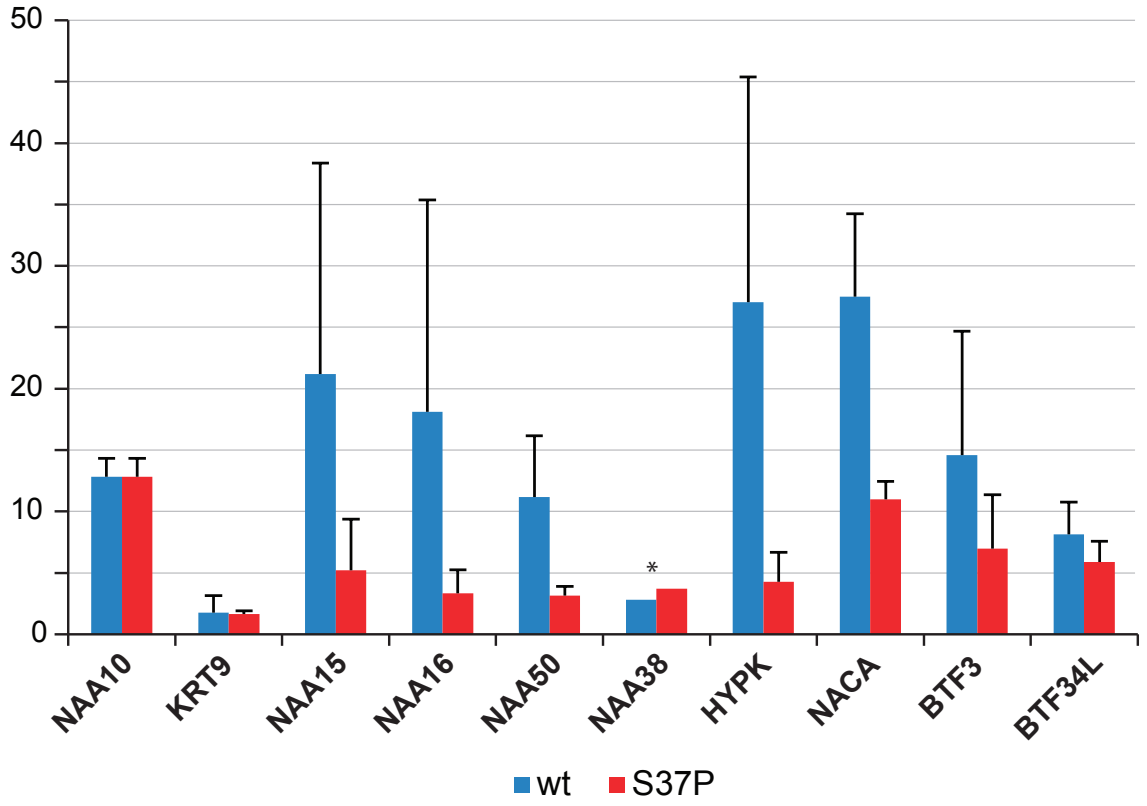

* Naa38 was only found in one set

NAC

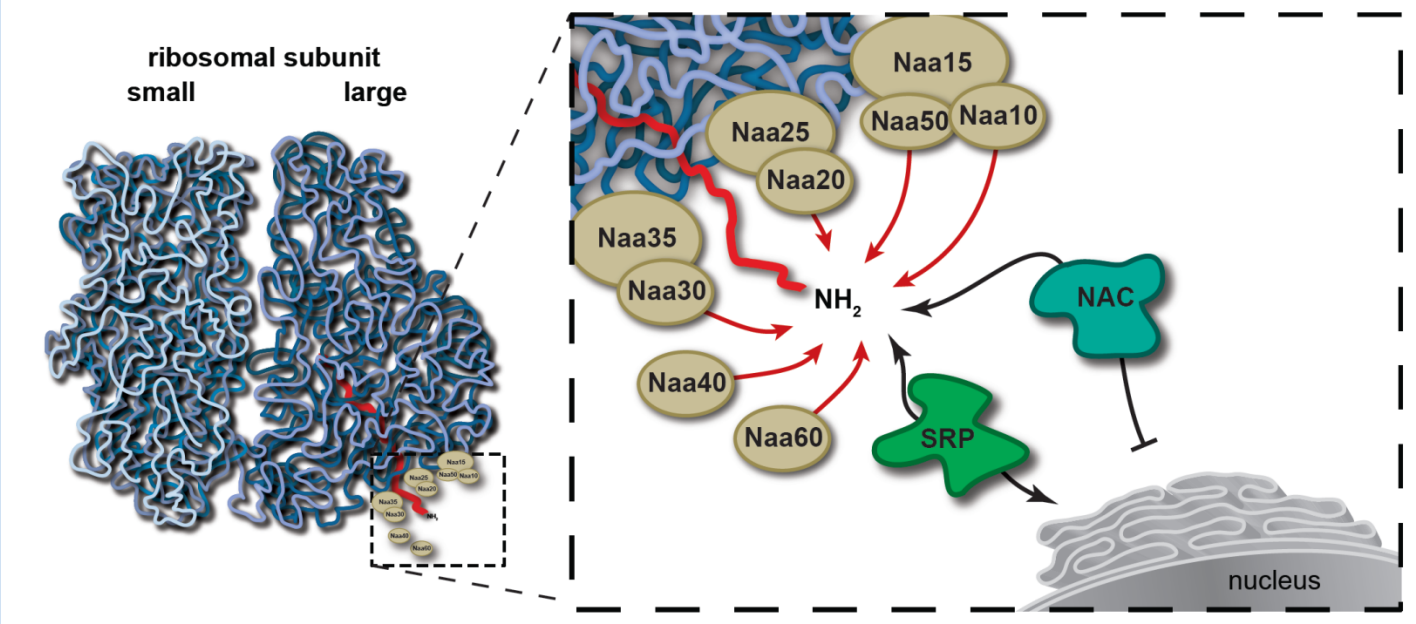
ribosomal subunit
small
large
Naa15
Naa50
Naa10
Naa25
Naa20
Naa35
Naa30
NH2
NAC
Naa40
Naa60
SRP
nucleus

interaction partners of Naa10

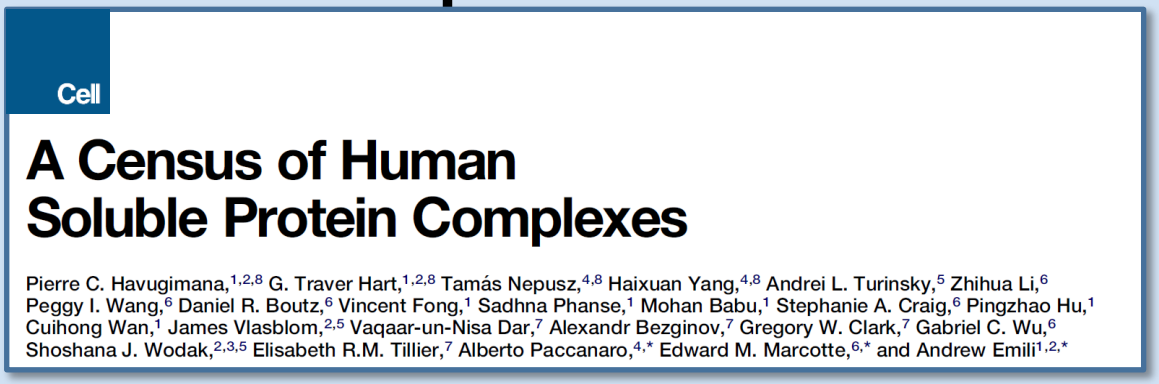

Cell

A Census of Human Soluble Protein Complexes

Pierre C. Havugimana,[1,2,8] G. Traver Hart,[1,2,8] Tamás Nepusz,[4,8] Haixuan Yang,[4,8] Andrei L. Turinsky,[5] Zhihua Li,[6] Peggy I. Wang,[6] Daniel R. Boutz,[6] Vincent Fong,[1] Sadhna Phanse,[1] Mohan Babu,[1] Stephanie A. Craig,[6] Pingzhao Hu,[1] Cuihong Wan,[1] James Vlasblom,[2,5] Vaqaar-un-Nisa Dar,[7] Alexandr Bezginov,[7] Gregory W. Clark,[7] Gabriel C. Wu,[6] Shoshana J. Wodak,[2,3,5] Elisabeth R.M. Tillier,[7] Alberto Paccanaro,[4,*] Edward M. Marcotte,[6,*] and Andrew Emili[1,2,*]

NAA15_HUMAN,NAA10_HUMAN,M89BB_HUMAN

PARP9_HUMAN,NHEJ1_HUMAN,NAA25_HUMAN,NAA20_HUMAN

TCEA1_HUMAN,PLCB3_HUMAN,NAA16_HUMAN,NAA10_HUMAN,MINA_HUMAN

RT21_HUMAN,NAA15_HUMAN,ML12A_HUMAN,HYPK_HUMAN,CAP1_HUMAN

TCEA1_HUMAN,PLCB3_HUMAN,NAA16_HUMAN,NAA10_HUMAN,MINA_HUMAN

WDR44_HUMAN,TF2B_HUMAN,TCEA2_HUMAN,SNAG_HUMAN,RMI2_HUMAN,PYRD1_HUMAN,PRP18_HUMAN,NAA38_HUMAN,METH_HUMAN,LSM7_HUMAN,LSM6_HUMAN,LSM5_HUMAN,LSM4_HUMAN,LSM3_HUMAN,LSM2_HUMAN,HELQ_HUMAN,GON4L_HUMAN,GCC2_HUMAN,EHD2_HUMAN,DHX16_HUMAN

Top 20 hits

Nr.	Name	Description	Enrichment	
			wt	S37P
1	RPLP1*	60S acidic ribosomal protein P1	30.3	23.7
2	RPS25*	40S ribosomal protein S25	29.4	18.1
3	NACA	Nascent polypeptide-associated complex subunit alpha, muscle-specific form (Fragment)	27.5	11.0
4	HYPK	Huntingtin-interacting protein K	27.0	4.3
5	RPL38*	60S ribosomal protein L38	26.8	18.3
6	RPL8*	60S ribosomal protein L8	24.7	14.4
7	RPS13*	40S ribosomal protein S13	24.1	13.5
8	RPS28*	40S ribosomal protein S28	23.8	14.6
9	FAU*	40S ribosomal protein S30	23.7	15.9
10	RPL27A*	60S ribosomal protein L27a	21.9	11.9
11	RPL6*	60S ribosomal protein L6	21.8	13.7
12	CAPRIN1	Caprin-1	21.7	12.4
13	GPATCH4	G patch domain-containing protein 4	21.4	15.3
14	NAA15	N-alpha-acetyltransferase 15, NatA auxiliary subunit	21.2	5.2
15	RPS18*	40S ribosomal protein S18	20.9	12.0
16	RPS14*	40S ribosomal protein S14	20.7	11.6
17	RPS19*	40S ribosomal protein S19	20.3	12.8
18	RPL13*	60S ribosomal protein L13	19.9	11.5
19	NDNL2	Melanoma-associated antigen G1	19.6	4.7
20	RPS16*	40S ribosomal protein S16	19.5	13.6

*ribosomal protein

ARTICLE

Received 24 Feb 2014 | Accepted 21 May 2014 | Published 18 Jun 2014

DOI: 10.1038/ncomms5180

Interplay between trigger factor and other protein biogenesis factors on the ribosome

Thomas Bornemann[1], Wolf Holtkamp[1] & Wolfgang Wintermeyer[1]

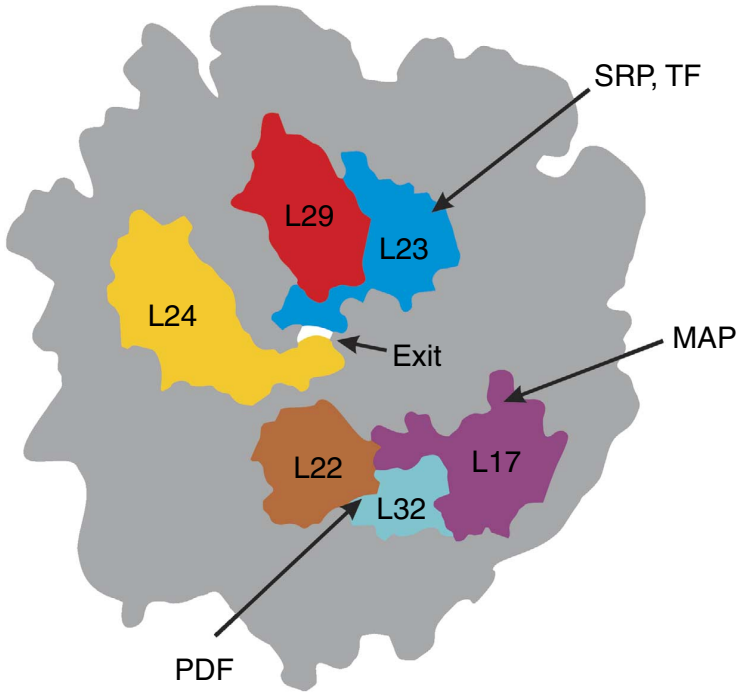

Figure 1 | Binding platform for RPBs at the peptide exit of the bacterial 50S ribosomal subunit. Ribosomal proteins at or near the peptide exit of the 50S subunit (grey outline) are indicated along with the RPBs binding to protein L23 (SRP, TF), L22 (PDF) or L17 (MAP) (for references, see text).

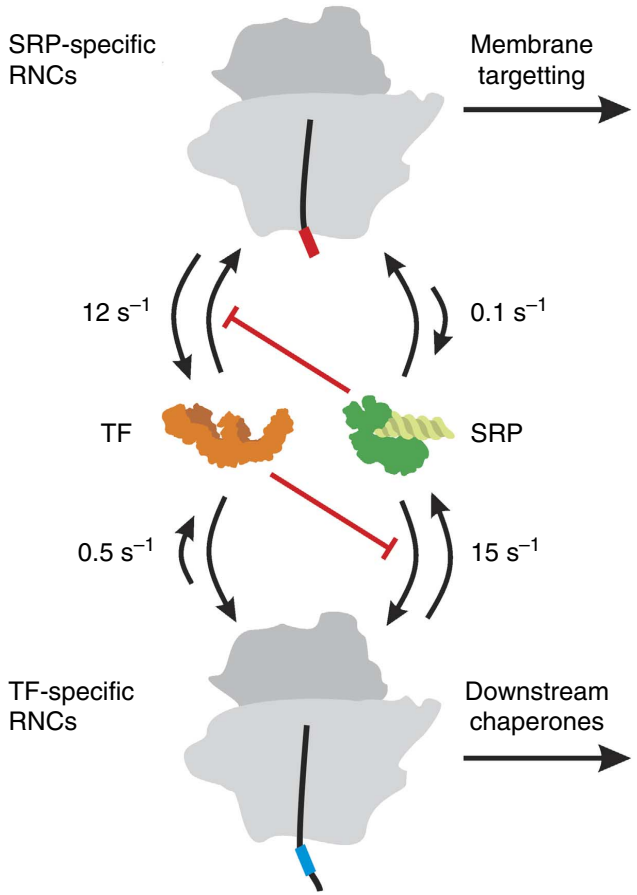

Figure 6 | Interplay of TF and SRP on translating ribosomes. Concurrent binding of TF or SRP to RNCs presenting the respective specific nascent chain (SRP-specific SAS, red; TF-specific sequence, blue) leads to weakening of the binding of the respective other ligand (values of K_d increased eightfold or >15-fold, respectively (Fig. 3)), as indicated by red lines. Because SRP dissociates from RNCs in three steps, average values of k_{off} calculated from the three rate constants k_{-1}, k_{-2} and k_{-3} are given[13]. Values of k_{off} for TF dissociation from RNCs are taken from Table 1. Second-order rate constants for TF or SRP binding to RNCs ranged from about 100 to 200 $\mu M^{-1} s^{-1}$ (Table 1 and ref. 13), indicating near diffusion-controlled binding.

The End
Extra Slides to Follow

The mechanism of eukaryotic translation initiation and principles of its regulation

Richard J. Jackson, Christopher U. T. Hellen‡ and Tatyana V. Pestova‡*

Abstract | Protein synthesis is principally regulated at the initiation stage (rather than during elongation or termination), allowing rapid, reversible and spatial control of gene expression. Progress over recent years in determining the structures and activities of initiation factors, and in mapping their interactions in ribosomal initiation complexes, have advanced our understanding of the complex translation initiation process. These developments have provided a solid foundation for studying the regulation of translation initiation by mechanisms that include the modulation of initiation factor activity (which affects almost all scanning-dependent initiation) and through sequence-specific RNA-binding proteins and microRNAs (which affect individual mRNAs).

Table 1 | **Eukaryotic initiation factors**

Name	Number of subunits and their molecular mass (kDa)	Function
Core initiation factors		
eIF2	3 (36.1, 38.4 and 51.1)	Forms an eIF2–GTP–Met-tRNA$_i$ ternary complex that binds to the 40S subunit, thus mediating ribosomal recruitment of Met-tRNA$_i$
eIF3	13 (800 total)	Binds 40S subunits, eIF1, eIF4G and eIF5; stimulates binding of eIF2–GTP–Met-tRNA$_i$ to 40S subunits; promotes attachment of 43S complexes to mRNA and subsequent scanning; and possesses ribosome dissociation and anti-association activities, preventing joining of 40S and 60S subunits
eIF1	1 (12.7)	Ensures the fidelity of initiation codon selection; promotes ribosomal scanning; stimulates binding of eIF2–GTP–Met-tRNA$_i$ to 40S subunits; and prevents premature eIF5-induced hydrolysis of eIF2-bound GTP and P_i release
eIF1A	1 (16.5)	Stimulates binding of eIF2–GTP–Met-tRNA$_i$ to 40S subunits and cooperates with eIF1 in promoting ribosomal scanning and initiation codon selection
eIF4E	1 (24.5)	Binds to the m^{7}GpppG 5′ terminal 'cap' structure of mRNA
eIF4A*	1 (46.1)	DEAD-box ATPase and ATP-dependent RNA helicase
eIF4G‡	1 (175.5)	Binds eIF4E, eIF4A, eIF3, PABP, SLIP1 and mRNA (see FIG. 3a) and enhances the helicase activity of eIF4A
eIF4F	3 (246.1 total)	A cap-binding complex, comprising eIF4E, eIF4A and eIF4G; unwinds the 5′ proximal region of mRNA and mediates the attachment of 43S complexes to it; and assists ribosomal complexes during scanning
eIF4B	1 (69.3)	An RNA-binding protein that enhances the helicase activity of eIF4A
eIF4H	1 (27.4)	An RNA-binding protein that enhances the helicase activity of eIF4A and is homologous to a fragment of eIF4B
eIF5	1 (49.2)	A GTPase-activating protein, specific for GTP-bound eIF2, that induces hydrolysis of eIF2-bound GTP on recognition of the initiation codon
eIF5B	1 (138.9)	A ribosome-dependent GTPase that mediates ribosomal subunit joining
eIF2B	5 (33.7, 39.0, 50.2, 59.7 and 80.3)	A guanosine nucleotide exchange factor that promotes GDP–GTP exchange on eIF2
Auxiliary factors		
DHX29	1 (155.3)	A DExH box-containing protein that binds 40S subunit and promotes ribosomal scanning on mRNAs with long, highly structured 5′ UTRs
Ded1	1 (65.6)	A DEAD box-containing NTPase and RNA helicase that potentially promotes scanning in *Saccharomyces cerevisiae*
eIF6	1 (26.6)	An anti-association factor that binds 60S subunits and prevents them from joining to 40S subunits
p97	1 (102.4)	Closely related to the carboxy-terminal two-thirds of eIF4G; binds eIF4A and eIF3; and promotes initiation in a potentially mRNA-specific manner
PABP	1 (70.7)	Binds to the 3′ poly(A) tail of mRNA, eIF4G and eRF3; enhances binding of eIF4F to the cap; and might facilitate recruitment of recycled post-termination 40S subunits back to the 5′ end of mRNA

Ded1, DEAD box helicase 1; DHX29, DExH box protein 29; eIF, eukaryotic initiation factor; PABP, poly(A)-binding protein. *Two paralogues (eIF4AI and eIF4AII), encoded by different genes, are functionally indistinguishable, but eIF4AIII has no activity as an eIF. ‡Two paralogues (eIF4GI and eIF4GII), encoded by different genes, are functionally similar but show some selectivity towards different mRNAs. eIF4GI is generally the more abundant.

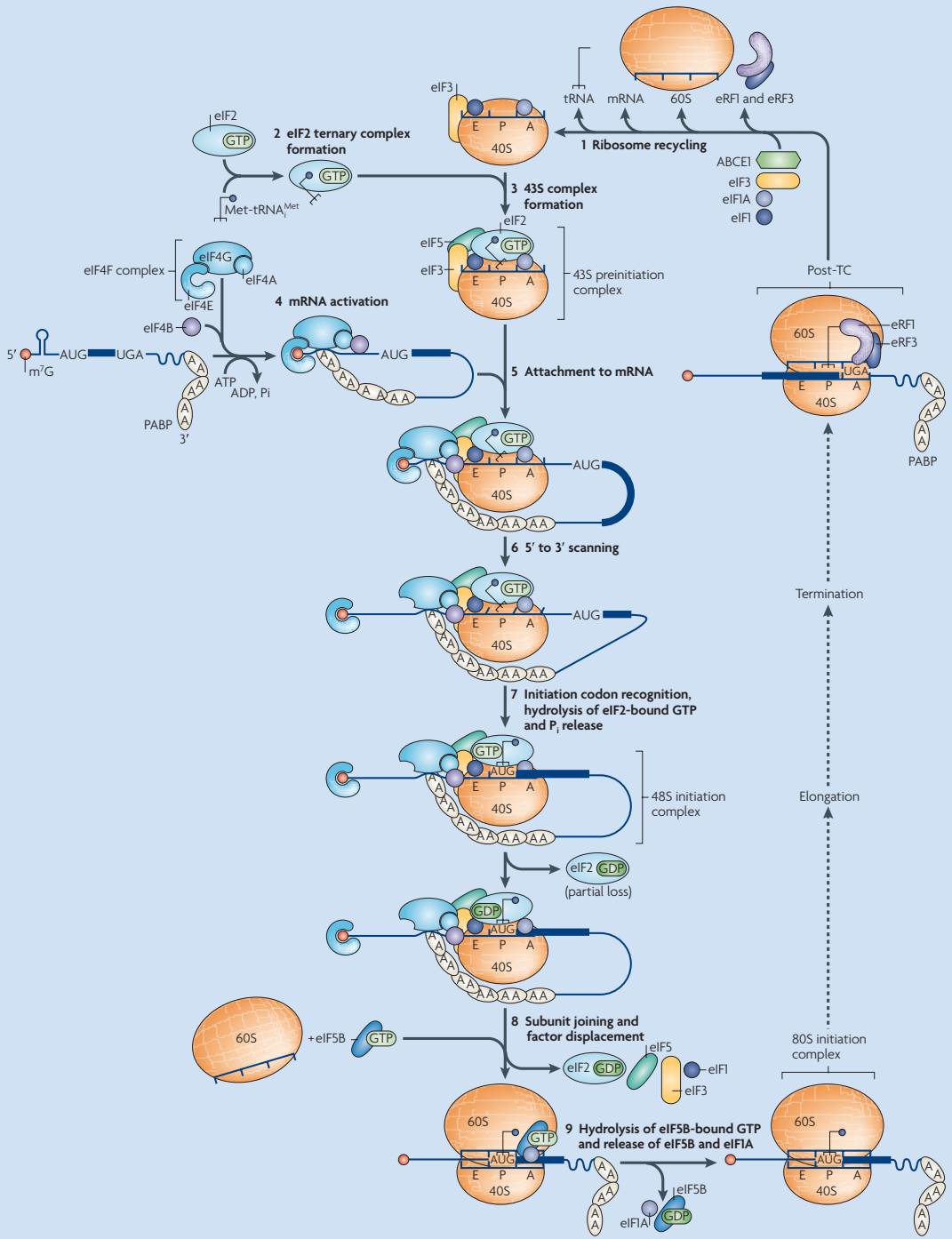
eIF3
tRNA
mRNA
60S
eRF1 and eRF3
1 Ribosome recycling
ABCE1
eIF3
eIF1A
eIF1
eIF2
GTP
2 eIF2 ternary complex formation
Met-tRNA$_i^{Met}$
3 43S complex formation
eIF5
43S preinitiation complex
eIF4F complex
eIF4G
eIF4A
eIF4E
eIF4B
4 mRNA activation
5′
m^{7}G
AUG
UGA
PABP
3′
ATP
ADP, Pi
5 Attachment to mRNA
Post-TC
eRF1
eRF3
6 5′ to 3′ scanning
7 Initiation codon recognition, hydrolysis of eIF2-bound GTP and P$_i$ release
48S initiation complex
eIF2 GDP
(partial loss)
8 Subunit joining and factor displacement
+eIF5B
eIF5
eIF1
eIF3
80S initiation complex
9 Hydrolysis of eIF5B-bound GTP and release of eIF5B and eIF1A
eIF5B
eIF1A
Termination
Elongation

◀ Figure 1 | **Model of the canonical pathway of eukaryotic translation initiation.** The canonical pathway of eukaryotic translation initiation is divided into eight stages (**2**–**9**). These stages follow the recycling of post-termination complexes (post-TCs; **1**) to yield separated 40S and 60S ribosomal subunits, and result in the formation of an 80S ribosomal initiation complex, in which Met-tRNA$^{Met}_{i}$ is base paired with the initiation codon in the ribosomal P-site and which is competent to start the translation elongation stage. These stages are: eukaryotic initiation factor 2 (eIF2)–GTP–Met-tRNA$^{Met}_{i}$ ternary complex formation (**2**); formation of a 43S preinitiation complex comprising a 40S subunit, eIF1, eIF1A, eIF3, eIF2–GTP–Met-tRNA$^{Met}_{i}$ and probably eIF5 (**3**); mRNA activation, during which the mRNA cap-proximal region is unwound in an ATP-dependent manner by eIF4F with eIF4B (**4**); attachment of the 43S complex to this mRNA region (**5**); scanning of the 5′ UTR in a 5′ to 3′ direction by 43S complexes (**6**); recognition of the initiation codon and 48S initiation complex formation, which switches the scanning complex to a 'closed' conformation and leads to displacement of eIF1 to allow eIF5-mediated hydrolysis of eIF2-bound GTP and P_i release (**7**); joining of 60S subunits to 48S complexes and concomitant displacement of eIF2–GDP and other factors (eIF1, eIF3, eIF4B, eIF4F and eIF5) mediated by eIF5B (**8**); and GTP hydrolysis by eIF5B and release of eIF1A and GDP-bound eIF5B from assembled elongation-competent 80S ribosomes (**9**). Translation is a cyclical process, in which termination follows elongation and leads to recycling (**1**), which generates separated ribosomal subunits. The model omits potential 'closed loop' interactions involving poly(A)-binding protein (PABP), eukaryotic release factor 3 (eRF3) and eIF4F during recycling (see Supplementary information S5 (box)), and the recycling of eIF2–GDP by eIF2B. Whether eRF3 is still present on ribosomes at the recycling stage is unknown.

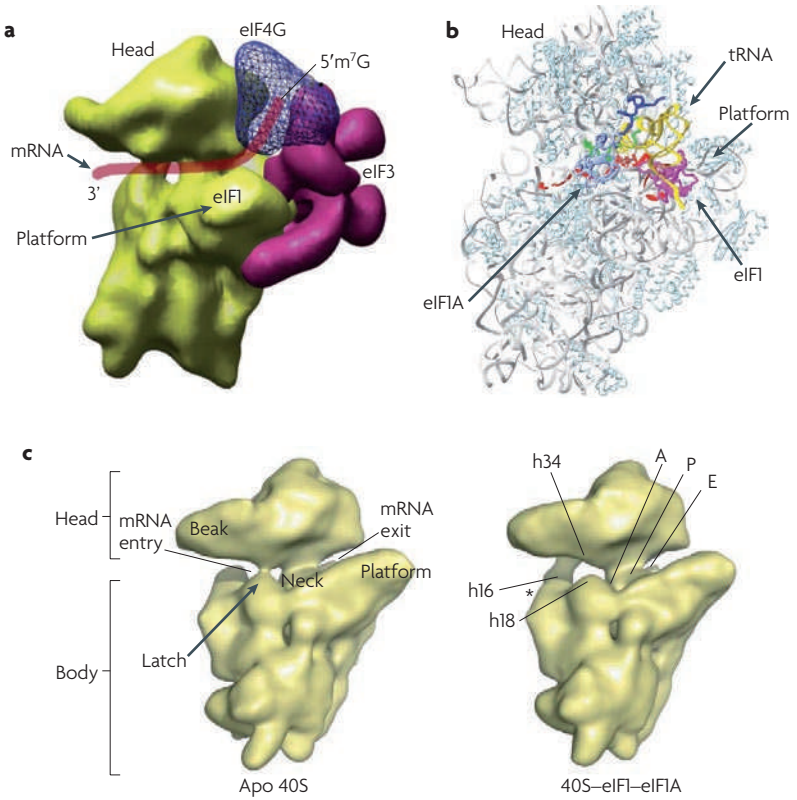

Figure 2 | **Architecture of ribosomal initiation complexes. a** | Model of a 40S subunit with eIF3 (magenta) on its exterior (solvent) surface and eIF4G (purple) bound to eIF3 near the E-site, based on cryoelectron microscopy analysis, and showing positions of mRNA (red line) and eIF1 (green) on the subunit interface. Binding of eIF3 to the solvent surface of the 40S subunit is compatible with its potential partial retention on ribosomes during translation of short upstream open reading frames (uORFs). **b** | Positions of eIF1 (magenta) and eIF1A (with its structured domain in light blue, its carboxy-terminal tail in dark blue and its amino-terminal tail in green) on the 40S subunit, relative to mRNA (red) and P-site tRNA (yellow), based on directed hydroxyl radical probing data[10,13] and modelled using *Thermus thermophilus* 30S subunit crystal structures (protein data bank codes 1JGO and 1JGP). **c** | Cryoelectron microscopy reconstructions of yeast apo 40S subunits (left panel) and 40S–eIF1–eIF1A complexes (right panel), labelled to indicate the A-site, P-site and E-site in the mRNA-binding channel and the positions of rRNA helices h16, h18 and h34, which are involved in forming the mRNA entry channel (h18–h34) and the eIF1- and eIF1A-induced head–shoulder connection (h16–ribosomal protein S3 (rpS3); indicated by an asterisk). Part **a** is adapted, with permission, from REF. 8 © American Association for the Advancement of Science (2005). Part **c** is adapted, with permission, from REF. 14 © Cell (2007).

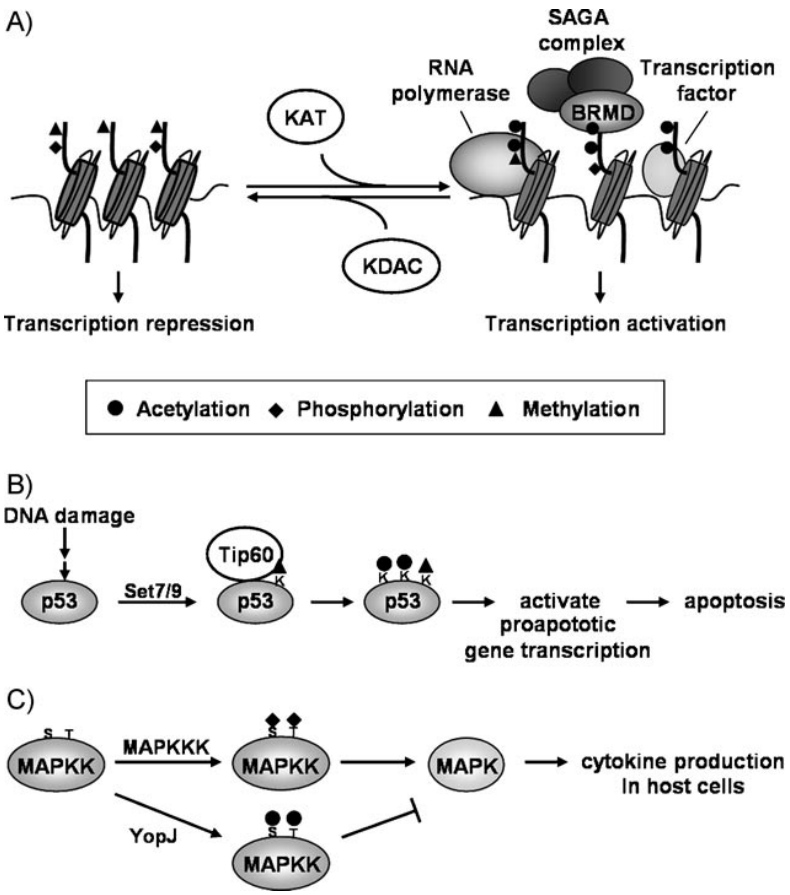

Scheme 2. Schematic representation of the biological functions of protein acetylation in gene transcription and bacterial infection. A) Lysine acetylation on histones activates gene transcription by opening the access of promoter region to RNA polymerases and transcription factors and by recruiting the chromatin-remodeling complex containing bromodomain (BRMD), such as SAGA complex. B) In response to genotoxic stress, lysine methylation on p53 recruits KATs such as Tip60 for lysine acetylation which leads to activation of proapototic gene transcription, thereby cell apoptosis.[20,21] C) *Yersinia* effector protein YopJ, functioning as an acetyltransferase in host cells, blocks specific Ser/Thr phosphorylation sites of MAPKK with acetyl groups to inhibit the downstream MAPK signaling pathway.[10]

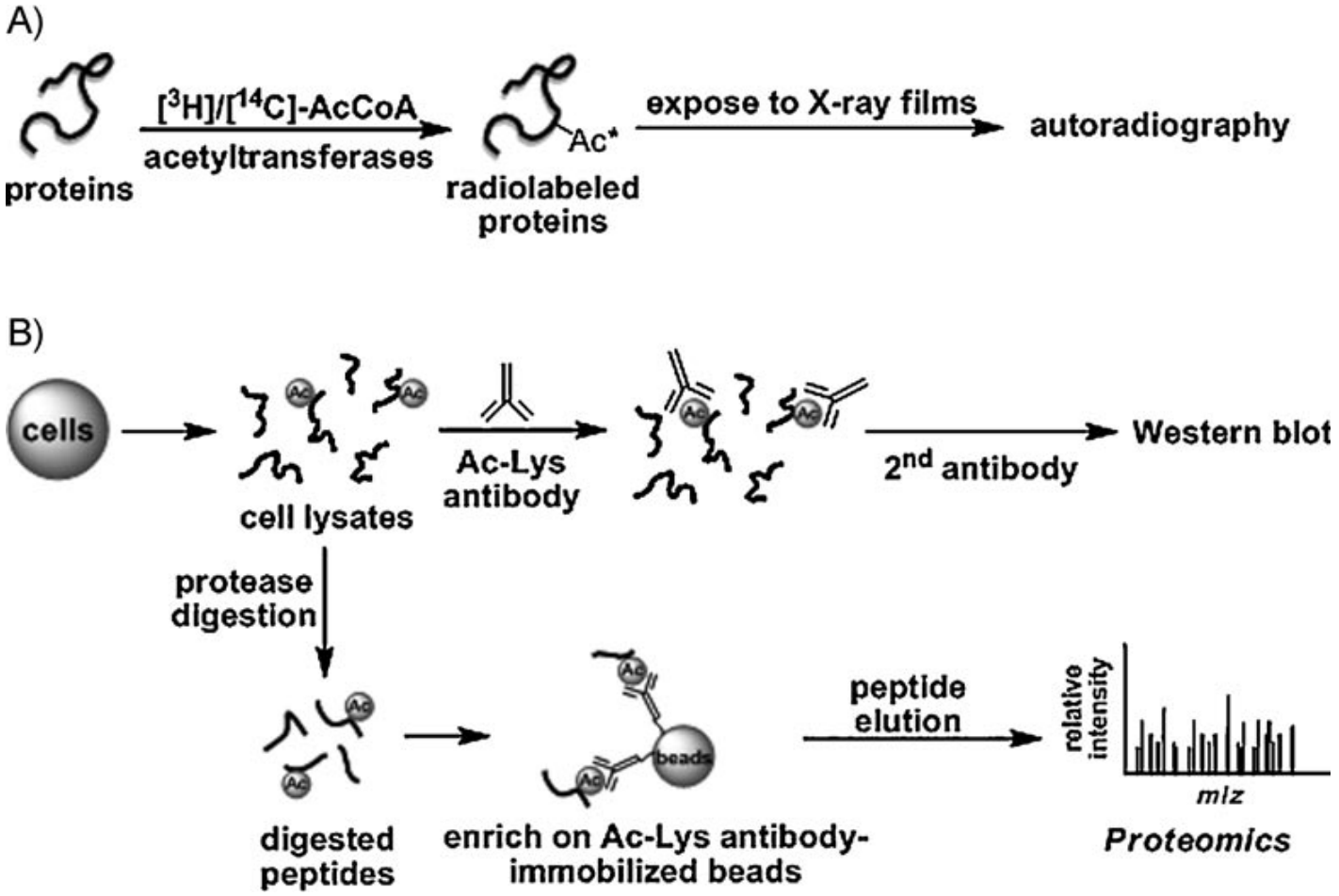

Scheme 3. Detection methods for the visualization and identification of acetylated proteins. A) Radiolabeling of proteins with [^{3}H]/[^{14}C]-AcCoA enable the detection of KAT activity in vitro. B) Anti-AcLys antibodies can be utilized to either visualize acetylated proteins by immunoblotting or retrieve acetylated peptides from biological mixtures for LC-MS/MS analysis.

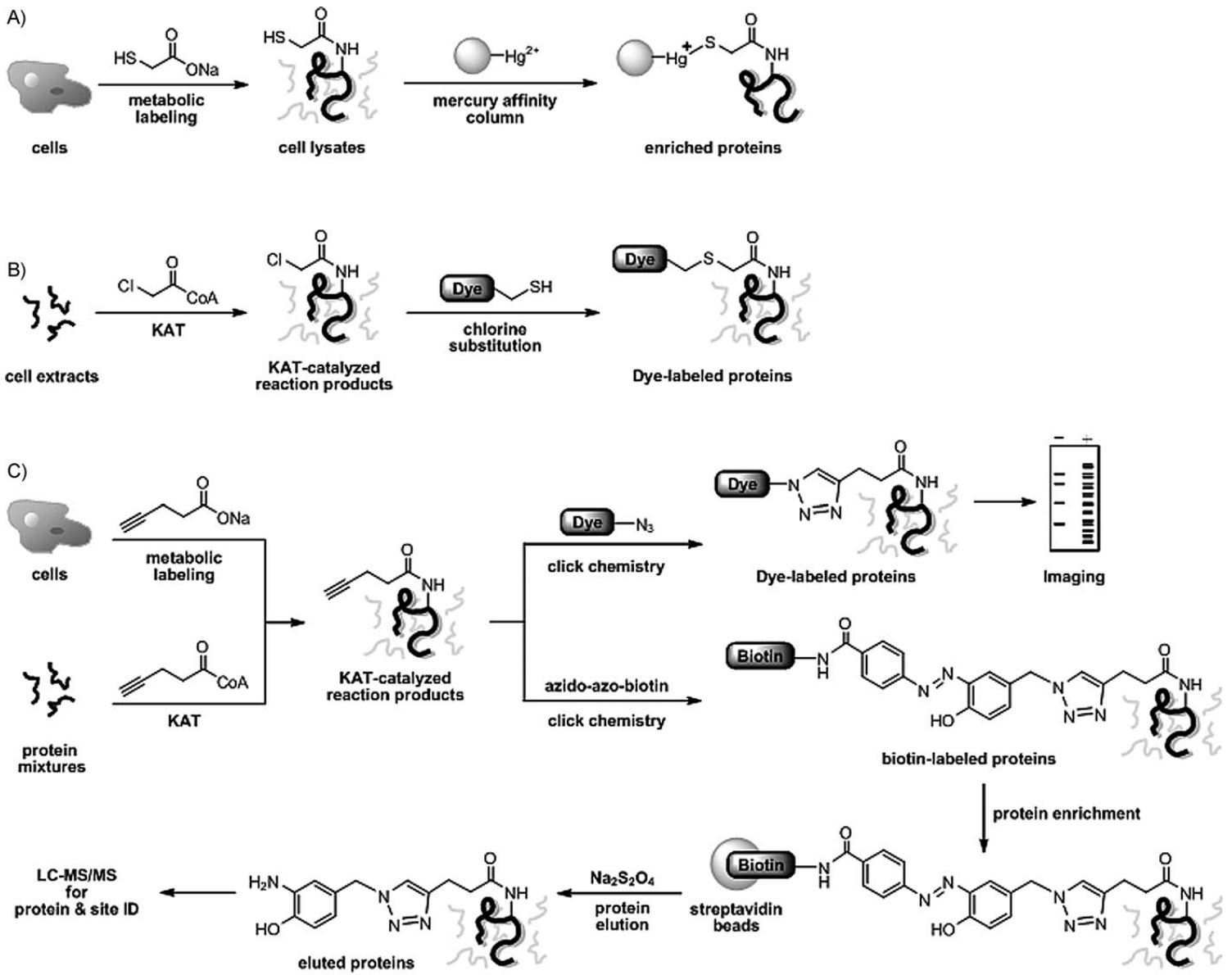

Scheme 4. Detection of acetylated proteins by using acetylation chemical reporters. A) Mercaptoacetate-labeled proteins can be retrieved from the biological mixtures by mercury-affinity column chromatography for LC-MS/MS analysis.[48] B) Chloroacetyl-CoA can be utilized by RimL and Hat1 to label proteins in vitro. KAT activity can be monitored by reaction of chloroacetyl groups appended on proteins with a thiol-containing visualization tag, cysteamine-TAMRA.[49] C) Sodium 4-pentynoate and 4-pentynoyl-CoA can be respectively utilized by KATs in living cells and in vitro.[50] The incorporated alkyne group serves as a unique functionality in cell lysates, which can be further elaborated with an azide-functionalized fluorescent tag for visualization or a cleavable biotin tag for acetylome profiling.

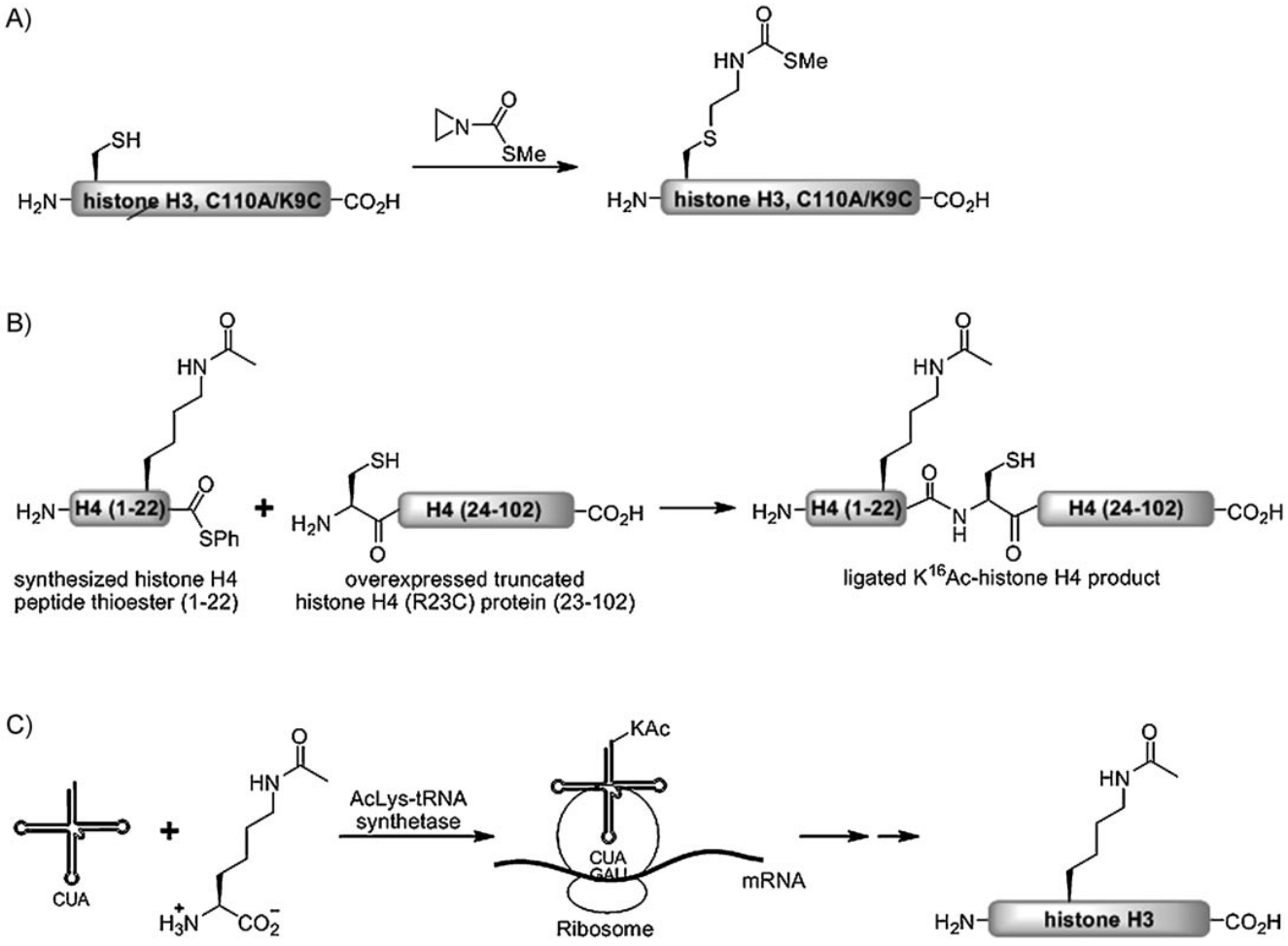

Scheme 5. Synthesis of homogeneously acetylated proteins for structure–function analysis. A) Chemoselective modification of cysteine residues to install AcLys mimics onto the specific sites of proteins.[66] B) Semisynthesis of proteins with defined acetylation site by expressed protein ligation.[74] C) Site-specific incorporation of AcLys into recombinant proteins by using N^{ε}-AcLys-tRNA synthetases/$tRNA_{CUA}$ pair.[76–78]